Supporting Information

Ditriphenylenothiophene Butterfly-Shape Liquid Crystals. The Influence of Polyarene Core Topology on Self-Organization, Fluorescence and Photoconductivity

Wen-Jing Deng,[a] Shuai Liu,[a] Hang Lin,[a] Ke-Xiao Zhao,[a] Xiao-Yan Bai,[a] Ke-Qing Zhao,[a,*] Ping Hu,[a] Bi-Qin Wang,[a] Hirosato Monobe,[b,*], Bertrand Donnio[c,*]

(a) College of Chemistry and Materials Science, Sichuan Normal University, Chengdu, 610066, China. E-mail: kqzhao@sicnu.edu.cn
(b) Nanomaterials Research Institute, National Institute of Advanced Industrial Science and Technology (AIST), Ikeda, Osaka, 5638577, Japan. E-mail: monobe-hirosato@aist.go.jp
(c) Institut de Physique et Chimie des Materiaux de Strasbourg (IPCMS), CNRS-Universite de Strasbourg (UMR 7504), Strasbourg, 67034, France. E-mail: bertrand.donnio@ipcms.unistra.fr

Contents

1. Materials and Methods

Chemicals. All commercially available starting materials were used directly without further purification. The solvents of air- and moisture-sensitive reactions were carefully distilled from appropriate drying agents before use.

Experimental. Air- and moisture-sensitive reactions were assembled on a Schlenk vacuum line or in a glovebox using oven-dried glassware with a Teflon screw cap under Ar atmosphere. Air- and moisture-sensitive liquids and solutions were transferred by syringe. Reactions were stirred using Teflon-coated magnetic stir bars. Elevated temperatures were maintained using Thermostat-controlled air baths. Organic solutions were concentrated using a rotary evaporator with a diaphragm vacuum pump.

Analytical. ^{1}H-NMR/^{13}C NMR spectra were recorded using a Varian UNITY INOVA 400/100 MHz or Bruker 600 MHz spectrometers in $CDCl_3$, and TMS as the internal standard. High-resolution mass spectra (HRMS) spectra were recorded at the Bruker Fourier Transform High Resolution Mass Spectrometry (solariX XR) with MALDI as the ion source. Elemental analyses (EA) were performed on a Vario Micro Select (Elementar Company, German). The thermal gravimetrical analysis (TGA) was measured on a TA-TGA Q500 instrument with heating rate of 20 °C/min in N_2 atmosphere. The phase transition temperatures and enthalpy changes were investigated using a TA-DSC Q100 differential scanning calorimeter (DSC) under N_2 atmosphere with heating or cooling rate of 10 °C/min. Liquid crystalline optical textures were observed and recorded on an Olympus BH2 Polarized Optical Microscope equipped with a Mettler FP82HT hot-stages of which temperatures were controlled by XPR-201 and Mettler FP90. Temperature-variation SAXS (small-angle X-ray scattering) and WAXS (wide-angle X-ray scattering) experiments on Rigaku Smartlab. UV/Vis. absorption spectra were recorded on a Perkin Elmer Lambda 950 spectrophotometer at room temperature. Fluorescence was measured on a HORIBA Fluoromax-4p, and the quantum yields were measured by a HORIB-F-3029 Integrating Sphere, HORIBA, Kyoto, Japan.

Photocurrent time-of-flight (TOF) technique uses N_2 gas laser (KEN-1520, Usho, 600 ps pulse width, λ = 337 nm) and hot stage to measure compound electron and hole mobilities. The liquid crystalline sample cell with indium-tin-oxide (ITO) electrodes was mounted on a handmade hot stage, and electric bias was applied by dry cell batteries. The polarity (20 to 50 kV/cm) electric field is applied, a positive or negative charge carriers hopping through the self-organized aligned sample, causing displacement photocurrent, which was detected on a digital oscilloscope (DSO5052A, Agilent Technology) with a commercially available current amplifier (DHPCA-100, FEMTO). Thickness of the cell used for measurements was in range of 15~20μm.

The cells were filled with the sample in its isotropic liquid state by capillary forces, and then cooled down to the columnar mesophase. POM images showed a low-birefringent textures with homeotropic domains, and the laser focused on a spot with homeotropic aligned sample area.

2. Synthesis and Characterization

The synthesis of 4-bromobenzene-1,2-diol (**1**),[1] 4-bromo-1,2-bis(alkoxy)benzene (**2a-c**),[1] 2-(3,4-bis(alkoxy)phenyl)-4,4,5,5-tetramethyl-1,3,2-dioxaborolane (**3a-c**),[2,3] 2,3,7,8-tetrabromodibenzothiophene (**4**),[4] 3,3',4,4'-tetrakis(alkoxy)-1,1'-biphenyl (**5a-c**), 2-bromo-3',4,4',5-tetrakis(alkoxy)-1,1'-biphenyl (**6a-c**) and 4,4,5,5-tetramethyl-2-(3',4,4',5-tetrakis(alkoxy)-[1,1'-biphenyl]-2-yl)-1,3,2-dioxaborolane (**7a-c**)[5] were performed according to reported methods. All other materials were used as purchased without further purification.

2.1 Synthesis of the phenylboronic ester derivatives

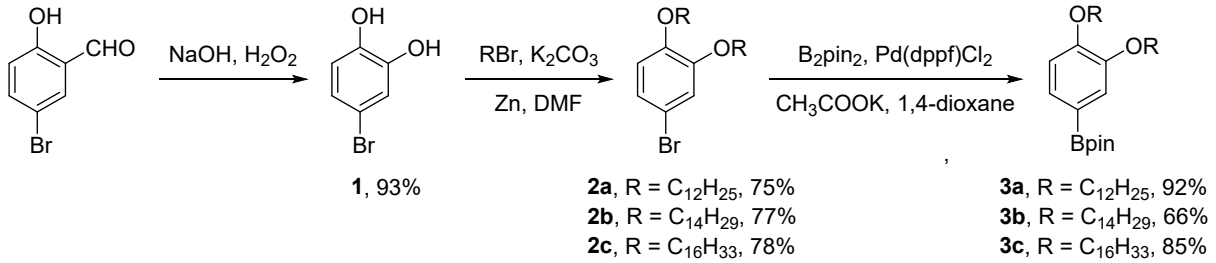

Scheme S1. Preparation of the phenylboronic esters.

---

[1] K. Q. Zhao, Y. Gao, W. H. Yu, P. Hu, B. Q. Wang, B. Heinrich and B. Donnio. Discogens Possessing Aryl Side Groups Synthesized by Suzuki Coupling of Triphenylene Triflates and Their Self-Organization Behavior. *Eur. J. Org. Chem.*, 2016, 2802-2814.

[2] C. X. Liu, H. Wang, J. Q. Du, K. Q. Zhao, P. Hu, B. Q. Wang, H. Monobe, B. Heinrich, and B. Donnio. Molecular Design of Benzothienobenzothiophene-Cored Columnar Mesogens: Facile Synthesis, Mesomorphism, and Charge Carrier Mobility, *J. Mater. Chem. C*, 2018, **6**, 4471-4478.

[3] T. Ma, H. F. Wang, K. Q. Zhao, B. Q. Wang, P. Hu, H. Monobe, B. Heinrich and B. Donnio. Nonlinear Nonacenes with a Dithienothiophene Substructure: Multifunctional Compounds that Act as Columnar Mesogens, Luminophores, π Gelators, and p-Type Semiconductors, *ChemPlusChem*, 2019, **84**, 1439- 1448.

[4] T. Oyama, T. Mori, T. Hashimoto, M. Kamiya, T. Ichikawa, H. Komiyama, Y. S. Yang and T. Yasuda, High-Mobility Regioisomeric Thieno[*f,f'*]bis[1]benzothiophenes: Remarkable Effect of *Syn*/*Anti* Thiophene Configuration on Optoelectronic Properties, Self-Organization, and Charge-Transport Functions in Organic Transistors. *Adv. Electron. Mater.*, 2018, **4**, 1700390.

[5] J. F. Hang, H. Lin, K. Q. Zhao, P. Hu, B. Q. Wang, H. Monobe, C. H. Zhu and B. Donnio, Butterfly Mesogens Based on Carbazole, Fluorene or Fluorenone: Mesomorphous, Gelling, Photophysical, and Photoconductive Properties. *Eur. J. Org. Chem.*, 2021, **2021**, 1989-2002.

4-Bromobenzene-1,2-diol (**1**): Into a solution of NaOH (17.30 g, 10.40 mol) in H_2O (220 mL) was added 5-bromosalicylaldehyde (80.00 g, 0.40 mol), the mixture then heated at 60 °C until all reactants dissolved. The clarified mixture was cooled by an ice-water bath, and 30% of H_2O_2 (51 mL) was added slowly by a constant-pressure dropping funnel. The resulting solution was stirred at room temperature for 2 h. To the reaction mixture, was added NaCl to saturated, and extracted with Et_2O. The combined organic layers were dried over anhydrous $MgSO_4$ and concentrated in vacuum to give **1** as yellow oil (9.80 g, 93 %).

4-Bromo-1,2-bis(alkoxy)benzene (**2**): **1** (10.58 mmol, 1.0 equiv.), potassium carbonate (52.90 mmol, 5.0 equiv.), zinc powder (21.16 mmol, 2.0 equiv.) were weighed in a round bottom flask. Subsequently, DMF (60 mL) and 1-bromoalkane (26.45 mmol, 2.5 equiv.) were added. The resulting solution was stirred at 90°C for 48 h. The reaction mixture was cooled and poured into ice-water, dilute hydrochloric acid was added until acidic pH. Then, the precipitated solid was filtered, washed with MeOH and dried. The crude product was purified by column chromatography on silica gel with dichloromethane/petroleum ether (1/3) mixture as eluent to give liquid or white solid **2** in yield of 75-78%.

2-(3,4-Bis(alkoxy)phenyl)-4,4,5,5-tetramethyl-1,3,2-dioxaborolane (**3**). **2** (1.0 equiv.), bis(pinacolato)diboron (2.0 equiv.), CH_3COOK (4.0 equiv.), $Pd(dppf)Cl_2$ (8 mol%), 1,4-dioxane (0.08 M) were added in a round bottom flask. The resulting solution was stirred under nitrogen at 90ºC for 24 h. The reaction mixture was cooled to room temperature and extracted with dichloromethane. The combined organic layers were dried over anhydrous $MgSO_4$ and concentrated in vacuum. The crude product was purified by column chromatography on silica gel with dichloromethane/petroleum ether (1/2) mixture as eluent to give **3** in yield of 75-92%.

2-(3,4-Bis(dodecyloxy)phenyl)-4,4,5,5-tetramethyl-1,3,2-dioxaborolane (**3a**): Following the general procedure, substrate **2a** (2.0 g, 3.80 mmol) was converted to the white solid **3a** (2.0 g, 92%). **^{1}H NMR** ($CDCl_3$, TMS, 400 MHz) δ(ppm): 7.38 (d, J = 8.0 Hz, 1H, ArH), 7.29 (s, 1H, ArH), 6.87 (d, J = 8.0 Hz, 1 H, ArH), 4.04-3.99 (m, 4H, OCH_2), 1.85-1.78 (m, 4H, CH_2), 1.47-1.42 (m, 4H, CH_2), 1.35-1.26 (m, 44H, CH_2), 0.88 (t, J = 6.8 Hz, 6H, CH_3).

2-(3,4-Bis(tetradecyloxy)phenyl)-4,4,5,5-tetramethyl-1,3,2-dioxaborolane (**3b**): Following the general procedure, substrate **2b** (4.0 g, 6.88 mmol) was converted to the white solid **3b** (2.86 g, 66%). **^{1}H NMR** ($CDCl_3$, TMS, 400 MHz) δ(ppm): 7.38 (d, J = 8.0 Hz, 1 H, ArH), 7.29 (s, 1H, ArH), 6.87 (d, J = 8.0 Hz, 1

H, ArH), 4.04-3.99 (m, 4H, OCH_2), 1.85-1.78 (m, 4H, CH_2), 1.47-1.43 (m, 4H, CH_2), 1.38-1.21 (m, 52H, CH_2), 0.88 (t, J = 6.8 Hz, 6H, CH_3).

2-(3,4-Bis(hexadecyloxy)phenyl)-4,4,5,5-tetramethyl-1,3,2-dioxaborolane (**3c**): Following the general procedure, substrate **2c** (5.0 g, 7.84 mmol) was converted to the white solid **3c** (4.55 g, 85%). **^{1}H NMR** ($CDCl_3$, TMS, 400 MHz) δ(ppm): 7.38 (d, J = 8.0 Hz, 1 H, ArH), 7.29 (s, 1H, ArH), 6.87 (d, J = 8.0 Hz, 1 H, ArH), 4.04-3.99 (m, 4H, OCH_2), 1.85-1.78 (m, 4H, CH_2), 1.48-1.43 (m, 4H, CH_2), 1.35-1.26 (m, 60H, CH_2), 0.88 (t, J = 6.8 Hz, 6H, CH_3).

2.2 Synthesis of the DTPTB*n*

2,3,7,8-Tetrabromodibenzothiophene (**4**): Dibenzothiophene (1.00 g, 5.40 mmol) was dissolved in dry chloroform (40 mL), and bromine (6.19 g, 37.90 mmol) diluted with chloroform (20 mL) was added slowly by a constant-pressure dropping funnel. The resulting solution was stirred under heating reflux for 24 h. The reaction mixture was quenched with aqueous solution of $NaHSO_3$. Filtration gave the product as a white solid (3.14 g, 86%).

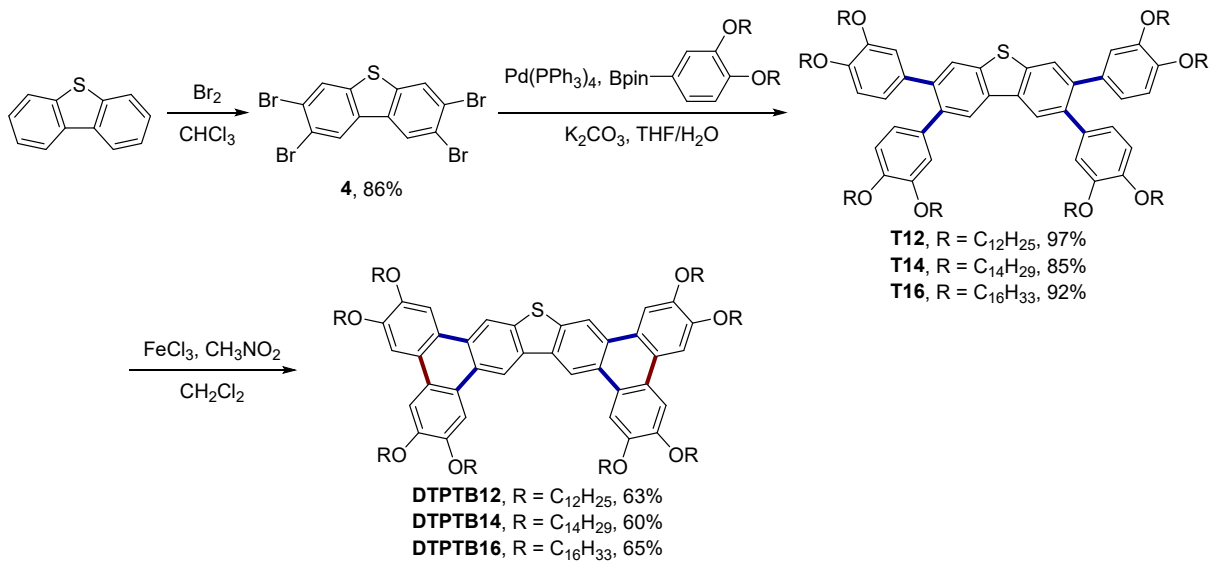

Scheme S2. Preparation of 2,3,6,7,13,14,17,18-octa(alkoxy)ditriphenylenothiophene butterfly-shape molecules.

2,3,7,8-Tetra(3,4-di(alkoxy)phenyl)dibenzothiophene (**T*n***). Under argon, **4** (0.20 mmol, 1.0 equiv.), 3,4-di(alkoxyphenyl)borate (1.00 mmol, 5.0 equiv.), K_2CO_3 (10.00 mmol, 50.0 equiv.), $Pd(PPh_3)_4$ (0.04 mmol, 20 mol%), THF/H_2O (4/1, 15 mL) were added in a reaction tube. The resulting solution was stirred at 70°C for 48

h. The reaction mixture was cooled to room temperature and extracted with dichloromethane. The combined organic layers were dried over anhydrous $MgSO_4$ and concentrated in vacuum. The residue was purified by column chromatography on silica gel with dichloromethane/petroleum ether (1/2) mixture as eluent to give **T*n*** in yield of 85-97%.

2,3,7,8-Tetra(3,4-di(dodecyloxy)phenyl)dibenzothiophene (**T12**): Following the general procedure, substrate **4** (100.0 mg, 0.20 mmol) was converted to the white solid **T12** (384.3 mg, 97%). **^{1}H NMR** ($CDCl_3$, TMS, 400 MHz) δ(ppm): 8.16 (s, 2H, ArH), 7.88 (s, 2H, ArH), 6.78-6.86 (m, 8H, ArH), 6.69 (s, 4H, ArH), 3.97 (t, J = 6.6 Hz, 8H, OCH_2), 3.72 (t, J = 6.6 Hz, 8H, OCH_2), 1.85-1.80 (m, 8H, CH_2), 1.70-1.63 (m, 8H, CH_2), 1.50-1.43 (m, 8H, CH_2), 1.37-1.27 (m, 136H, CH_2), 0.89-0.86 (m, 24H, CH_3). **^{13}C NMR** ($CDCl_3$, 101 MHz) δ(ppm): 148.42, 148.33, 147.96, 147.88, 139.52, 138.80, 137.48, 134.50, 134.46, 134.12, 124.12, 123.16, 122.05, 116.02, 115.88, 113.26, 113.12, 69.24, 69.17, 69.10, 69.05, 31.96, 29.79, 29.75, 29.72, 29.70, 29.54, 29.48, 29.43, 29.41, 29.36, 29.35, 29.13, 26.09, 26.05, 22.72, 14.16. **Elemental Analysis** ($C_{132}H_{216}O_8S$, MW 1963.23): calc. C 80.76%, H 11.09%, S 1.63%; found C 80.63%, H 11.00%, S 1.61%. **HRMS** (ESI) calcd for $C_{132}H_{216}O_8S$ $[M]^{+\bullet}$m/z: 1962.6249 (100.0%), 1961.6216 (70.0%), 1963.6283 (40.9%), 1964.6317 (15.8%); found: 1962.6233 (100%), 1961.6199 (66.21%), 1963.6271 (85.52%), 1964.6314 (48.27%);.

2,3,7,8-Tetra(3,4-di(tetradecyloxy)phenyl)dibenzothiophene (**T14**)**:** Following the general procedure, substrate **4** (100.0 mg, 0.20 mmol) was converted to the white solid **T14** (371.7 mg, 85%). **^{1}H NMR** ($CDCl_3$, TMS, 400 MHz) δ(ppm): 8.16 (s, 2H, ArH), 7.88 (s, 2H, ArH), 6.86-6.79 (m, 8H, ArH), 6.69 (s, 4H, ArH), 3.97 (t, J = 6.6 Hz, 8H, OCH_2), 3.71 (t, J = 6.6 Hz, 8H, OCH_2), 1.85-1.78 (m, 8H, CH_2), 1.71-1.63 (m, 8H, CH_2), 1.48-1.44 (m, 8H, CH_2), 1.37-1.26 (m, 168H, CH_2), 0.89-0.86 (m, 24H, CH_3). **^{13}C NMR** (101 MHz, $CDCl_3$) δ(ppm): 148.48, 148.40, 148.02, 147.94, 139.53, 138.81, 137.50, 134.51, 134.17, 124.11, 123.14, 122.08, 116.14, 116.01, 113.39, 113.25, 69.29, 69.22, 69.15, 69.10, 31.94, 29.78, 29.76, 29.74, 29.69, 29.52, 29.46, 29.39, 29.15, 26.09, 26.05, 22.70, 14.12. **Elemental Analysis** ($C_{148}H_{248}O_8S$, MW 2187.66): calc. C 81.26%, H 11.43%, S 1.47%; found C 81.17%, H 11.23%, S 1.54%. **HRMS** (ESI) calcd for $C_{148}H_{248}O_8SNa[M+Na]^{+\bullet}$ m/z: 2209.8651 (100%), 2210.8685 (79.5%), 2208.8618 (62.5%), 2211.8718 (34.5%); found: 2209.8630 (100%), 2210.8688 (85.80%), 2208.8574 (48.74%), 2211.8740 (40.74%).

2,3,7,8-Tetra(3,4-di(hexadecyloxy)phenyl)dibenzothiophene (**T16**): Following the general procedure, substrate **4** (100.0 mg, 0.20 mmol) was converted to the white solid **T16** (441.6 mg, 92%). **^{1}H NMR** ($CDCl_3$, TMS, 400 MHz) δ(ppm): 8.16 (s, 2H, ArH), 7.88 (s, 2H, ArH), 6.86-6.77 (m, 8H, ArH), 6.69 (s, 4H, ArH), 3.97 (t, J = 6.6 Hz, 8H, OCH_2), 3.72 (t, J = 6.6 Hz, 8H, OCH_2), 1.85-1.78 (m, 8H, CH_2), 1.71-1.65 (m, 8H,

CH_2), 1.50-1.43 (m, 8H, CH_2), 1.37-1.26 (m, 200H, CH_2), 0.88 (t, J = 6.4 Hz, 24H, CH_3). **^{13}C NMR** ($CDCl_3$, 101 MHz) δ(ppm): 148.42, 148.34, 147.97, 147.89, 139.52, 138.81, 137.48, 134.50, 134.47, 134.12, 124.12, 123.15, 122.05, 116.04, 115.89, 113.27, 113.13, 69.25, 69.17, 69.10, 69.05, 31.95, 29.79, 29.77, 29.71, 29.55, 29.54, 29.48, 29.41, 29.38, 29.36, 29.13, 26.10, 26.06, 22.72, 14.16. **Elemental Analysis** ($C_{164}H_{280}O_8S$, MW 2412.10): calc. C 81.66%, H 11.70%, S 1.33%; found C 81.67%, H 11.40%, S 1.32%. **HRMS** (ESI) calcd for $C_{164}H_{280}O_8S$ $[M]^{+\bullet}$ m/z: 2411.1258 (100.0%), 2412.1291 (64.0%), 2410.1224 (56.4%), 2413.1325 (44.9%); found: 2411.1240 (100.0%), 2412.1274 (89.70%), 2410.1250 (34.56%), 2413.1346 (34.56%).

2,3,6,7,13,14,17,18-Octa(alkoxy)ditriphenylenethiophene (**DTPTB*n***). To a stirred solution of **T*n*** (1.0 equiv.) in CH_2Cl_2 (0.002 M), a solution of $FeCl_3$ (6.0 equiv.) in CH_3NO_2 (0.02 M) was added. The resulting solution was stirred at room temperature until completion of the reaction. The reaction mixture was quenched with methanol and extracted with dichloromethane. The combined organic layers were dried over anhydrous $MgSO_4$ and concentrated in vacuum. The residue was purified by column chromatography on Al_2O_3 with dichloromethane /petroleum ether (1/2.5) mixture as eluent to give **DTPTB*n*** in yield of 60-65%.

2,3,6,7,13,14,17,18-Octa(dodecyloxy)ditriphenylenothiophene (**DTPTB12**): Following the general procedure, substrate **T12** (100.0 mg, 0.05 mmol) was converted to the yellow solid **DTPTB12** (62.9 mg, 63%). **^{1}H NMR** ($CDCl_3$, TMS, 400 MHz) δ(ppm): 8.94 (s, 2H, ArH), 8.60 (s, 2H, ArH), 8.16 (s, 2H, ArH), 7.79 (s, 2H, ArH), 7.65 (s, 2H, ArH), 7.62 (s, 2H, ArH), 4.42 (t, J = 6.0 Hz, 4H, OCH_2), 4.23-4.17 (m, 12H, OCH_2), 2.10-1.94 (m, 16H, CH_2), 1.74-1.60 (m, 16H, CH_2), 1.52-1.25 (m, 128H, CH_2), 0.91-0.84 (m, 24H, CH_3). **Elemental Analysis** ($C_{132}H_{212}O_8S$, MW 1959.20): calc. C 80.92%, H 10.91%, S 1.64%; found C 80.60%, H 10.64%, S 1.67%. **HRMS** (ESI) calcd for $C_{132}H_{212}O_8S$ $[M]^{+\bullet}$ m/z: 1958.5936 (100%), 1957.5903 (70.0%), 1959.5970 (40.9%), 1960.6004 (24.0%); found: 1958.5920 (100%), 1957.5910 (58.11%), 1959.5910 (77.70%), 1960.6030 (33.78%).

2,3,6,7,13,14,17,18-Octa(tetradecyloxy)ditriphenylenothiophene (**DTPTB14**)**:** Following the general procedure, substrate **T14** (100.0 mg, 0.05 mmol) was converted to the green solid **DTPTB14** (60.0 mg, 60%). **^{1}H NMR** ($CDCl_3$, TMS, 400 MHz) δ(ppm): 8.98 (s, 2H, ArH), 8.63 (s, 2H, ArH), 8.18 (s, 2H, ArH), 7.81 (s, 2H, ArH), 7.67 (s, 2H, ArH), 7.64 (s, 2H, ArH), 4.41 (t, J = 6.0 Hz, 4H, OCH_2), 4.23-4.18 (m, 12H, OCH_2), 2.07-1.97 (m, 16H, CH_2), 1.71-1.60 (m, 16H, CH_2), 1.47-1.23 (m, 160H, CH_2), 0.90-0.84 (m, 24H, CH_3). **Elemental Analysis** ($C_{148}H_{244}O_8S$, MW 2183.63): calc. C 81.41%, H 11.26%, S 1.47%; found C 80.95%, H 10.85%, S 1.56%. **HRMS** (ESI) calcd for $C_{148}H_{244}O_8S$ $[M]^{+\bullet}$ m/z: 2182.8441 (100%), 2183.8474 (79.5%),

2181.8407 (62.5%), 2184.8508 (34.5%); found: 2182.8421 (100%), 2183.8493 (82.87%), 2181.8492 (34.27%), 2184.8632 (46.42%).

2,3,6,7,13,14,17,18-Octakis(hexadecyloxy)ditriphenylenethiophene (**DTPTB16**): Following the general procedure, substrate **T16** (100.0 mg, 0.04 mmol) was converted to the orange solid **DTPTB16** (65.0 mg, 65%). **^{1}H NMR** ($CDCl_3$, TMS, 600 MHz) δ(ppm): 9.02 (s, 2H, ArH), 8.67 (s, 2H, ArH), 8.19 (s, 2H, ArH), 7.84 (s, 2H, ArH), 7.69 (s, 2H, ArH), 7.67 (s, 2H, ArH), 4.41 (t, J = 6.0 Hz, 4H, OCH_2), 4.26-4.20 (m, 12H, OCH_2), 2.05-1.96 (m, 16H, CH_2), 1.70-1.67 (m, 4H, CH_2), 1.62-1.58 (m, 12H, CH_2), 1.51-1.43 (m, 16H, CH_2), 1.40-1.23 (m, 176H, CH_2), 0.89-0.85 (m, 24H, CH_3). **Elemental Analysis** ($C_{164}H_{276}O_8S$, MW 2408.06): calc. C 81.80%, H 11.55%, S 1.33%; found C 81.44%, H 11.28%, S 1.37%. **HRMS** (ESI) calcd for $C_{164}H_{276}O_8S$ $[M]^{+\bullet}$ m/z: 2407.0945 (100%), 2408.0978 (64.0%), 2406.0911 (56.4%), 2409.1012 (44.9%); found: 2407.0939 (100%), 2408.0996 (92.35%), 2406.0876 (37.58%), 2409.1058 (40.94%).

2.3 Synthesis of the biphenylboronic ester derivatives

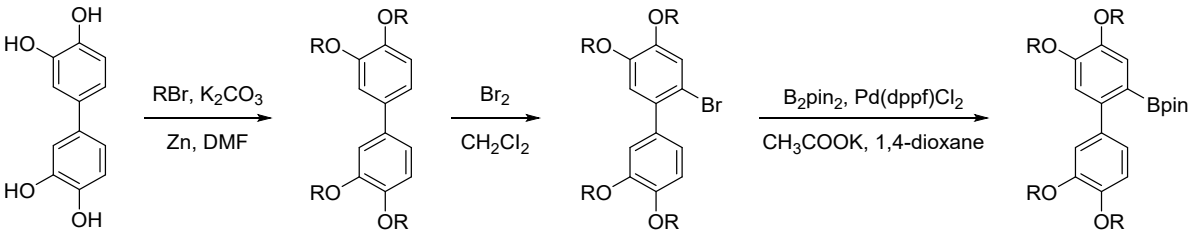

5a, R = C_8H_{17}, 55%
5b, R = $C_{10}H_{21}$, 60%
5c, R = $C_{12}H_{25}$, 88%

6a, R = C_8H_{17}, 90%
6b, R = $C_{10}H_{21}$, 94%
6c, R = $C_{12}H_{25}$, 97%

7a, R =C_8H_{17}, 82%
7b, R = $C_{10}H_{21}$, 40%
7c, R = $C_{12}H_{25}$, 53%

Scheme S3. Preparation of the biphenylboronic esters.

3,3',4,4'-Tetrakis(alkoxy)-1,1'-biphenyl (**5**): [1,1'-biphenyl]-3,3',4,4'-tetraol (1.0 equiv.), potassium carbonate (30.0 equiv.), zinc powder (4.0 equiv.) were weighed into a round bottom flask. Subsequently, DMF (0.1 M) and 1-bromoalkane (4.5 equiv.) were added. The resulting solution was stirred at 100°C for 24 h. The reaction mixture was cooled and poured into ice-water, dilute hydrochloric acid was added until acidic pH. Then, the precipitated solid was filtered and dried. The crude product was purified by column chromatography on silica gel with dichloromethane:petroleum ether (1:3) mixture as eluent. Finally, recrystallized from ethyl acetate and ethanol gave **5** in yield of 55-88%.

3,3',4,4'-Tetrakis(octyloxy)-1,1'-biphenyl (**5a**): Following the general procedure, [1,1'-biphenyl]-3,3',4,4'-tetraol (1.19 g, 5.47 mmol) was converted to the white solid **5a** (2.00 g, 55%). **^{1}H NMR** ($CDCl_3$, TMS, 400

MHz) δ(ppm):7.09-7.05 (m, 4H, ArH), 6.93 (d, J = 8.0 Hz, 2H, ArH), 4.08-4.01 (m, 8H, OCH_2), 1.88-1.81 (m, 8H, CH_2), 1.53-1.46 (t, J = 8.0 Hz ,8H, CH_2), 1.35-1.30 (m, 32H, CH_2),0.90 (t, J = 6.2 Hz, 12H, CH_3).

3,3',4,4'-Tetrakis(decyloxy)-1,1'-biphenyl (**5b**): Following the general procedure, [1,1'-biphenyl]-3,3',4,4'-tetraol (0.40 g, 1.83 mmol) was converted to the white solid **5b** (0.86 g, 60%). **^{1}H NMR** ($CDCl_3$, TMS, 400 MHz) δ(ppm): 7.08-7.04 (m, 4H, ArH), 6.92 (d, J = 8.0 Hz, 2H, ArH), 4.08-4.01 (m, 8H, OCH_2), 1.88-1.81 (m, 8H, CH_2), 1.53-1.46 (m, 8H, CH_2), 1.38-1.26 (m, 48H, CH_2), 0.89 (t, J = 6.5 Hz, 12H, CH_3).

3,3',4,4'-Tetrakis(dodecyloxy)-1,1'-biphenyl (**5c**): Following the general procedure, [1,1'-biphenyl]-3,3',4,4'-tetraol (1.20 mg, 5.50 mmol) was converted to the white solid **5a** (3.78 g, 88%). **^{1}H NMR** ($CDCl_3$, TMS, 400 MHz) δ(ppm): 7.06 (s, 2H, ArH), 7.05 (d, J = 4.0 Hz, 2H, ArH), 6.92 (d, J = 8.1 Hz, 2H, ArH), 4.07-4.00 (m, 8H, OCH_2), 1.85-1.80 (m, 8H, CH_2), 1.50-1.26 (m, 72H, CH_2), 0.88 (t, J = 6.6 Hz, 12H, CH_3).

2-Bromo-3',4,4',5-tetrakis(alkoxy)-1,1'-biphenyl (**6**). **5** (1.0 equiv.) was dissolved in dry chloroform (0.015 M), and bromine (1.0 equiv.) diluted with chloroform (0.1 M) was added slowly by a constant-pressure dropping funnel. The resulting solution was stirred at room temperature until completion of the reaction. The reaction mixture was quenched with aqueous sodium hydrogen sulfite and extracted with dichloromethane. The combined organic layers were dried over anhydrous $MgSO_4$ and concentrated in vacuum. The crude product was purified by column chromatography on silica gel with dichloromethane/petroleum ether (1/2) mixture as eluent. Finally, recrystallized from ethyl acetate and ethanol gave **6** in yield of 90-97%.

2-Bromo-3',4,4',5-tetrakis(octyloxy)-1,1'-biphenyl (**6a**): Following the general procedure, **5a** (1.50 g, 2.25 mmol) was converted to the white solid **6a** (1.68 g, 90%). **^{1}H NMR** ($CDCl_3$, TMS, 400 MHz) δ(ppm): 7.10 (s, 1H, ArH), 6.94 (s, 1H, ArH), 6.89 (s, 2H, ArH), 6.84 (s, 1H, ArH), 4.04-3.95(m, 8H, OCH_2), 1.84-1.80 (m, 8H, CH_2), 1.48-1.29 (m, 40H, CH_2), 0.89-0.86 (m, 12H, CH_3).

2-Bromo-3',4,4',5-tetrakis(decyloxy)-1,1'-biphenyl (**6b**): Following the general procedure, **5b** (0.63 g, 0.81 mmol) was converted to the white solid **6b** (0.65 g, 94%). **^{1}H NMR** ($CDCl_3$, TMS, 400 MHz) δ(ppm): 7.10 (s, 1H, ArH), 6.95 (s, 1H, ArH), 6.89 (s, 2H, ArH), 6.84 (s, 1H, ArH), 4.03-3.97 (m, 8H, OCH_2), 1.84-1.81 (m, 8H, CH_2), 1.48-1.27 (m, 56H, CH_2), 0.88 (t, J = 5.3 Hz, 12H, CH_3).

2-Bromo-3',4,4',5-tetrakis(dodecyloxy)-1,1'-biphenyl (**6c**): Following the general procedure, **5c** (3.29 g, 3.70 mmol) was converted to the white solid **6c** (3.50 g, 97%). **^{1}H NMR** ($CDCl_3$, TMS, 400 MHz) δ(ppm): 7.10（s, 1H, ArH, 6.94 (s, 1H, ArH), 6.89 (s, 2H, ArH), 6.84 (s, 1H, ArH), 4.04-3.96 (m, 8H, OCH_2), 1.84-1.80 (m, 8H, CH_2), 1.47-1,42 (m, 8H, CH_2), 1.35-1.26 (m, 64H, CH_2), 0.88 (t, J = 6.1 Hz, 12H, CH_3).

4,4,5,5-Tetramethyl-2-(3',4,4',5-tetrakis(alkoxy)-[1,1'-biphenyl]-2-yl)-1,3,2-dioxaborolane (**7**). **6** (1.0 equiv.), bis(pinacolato)diboron (1.5 equiv.), CH_3COOK (3.0 equiv.), $Pd(dppf)Cl_2$ (5 mol%), 1,4-dioxane (0.06 M) were added in a round bottom flask. The resulting solution was stirred under nitrogen at 90°C for 24 h. The reaction mixture was cooled to room temperature and extracted with dichloromethane. The combined organic layers were dried over anhydrous $MgSO_4$ and concentrated in vacuum. The crude product was purified by column chromatography on silica gel with dichloromethane:petroleum ether (1:3) mixture as eluent. Finally, recrystallized from ethyl acetate and methanol gave **7** in yield of 40-82%.

4,4,5,5-Tetramethyl-2-(3',4,4',5-tetrakis(octyloxy)-[1,1'-biphenyl]-2-yl)-1,3,2-dioxaborolane (**7a**): Following the general procedure, **6a** (4.00 g, 5.37 mmol) was converted to the white solid **7a** (3.51 g, 82%). **^{1}H NMR** ($CDCl_3$, TMS, 400 MHz) δ(ppm): 7.20 (s, 1H, ArH), 6.92 (s, 1H, ArH), 6.85 (s, 3H, ArH), 4.06-3.99 (m, 8H, OCH_2), 1.83-1.80 (m, 8H, CH_2), 1.48-1.46 (m, 8H, CH_2), 1.28-1.19 (m, 32H, CH_2), 1.19 (s, 12H, CH_3), 0.88 (d, J = 3.7 Hz, 12H, CH_3).

4,4,5,5-Tetramethyl-2-(3',4,4',5-tetrakis(decyloxy)-[1,1'-biphenyl]-2-yl)-1,3,2-dioxaborolane (**7b**): Following the general procedure, **6b** (1.20 g, 1.40 mmol) was converted to the white solid **7b** (1.27 g, 40%). **^{1}H NMR** ($CDCl_3$, TMS, 400 MHz) δ(ppm): 7.21 (s, 1H, ArH), 6.92 (s, 1H, ArH), 6.89 (s, 3H, ArH), 4.05-4.00 (m, 8H, OCH_2), 1.85-1.80 (m, 8H, CH_2), 1.48-1.27 (m, 56H, CH_2), 1.19 (s, 12H, CH_3), 0.88 (t, J = 5.7 Hz, 12H, CH_3).

4,4,5,5-Tetramethyl-2-(3',4,4',5-tetrakis(dodecyloxy)-[1,1'-biphenyl]-2-yl)-1,3,2-dioxaborolane (**7c**): Following the general procedure, **6c** (2.60 g, 2.70 mmol) was converted to the white solid **7c** (1.44 g, 53%). **^{1}H NMR** ($CDCl_3$, TMS, 400 MHz) δ(ppm): 7.21 (s, 1H, ArH), 6.92 (s, 1H, ArH), 6.85 (s, 3H, ArH), 4.05-4.00 (m, 8H, OCH_2), 1.85-1.80 (m, 8H, CH_2), 1.35-1.26 (m, 72H, CH_2), 1.19 (s, 12H, CH_3), 0.88 (t, J = 6.3 Hz, 12H, CH_3).

2.4 Synthesis of the DTPTA*n*

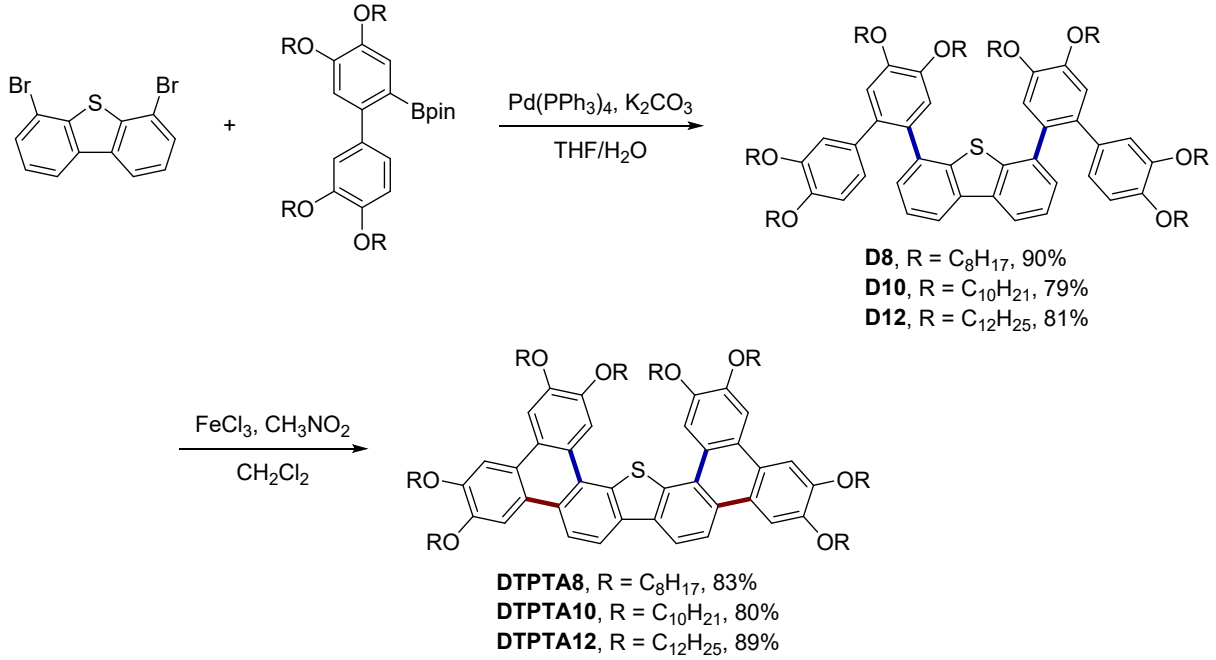

Scheme S4. Preparation of the 2,3,6,7,14,15,18,19-octakis(alkoxy)ditriphenylenethiophene.

2,3,6,7,14,15,18,19-Octakis(alkoxy)ditriphenylenothiophene (**DTPTA*n***). Under argon, 4,6-dibromodibenzothiophene (1.0 equiv.), 1,1'-biphenyl-2-borate (2.5 equiv.), K_2CO_3 (30.0 equiv.), $Pd(PPh_3)_4$ (20 mol%), THF/H_2O (4/1, 0.01 M) were added in a reaction tube. The resulting solution was stirred at 70°C for 48 h. The reaction mixture was cooled to room temperature and extracted with dichloromethane. The combined organic layers were dried over anhydrous $MgSO_4$ and concentrated in vacuum. The residue was purified by column chromatography on silica gel with dichloromethane/petroleum ether (1/3) mixture as eluent to give white solid **D*n*** in yield of 79-90%.

4,6-Bis(3',4,4',5-tetrakis(octyloxy)-[1,1'-biphenyl]-2-yl)dibenzo[b,d]thiophene (**D8**): Following the general procedure, substrate 4,6-dibromodibenzothiophene (50.0 mg, 0.15 mmol) was converted to the white solid **D8** (200.0 mg, 90%). **^{1}H NMR** ($CDCl_3$, TMS, 400 MHz) δ(ppm): 7.95 (d, *J* = 8.0 Hz, 2H, ArH), 7.28 (d, *J* = 8.0 Hz, 2H, ArH), 7.04 (d, *J* = 4.0 Hz, 2H, ArH), 6.99 (s, 2H, ArH), 6.95 (s, 2H, ArH), 6.69 (s, 2H, ArH), 6.63 (s, 2H, ArH), 6.49 (s, 2H, ArH), 4.08 (t, *J* = 6.0 Hz, 4H, OCH_2), 3.98 (t, *J* = 6.0 Hz, 4H, OCH_2), 3.85 (t, *J* = 6.0 Hz, 4H, OCH_2), 3.30 (s, 4H, OCH_2), 1.88-1.80 (m, 8H, CH_2), 1.74-1.69 (m, 4H, CH_2), 1.50-1.09 (m, 84H, CH_2), 0.90-0.85 (m, 24H, CH_3). **^{13}C NMR** ($CDCl_3$, 101 MHz) *δ* (ppm): 148.83, 147.86, 147.75, 147.46, 140.83, 137.01, 135.81, 133.74, 133.58, 130.82, 128.43, 124.40, 121.13, 119.73, 115.44, 115.15, 112.85, 69.35, 69.28, 69.01, 68.67, 31.89, 31.84, 31.82, 29.43, 29.42, 29.39, 29.36, 29.33, 29.31, 29.29, 29.27, 28.93,

26.11, 26.01, 25.71, 22.72, 22.71, 22.69, 22.67, 14.15, 14.14, 14.12.

4,6-Bis(3',4,4',5-tetrakis(decyloxy)-[1,1'-biphenyl]-2-yl)dibenzo[b,d]thiophene (**D10**): Following the general procedure, substrate 4,6-dibromodibenzothiophene (50.0 mg, 0.15 mmol) was converted to the white solid **D10** (200.0 mg, 79%). **^{1}H NMR** ($CDCl_3$, TMS, 400 MHz) δ(ppm): 7.95 (d, *J* = 7.9 Hz, 2H, ArH), 7.28 (d, *J* = 7.6 Hz, 2H, ArH), 7.03 (d, *J* = 7.3 Hz, 2H, ArH), 6.99 (s, 2H, ArH), 6.96 (s, 2H, ArH), 6.68 (s, 2H, ArH), 6.63 (s, 2H, ArH), 6.50 (s, 2H, ArH), 4.08 (t, *J* = 6.6 Hz, 4H, OCH_2), 3.98 (t, *J* = 6.5 Hz, 4H, OCH_2), 3.85 (t, *J* = 6.6 Hz, 4H, OCH_2), 3.31 (s, 4H, OCH_2), 1.88-1.79 (m, 8H, CH_2), 1.74-1.70 (m, 4H, CH_2), 1.50-1.11 (m, 116H, CH_2), 0.90-0.85 (m, 24H, CH_3). **^{13}C NMR** ($CDCl_3$, 101 MHz) *δ* (ppm): 148.83, 147.86, 147.74, 147.46, 140.83, 137.01, 135.81, 133.73, 133.57, 130.81, 128.44, 124.39, 121.12, 119.73, 115.43, 115.14, 112.83, 69.35, 69.28, 69.01, 68.67, 31.96, 31.94, 31.93, 31.92, 29.68, 29.67, 29.63, 29.61, 29.59, 29.49, 29.47, 29.43, 29.39, 29.37, 29.30, 28.93, 26.12, 26.01, 25.72, 22.73, 22.71, 22.70, 14.16, 14.15, 14.14.

4,6-Bis(3',4,4',5-tetrakis(dodecyloxy)-[1,1'-biphenyl]-2-yl)dibenzo[b,d]thiophene (**D12**): Following the general procedure, substrate 4,6-dibromodibenzothiophene (50.0 mg, 0.15 mmol) was converted to the white solid **D12** (232.4 mg, 81%). **^{1}H NMR** ($CDCl_3$, TMS, 400 MHz) δ(ppm): 7.95 (d, *J* = 8.0 Hz, 2H, ArH), 7.29 (s, 2H, ArH), 7.03 (d, *J* = 8.0 Hz, 2H, ArH), 6.99 (s, 2H, ArH), 6.96 (s, 2H, ArH), 6.68 (s, 2H, ArH), 6.63 (s, 2H, ArH), 6.50 (s, 2H, ArH), 4.08 (t, *J* = 6.0 Hz, 4H, OCH_2), 3.98 (t, *J* = 8.0 Hz, 4H, OCH_2), 3.85 (t, *J* = 6.0 Hz, 4H, OCH_2), 3.31 (s, 4H, OCH_2), 1.88-1.79 (m, 8H, CH_2), 1.73-1.68 (m, 4H, CH_2), 1.52-1.18 (m, 148H, CH_2), 0.89-0.86 (m, 24H, CH_3). **^{13}C NMR** ($CDCl_3$, 101 MHz) *δ* (ppm): 148.84, 147.87, 147.75, 147.46, 140.83, 137.01, 135.81, 133.74, 133.58, 130.82, 128.44, 124.39, 121.13, 119.73, 115.45, 115.16, 112.86, 69.36, 69.29, 69.02, 68.68, 31.96, 31.95, 31.94, 29.78, 29.76, 29.75, 29.72, 29.70, 29.69, 29.65, 29.51, 29.49, 29.43, 29.41, 29.38, 29.31, 28.94, 26.13, 26.02, 25.73, 22.72, 14.14.

To a stirred solution of **D*n*** (1.0 equiv.) in CH_2Cl_2 (0.0025 M), a solution of $FeCl_3$ (6.0 equiv.) in CH_3NO_2 (0.025 M) was added. The resulting solution was stirred at room temperature until completion of the reaction. The reaction mixture was quenched with methanol and extracted with dichloromethane. The combined organic layers were dried over anhydrous $MgSO_4$ and concentrated in vacuum. The residue was purified by column chromatography on SiO_2 with dichloromethane /petroleum ether (1/2.5) mixture as eluent to give **DTPTA*n*** in yield of 80-89%.

2,3,6,7,14,15,18,19-Octakis(octyloxy)ditriphenylenethiophene (**DTPTA8**): Following the general procedure, substrate **D8** (70.0 mg, 0.05 mmol) was converted to the green solid **DTPTA8** (58.0 mg, 83%).

^{1}H NMR ($CDCl_3$, TMS, 400 MHz) δ(ppm): 9.00 (s, 2H, ArH), 8.66 (d, *J* = 8.6 Hz, 2H, ArH), 8.47 (d, *J* = 8.7 Hz, 2H, ArH), 8.10 (s, 2H, ArH), 7.98 (s, 2H, ArH), 7.89 (s, 2H, ArH), 4.42 (t, *J* = 6.2 Hz, 4H, OCH_2), 4.34-4.25 (m, 12H, OCH_2), 2.02-1.97 (m, 16H, CH_2), 1.64-1.52 (m, 18H, CH_2), 1.47-1.30 (m, 50H, CH_2), 1.26-1.14 (m, 12H, CH_2), 0.91 (t, *J* = 4.3 Hz, 18H, CH_3), 0.80 (t, *J* = 6.7 Hz, 6H, CH_3). **^{13}C NMR** ($CDCl_3$, 101 MHz) δ(ppm): 149.55, 149.27, 149.14, 148.66, 134.49, 134.03, 128.44, 125.37, 125.00, 124.13, 123.95, 123.44, 120.45, 119.04, 112.34, 107.31, 107.10, 106.60, 70.46, 69.58, 69.57, 69.25, 31.94, 31.92, 31.89, 29.68, 29.62, 29.59, 29.53, 29.51, 29.43, 29.42, 26.33, 26.26, 22.74, 22.70, 22.57, 14.16, 14.14, 14.08. **Elemental Analysis** ($C_{100}H_{148}O_8S$, MW 1510.34): calc. C 79.53%, H 9.88%, S 2.12%; found C 79.18%, H 9.65%, S 2.10%. **HRMS** (ESI) calcd for $C_{100}H_{148}O_8S$ $[M]^{+\bullet}$ m/z: 1510.0928 (100%), 1509.0895 (92.5%), 1511.0962 (39.5%); found: 1510.0929 (100%), 1509.0930 (76.73%), 1511.0936 (52.45%).

2,3,6,7,14,15,18,19-Octakis(decyloxy)ditriphenylenethiophene (**DTPTA10**)：Following the general procedure, substrate **D10** (140.0 mg, 0.08 mmol) was converted to the green solid **DTPTA10** (112.0 mg, 80%). **^{1}H NMR** ($CDCl_3$, TMS, 400 MHz) δ(ppm): 9.00 (s, 2H, ArH), 8.66 (d, *J* = 8.7 Hz, 2H, ArH), 8.46 (d, *J* = 8.7 Hz, 2H, ArH), 8.10 (s, 2H, ArH), 7.98 (s, 2H, ArH), 7.89 (s, 2H, ArH), 4.42 (t, *J* = 6.2 Hz, 4H, OCH_2), 4.34-4.24 (m, 12H, OCH_2), 2.02-1.97 (m, 18H, CH_2), 1.63-1.53 (m, 16H, CH_2), 1.45-1.16 (m, 94H, CH_2), 0.89 (t, *J* = 6.5 Hz, 18H, CH_3), 0.81 (t, *J* = 6.9 Hz, 6H, CH_3). **^{13}C NMR** ($CDCl_3$, 101 MHz) δ(ppm): 149.54, 149.24, 149.12, 148.65, 134.54, 134.08, 128.47, 125.34, 125.07, 124.09, 123.95, 123.42, 120.53, 119.12, 112.11, 107.27, 107.03, 106.54, 70.38, 69.55, 69.24, 31.99, 31.95, 29.81, 29.78, 29.74, 29.71, 29.68, 29.63, 29.60, 29.56, 29.50, 29.47, 26.32, 26.27, 26.25, 22.75, 22.72, 14.19, 14.17, 14.14. **Elemental Analysis** ($C_{116}H_{180}O_8S$, MW 1734.77): calc. C 80.31%, H 10.46%, S 1.85%; found C 80.02%, H 10.25%, S 1.51%. **HRMS** (ESI) calcd for $C_{116}H_{180}O_8S$ $[M]^{+\bullet}$ m/z: 1734.3432 (100%), 1733.3399 (79.7%), 1735.3466 (34.1%); found: 1734.3438 (100%), 1733.3339 (68.96%), 1735.3466 (72.06%).

2,3,6,7,14,15,18,19-Octakis(dodecyloxy)ditriphenylenethiophene (**DTPTA12**)：Following the general procedure, substrate **D12** (50.0 mg, 0.03 mmol) was converted to the green solid **DTPTA12** (42.0 mg, 89%). **^{1}H NMR** ($CDCl_3$, TMS, 400 MHz) δ: 9.02 (s, 2H, ArH), 8.70 (d, *J* = 8.3 Hz, 2H, ArH), 8.50 (d, *J* = 8.4 Hz, 2H, ArH), 8.12 (s, 2H, ArH), 7.99 (s, 2H, ArH), 7.90 (s, 2H, ArH), 4.42 (t, *J* = 6.2 Hz, 4H, OCH_2), 4.32-4.28 (m, 12H, OCH_2), 2.04-1.93 (m, 16H, CH_2), 1.61-1.52 (m, 18H, CH_2), 1.47-1.21 (m, 106H, CH_2), 1.15 (s, 20H, CH_2), 0.90-0.82 (m, 24H, CH_3). **^{13}C NMR** ($CDCl_3$, 101 MHz) δ(ppm): 149.56, 149.24, 149.14, 148.66, 134.56, 134.08, 128.50, 125.34, 125.09, 124.10, 123.98, 123.43, 120.54, 119.14, 112.14, 107.30, 107.06, 106.54, 70.38, 69.56, 69.25, 31.98, 31.96, 29.82, 29.80, 29.76, 29.72, 29.69, 29.65, 29.59, 29.56, 29.50,

29.45, 26.32, 26.27, 26.26, 22.74, 22.72, 14.16, 14.15. **Elemental Analysis** ($C_{132}H_{212}O_8S$, MW 1959.20): calc. C 80.92%, H 10.91%, S 1.64%; found C 80.78%, H 10.67%, S 1.61%. **HRMS** (ESI) calcd for $C_{132}H_{212}O_8S$ $[M]^{+\bullet}$ m/z: 1958.5936 (100%), 1957.5903 (70.0%), 1959.5970 (40.9%); found: 1958.5941 (100%), 1957.5903 (57.26%), 1959.5989 (77.57%).

3. TGA

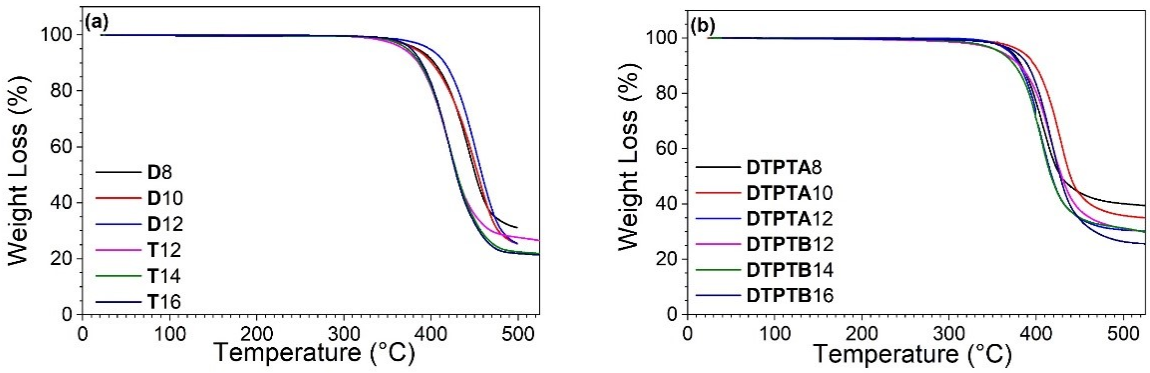

Figure S1. TGA thermograms of: (a) **D*n*** and **T*n***; (b) **DTPTA*n*** and **DTPTB*n***.

Table S1. Weight-loss temperatures of **D*n*** and **T*n***

Compound	T_{dec} /°C (1% loss)	T_{dec} /°C (2% loss)	T_{dec} /°C (5% loss)
D8	332	355	384
D10	332	355	382
D12	344	371	399
T12	324	345	369
T14	336	353	373
T16	345	361	377

Table S2. Weight-loss temperature of **DTPTA*n*** and **DTPTB*n***

Compound	T_{dec} /°C (1% loss)	T_{dec} /°C (2% loss)	T_{dec} /°C (5% loss)
DTPTA8	341	354	371
DTPTA10	339	360	384
DTPTA12	341	353	369
DTPTB12	312	322	360
DTPTB14	315	330	358
DTPTB16	328	352	376

4. POM

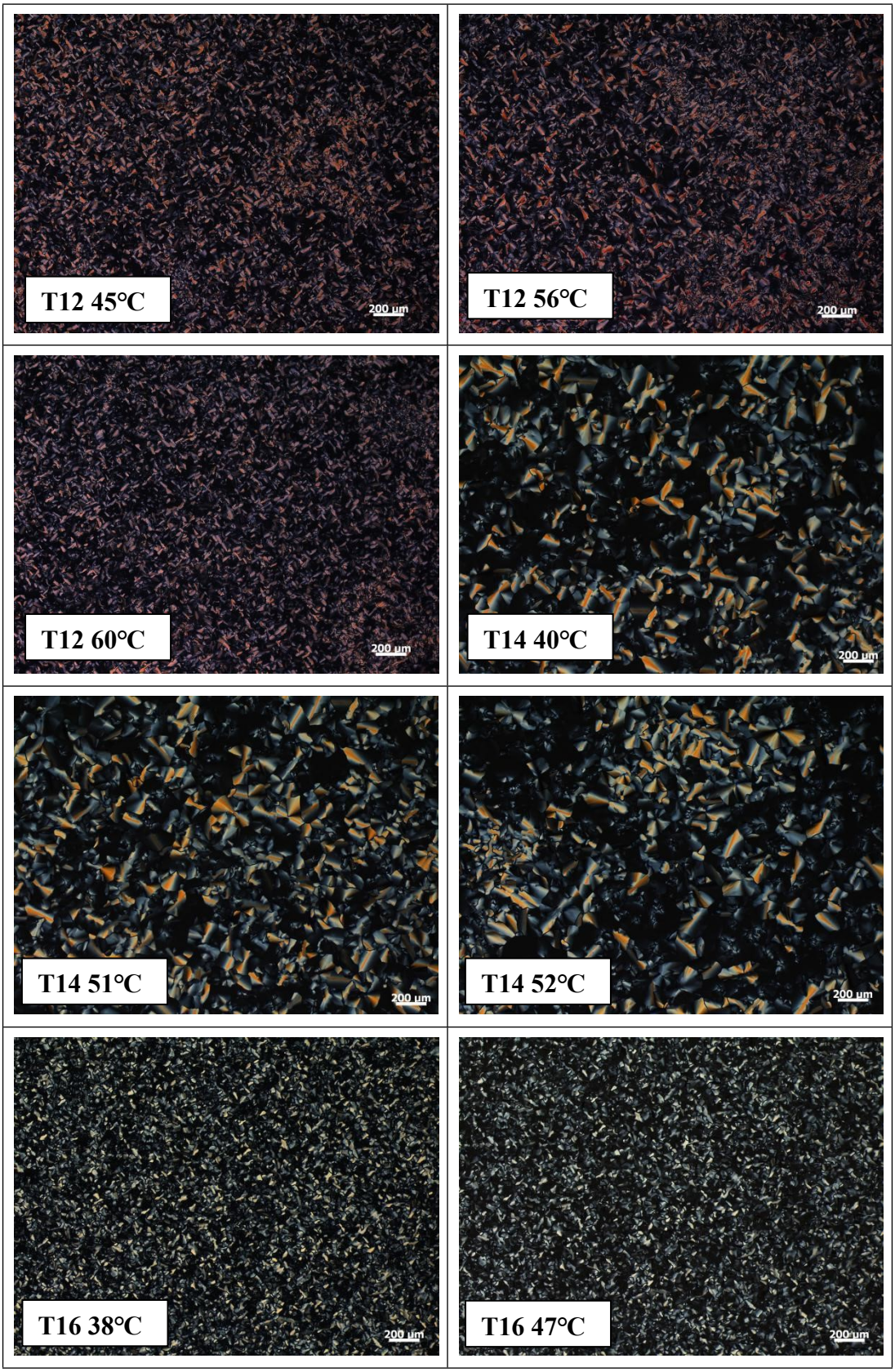
T12 45°C
200 µm
T12 56°C
200 µm
T12 60°C
200 µm
T14 40°C
200 µm
T14 51°C
200 µm
T14 52°C
200 µm
T16 38°C
200 µm
T16 47°C
200 µm

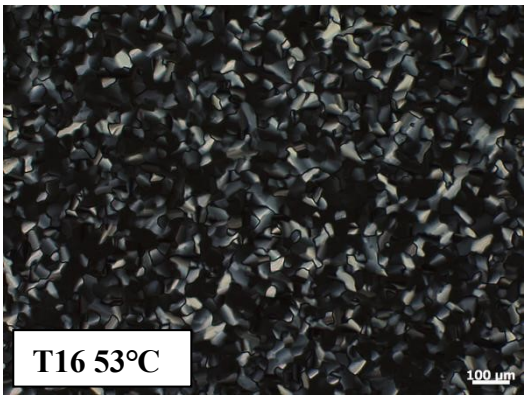
T16 53°C
100 μm

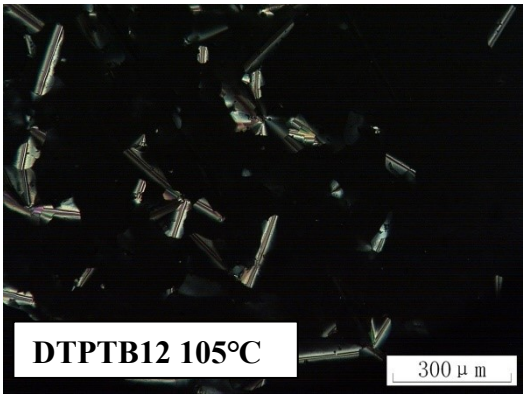
DTPTB12 105°C
300 μ m

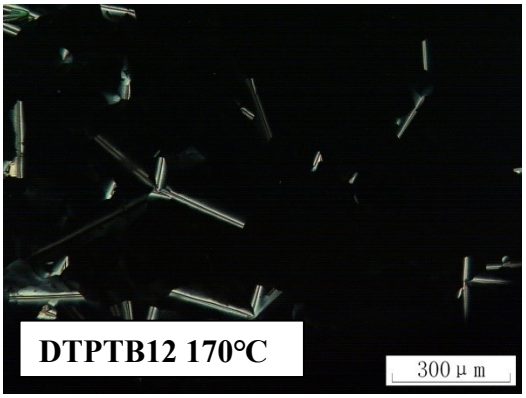
DTPTB12 170°C
300 μ m

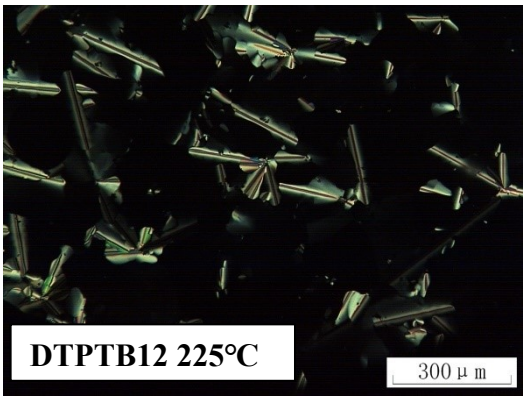
DTPTB12 225°C
300 μ m

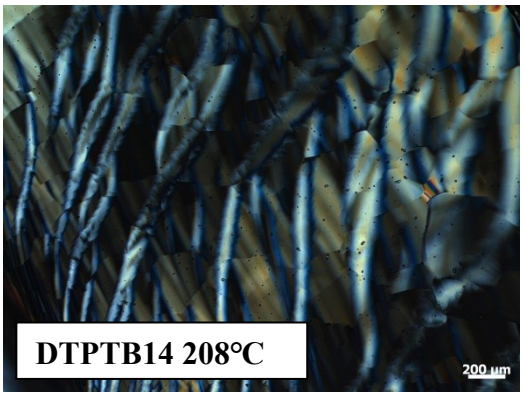
DTPTB14 208°C
200 μm

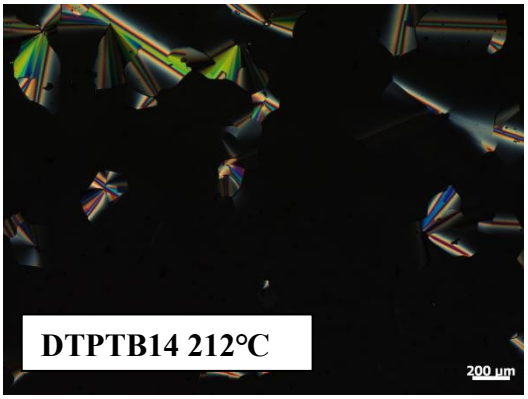
DTPTB14 212°C
200 μm

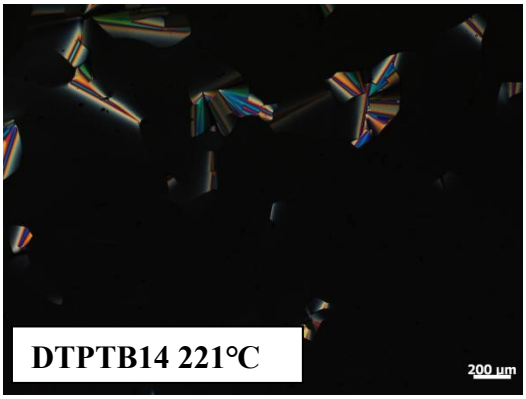
DTPTB14 221°C
200 μm

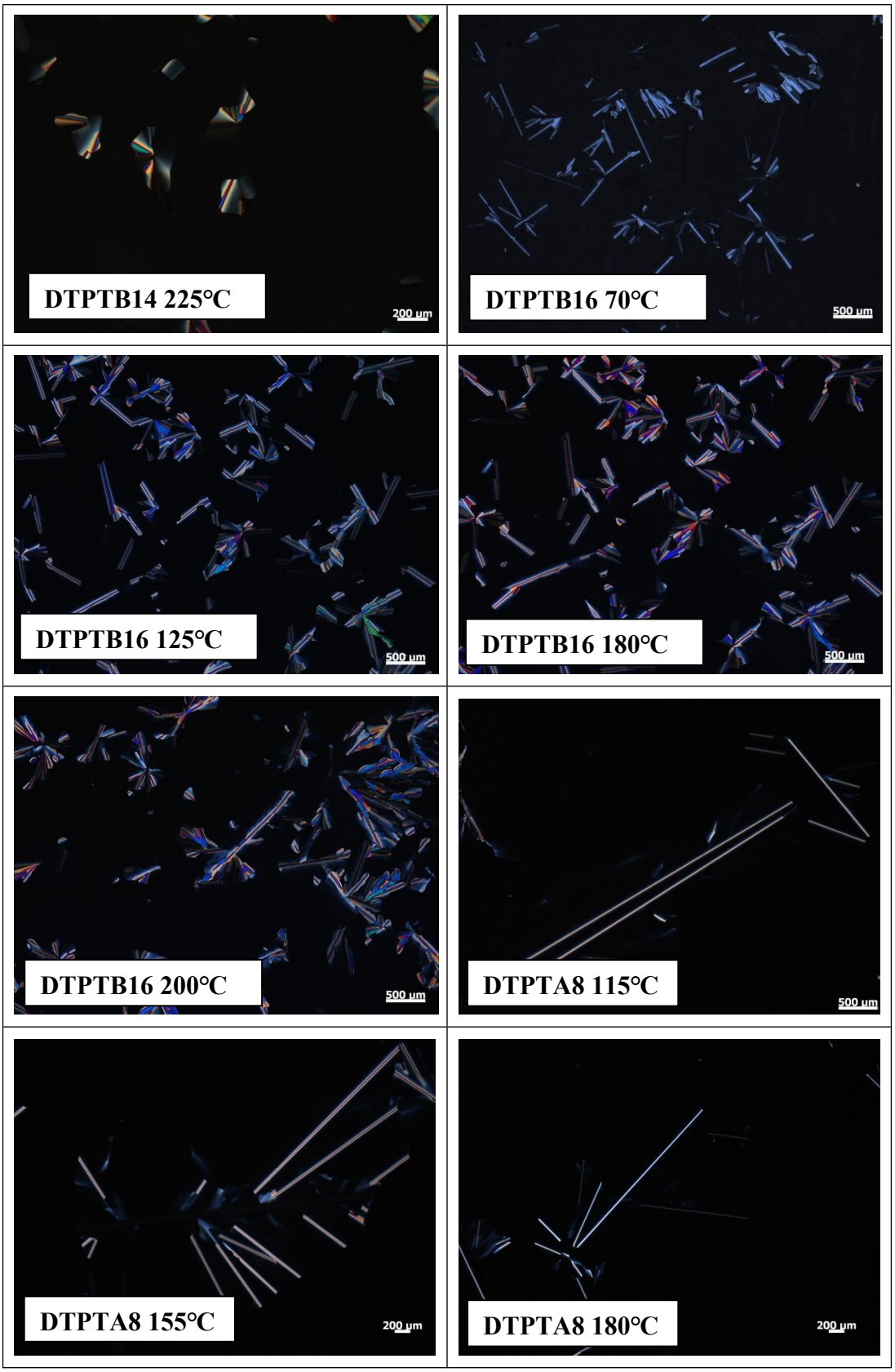
DTPTB14 225°C
200 µm
DTPTB16 70°C
500 µm
DTPTB16 125°C
500 µm
DTPTB16 180°C
500 µm
DTPTB16 200°C
500 µm
DTPTA8 115°C
500 µm
DTPTA8 155°C
200 µm
DTPTA8 180°C
200 µm

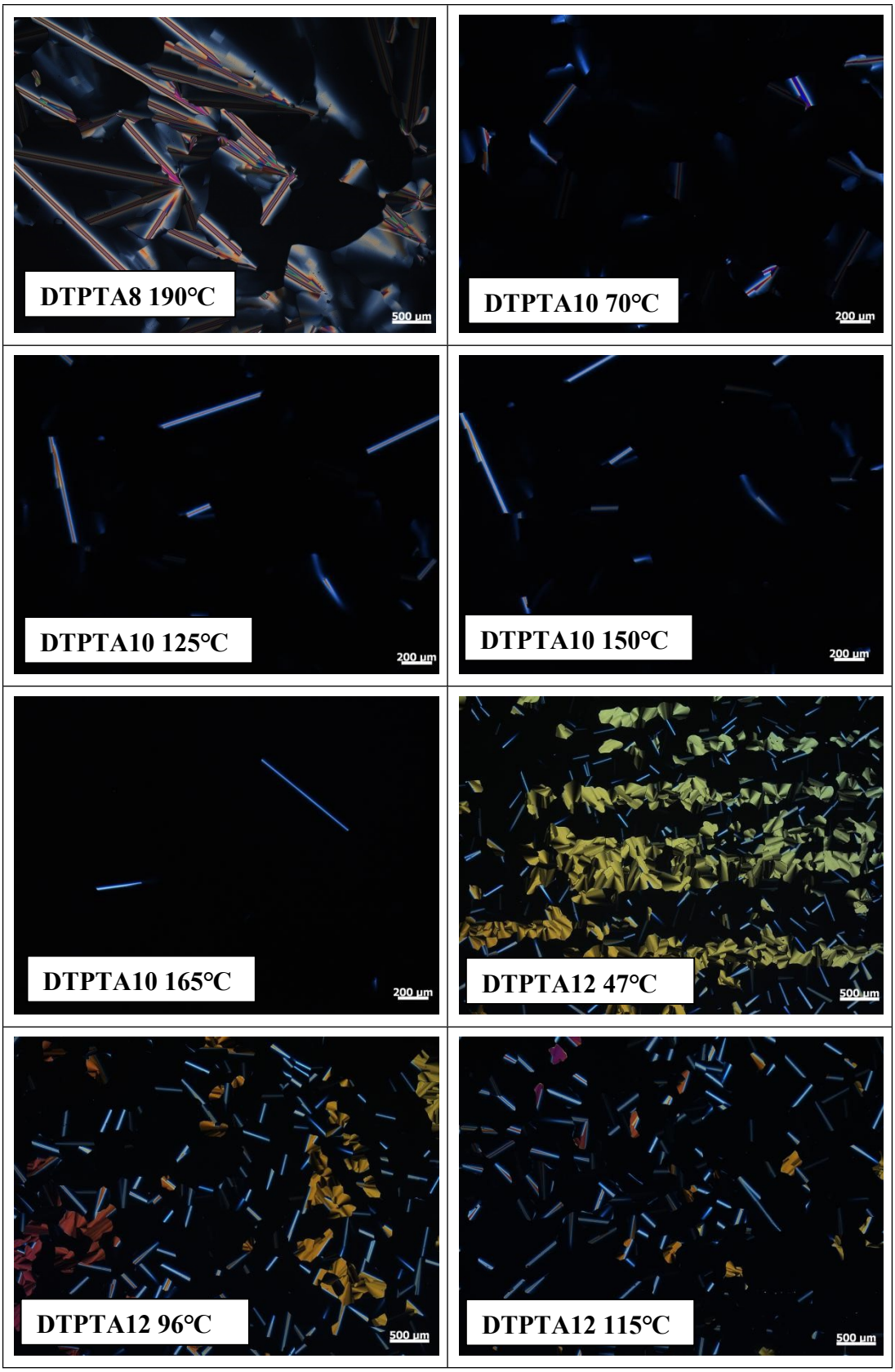
DTPTA8 190°C
500 µm
DTPTA10 70°C
200 µm
DTPTA10 125°C
200 µm
DTPTA10 150°C
200 µm
DTPTA10 165°C
200 µm
DTPTA12 47°C
500 µm
DTPTA12 96°C
500 µm
DTPTA12 115°C
500 µm

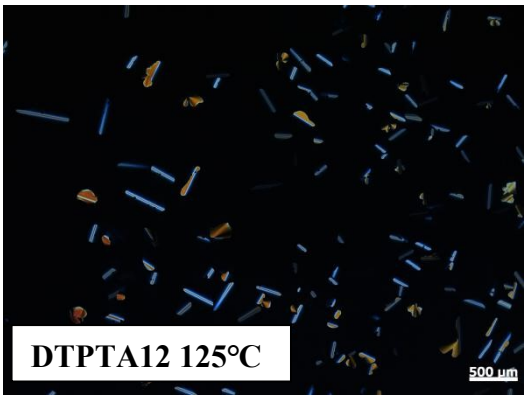

Figure S2a. POM textures of **T*n***, **DTPTA*n***, **DTPTB*n*** on cooling from the isotropic liquid.

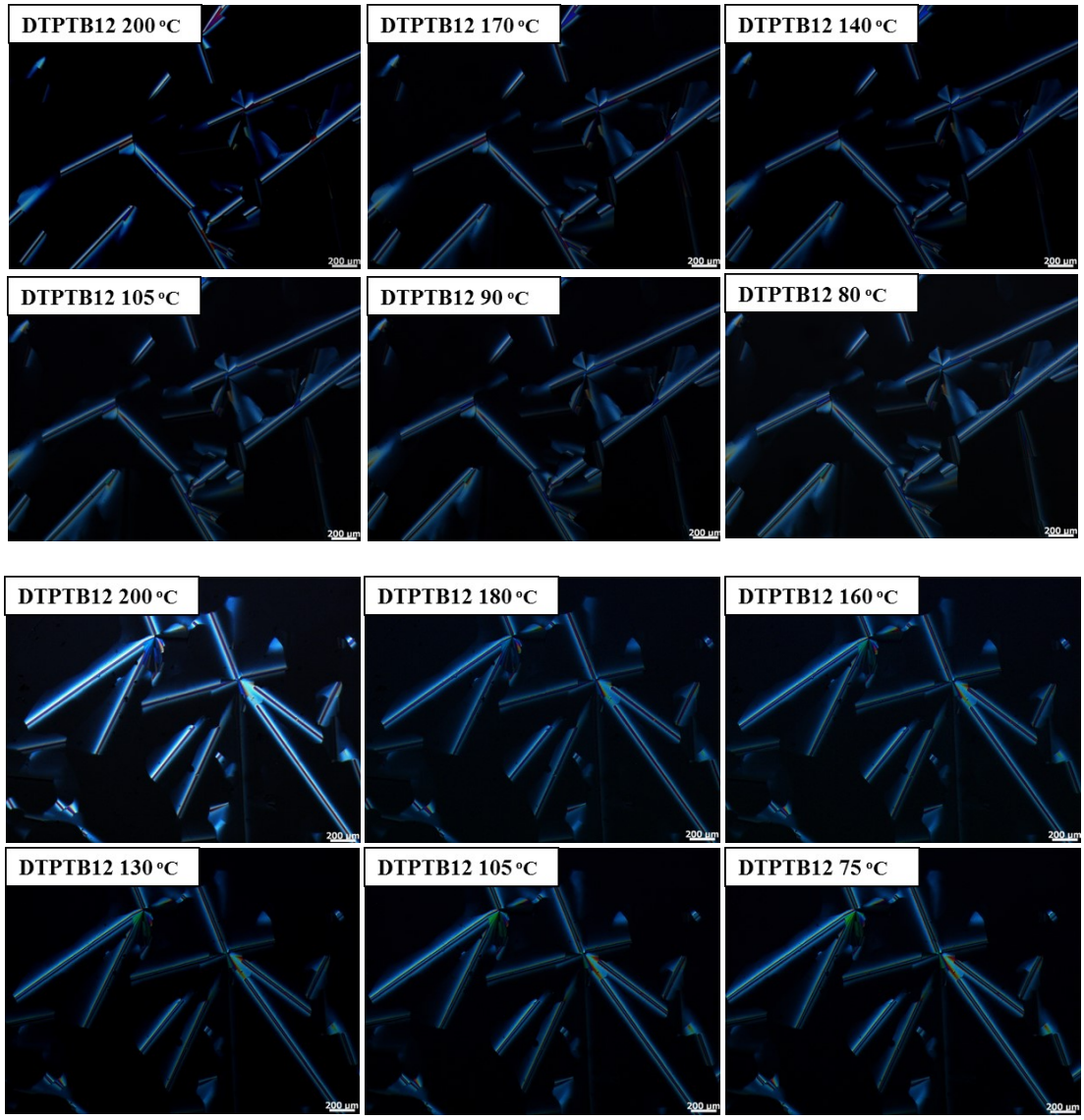

Figure S2b. POM textures of **DTPTB12** on slow cooling from the isotropic liquid (top: first cooling from isotropic liquid; Bottom: second cooling from isotropic after heating into isotropic liquid).

5. DSC

Table S3. Melting points of **D*n***

Compound	T [a] /℃
D8	52
D10	48
D12	46

[a] T, the temperature sample begins melting

Table S4. Mesophases, transition temperatures and enthalpy changes of **T*n***, **DTPTB*n***, **DTPTA*n***.

Compounds	Mesophases, transition temperature and enthalpy changes	
	2nd heating/°C (ΔH, kJ·mol^{-1})	**1st cooling/°C (ΔH, kJ·mol^{-1})**
T12	Cr 6 (22.92) Col_{hex} 65 (12.50) I	I 61 (-10.41) Col_{hex} -2 (-29.21) Cr
T14	Cr 21 (-) Cr' 38 (38.72)[b] Col_{hex} 57 (10.52) I	I 52 (-10.25) Col_{hex} 27 (-39.70)[b] Cr' 10 (-) Cr
T16	Cr 47 (-) Cr' 54 (30.72)* I	I 55 (-5.14) Col_{hex} 46 (-22.23)* Cr" 40 (-) Cr' 34 (-14.25) Cr
DTPTB12	Cr 89 (55.23) Col_{hex}' 132 (1.97) Col_{hex} 240 (1.36) I	I 236 (-2.85) Col_{hex} 110 (-1.42) Col_{hex}' 67 (-68.91) Cr
DTPTB14	Cr 82 (-) Cr' 88 (64.57)[b] Col_{hex} 232 (4.76) I	I 231 (-5.15) Col_{hex} 62 (-83.81) Cr
DTPTB16	Cr 89 (119.89) Col_{hex} 206 (4.73) I	I 202 (-3.56) Col_{hex} 70 (-118.50) Cr
DTPTA8	Cr 87 (71.27) Col_{hex} 193 (3.42) I	I 191 (-4.63) Col_{hex} 59 (-73.73) Cr
DTPTA10	Cr 86 (77.20) Col_{hex} 178 (2.06) I	I 174 (-2.13) Col_{hex} 61 (-79.19) Cr
DTPTA12	Cr 70 (89.56) Col_{hex} 167 (3.88) I	I 165 (-3.92) Col_{hex} 53 (-91.28) Cr

Cr, Cr': crystalline phases; Col_{hex}', Col_{hex}: hexagonal columnar mesophases; I: isotropic liquid. *Cumulated enthalpies.

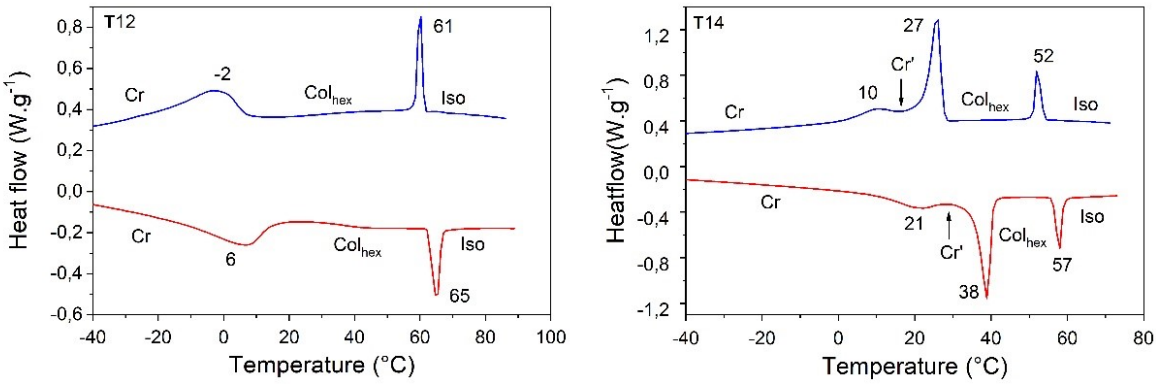

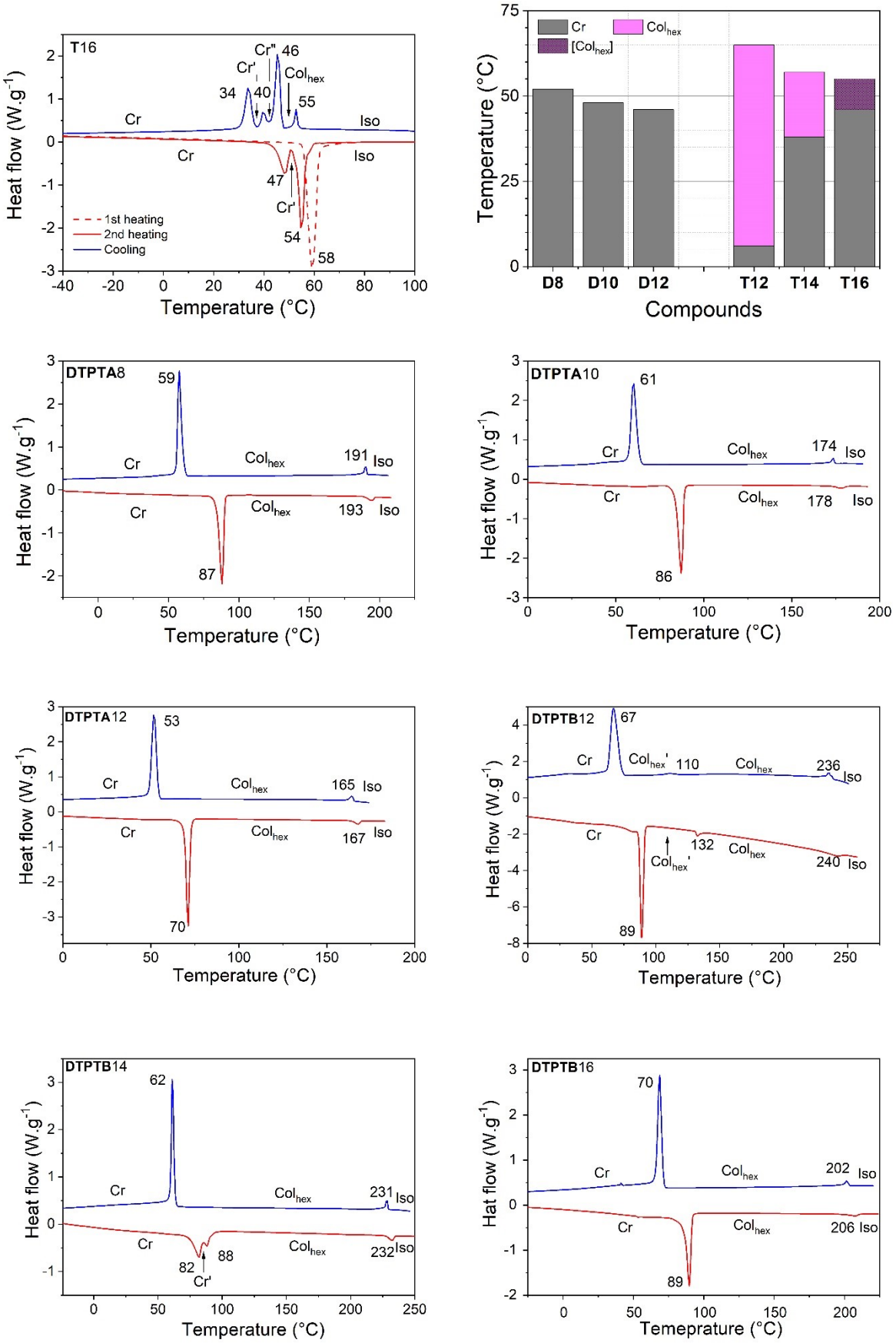

Figure S3. DSC of **T*n***, **DTPTB*n*** and **DTPTA*n***: second heating (red curves), cooling (blue curves), rate 10 °C/min (for **T16**, rate is 1°C/min). Phase diagram of **T*n*** and **D*n***.

6. S/WAXS

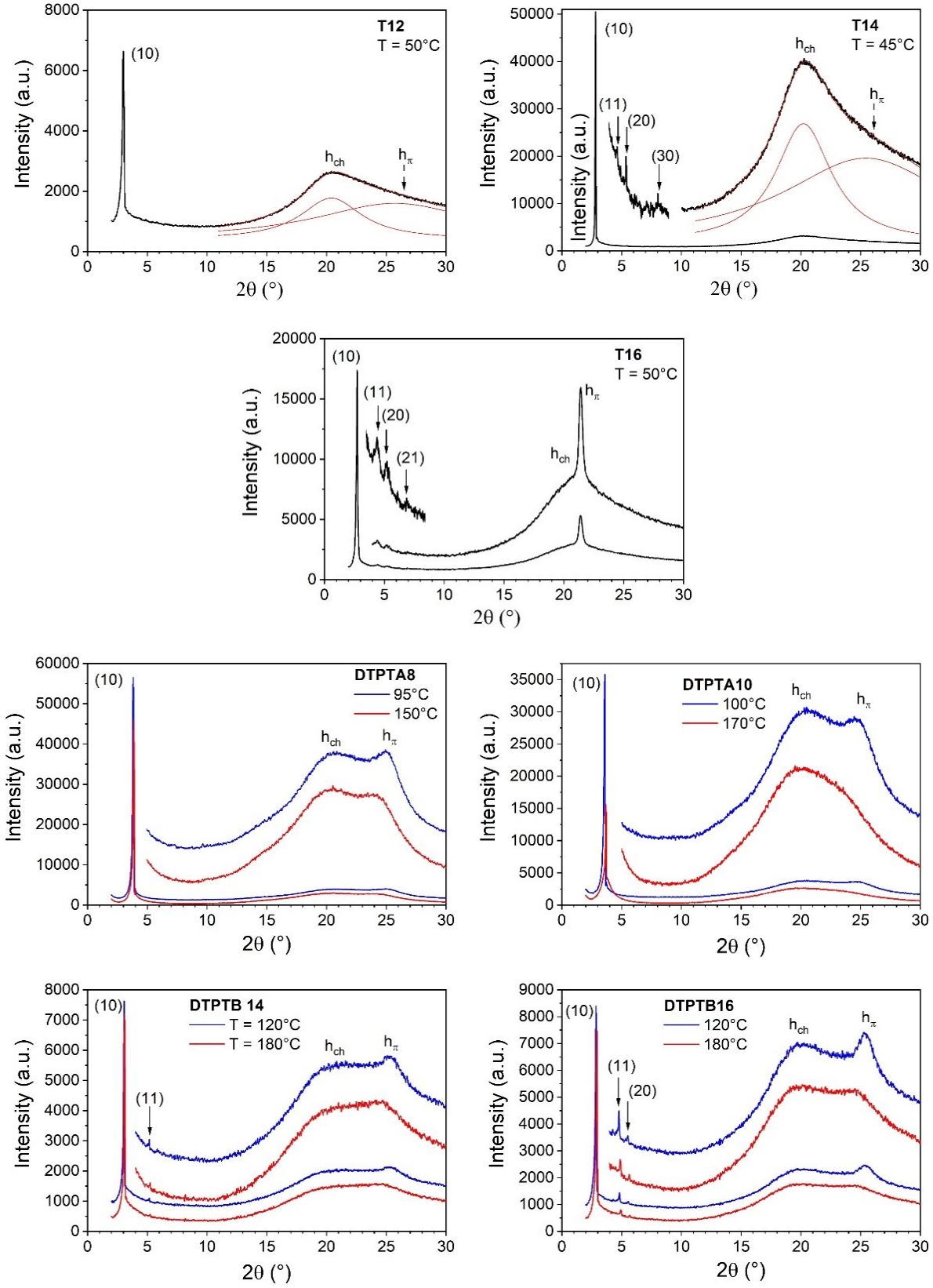

Figure S4. SAXS patterns of the mesophases of compound **T*n***, **DTPTA*n*** and **DTPTA*n*** (record on cooling).

Table S5. Indexation: $2\theta_{exp}$: measured diffraction angle (peak position); d_{exp} and d_{cal}: experimental and calculated spacings; I: relative intensity of diffracted peak in %, VS, S, W, VW (very strong, strong, weak, very weak), and sh and br (sharp and broad); *hk*: Miller indices; h_{ch}: average distance (Å) between alkyl chains; h_{π}: average distance (Å) of π-π stacking of molecules; ξ: correlation length (Å), determined by Debye-Scherrer formula; a: columnar lattice parameter, and A: lattice area $A = ½a^2\sqrt{3}$.

Compound	$2\theta_{exp}$ (°)	d_{exp} (Å)	d_{cal} (Å)	I (%)	*hk*/h_{ch}/h_{π} (ξ)	Lattice parameters (Å)
T12	2.892	30.52	30.52	100	10	Col_{hex}
(50°C)	20.36	4.36	-	VS (br)	h_{ch}	a = 35.24 Å
	25.97	3.43	-	VW (br)	h_{π} (-)	A = 1075.57 Å^2
T14	2.715	32.51	32.51	100	10	Col_{hex}
(45°C)	4.701	18.78	18.77	2.2	11	a = 37.54 Å
	5.433	16.25	16.26	6.3	20	A = 1220.40 Å^2
	8.155	10.83	10.83	2	30	
	20.24	4.38	-	VS (br)	h_{ch}	
	25.74	3.46	-	VW (br)	h_{π} (-)	
T16	2.584	34.16	34.16	100	10	Col_{rec}
(50°C)	4.477	19.72	19.72	7.2	11	a = 39.44 Å
	5169	17.08	17.08	6.3	20	A = 1347.43 Å^2
	6.840	12.91	12.91	2	21	
	20.16	4.40	-	VS (br)	h_{ch}	
	21.40	4.15	-	30.6 (sh)	h_{π} (181)	
DTPTB12	3.086	28.60	28.61	100	10	Col_{hex}
(95°C)	5.341	16.53	16.52	5	11	a = 33.04 Å
	20.93	4.24	-	VS (br)	h_{ch}	A = 945.16 Å^2
	25.65	3.47	-	VS (sh)	h_{π} (26)	
DTPTB12	3.078	28.68	28.68	100	10	Col_{hex}
(120°C)	5.332	16.56	16.56	8.5	11	a = 33.12 Å
	19.50	4.55	-	VS (br)	h_{ch}	A = 949.80 Å^2
	25.40	3.50	-	S (br)	h_{π} (11)	
DTPTB12	3.173	27.82	27.82	100	10	Col_{hex}
(210°C)	19.75	4.49	-	VS (br)	h_{ch}	a = 32.12 Å
	24.36	3.65	-	S (br)	h_{π} (-)	A = 893.68 Å^2
DTPTB14	2.990	29.52	29.55	100	10	Col_{hex}
(120°C)	5.169	17.08	17.06	14.4	11	a = 34.12 Å
	19.59	4.53	-	VS (br)	h_{ch}	A = 1008.29 Å^2
	25.40	3.50	-	S (br)	h_{π} (9)	
DTPTB14	3.022	29.21	29.20	100	10	Col_{hex}
(180°C)	5.240	16.85	16.86	13.8	11	a = 33.72 Å
	20.13	4.41	-	VS (br)	h_{ch}	A = 984.54 Å^2
	24.62	3.61	-	S (br)	h_{π} (-)	
DTPTB16	2.783	31.72	31.72	100	10	Col_{hex}
(120°C)	4.819	18.32	18.31	17.2	11	a = 36.63 Å
	5.567	15.86	15.86	13.3	20	A = 1161.81 Å^2
	19.68	4.51	-	VS (br)	h_{ch}	
	25.53	3.49	-	S (sh)	h_{π} (11)	
DTPTB16	2.846	31.02	31.02	100	10	Col_{hex}
(180°C)	4.938	17.88	17.91	16.5	11	a = 35.82 Å
	5.68	15.54	15.51	15.51	20	A = 1111.10 Å^2
	19.89	4.46	-	VS (br)	h_{ch}	
	24.64	3.61	-	S (br)	h_{π} (-)	
DTPTA8	3.737	23.62	23.62	100	10	Col_{hex}
(95°C)	20.65	4.30	-	VS (br)	h_{ch}	a = 27.27 Å
	25.11	3.55	-	VS (br)	h_{π} (20)	A = 644.21 Å^2
DTPTA8	3.794	23.27	23.27	100	10	Col_{hex}
(150°C)	19.99	4.44	-	VS (br)	h_{ch}	a = 26.87 Å
	24.49	3.63	-	S (br)	h_{π} (14)	A = 625.26 Å^2
DTPTA10	3.469	25.45	25.45	100	10	Col_{hex}
(100°C)	20.14	4.40	-	VS (br)	h_{ch}	a = 29.39 Å
	24.89	3.57	-	S (br)	h_{π} (14)	A = 747.90 Å^2
DTPTA10	3.574	24.70	24.70	100	10	Col_{hex}
(170°C)	20.15	4.40	-	VS (br)	h_{ch}	a = 28.52 Å
	23.51	3.78	-	W (br)	h_{π} (-)	A = 704.47 Å^2
DTPTA12	3.129	28.21	28.21	100	10	Col_{hex}
(80°C)	20.36	4.36	-	VS (br)	h_{ch}	a = 32.57 Å
	25.18	3.53	-	S (br)	h_{π} (-)	A = 918.91 Å^2
DTPTA12	3.271	26.99	26.99	100	10	Col_{hex}
(150°C)	20.36	4.36	-	VS (br)	h_{ch}	a = 31.16 Å
	24.23	3.67	-	W (br)	h_{π} (-)	A = 841.15 Å^2

7. SEM Images

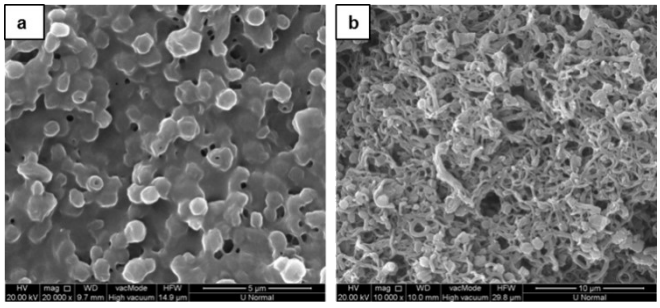

Figure S5. SEM images of xerogels from CH_2Cl_2/EtOH ("good/poor" solvent). (a) **DTPTB14**; (b) **DTPTA12**.

8. TOF

Table S6. TOF photoconductivity (hole) of **DTPTB12** recorded on cooling (cell thickness 17.7 μm).

T (°C)	*E* (V cm^{-1})	τ_{hole} (s)	μ_{hole} (cm^2 V^{-1} s^{-1})	μaverage hole (cm^2 V^{-1} s^{-1})
220	2×10^4	1.66×10^{-5}	2.14×10^{-3}	2.14×10^{-3}
	3×10^4	2.06×10^{-5}	2.12×10^{-3}	
	4×10^4	2.78×10^{-5}	2.15×10^{-3}	
	5×10^4	4.14×10^{-5}	2.13×10^{-3}	
210	2×10^4	4.15×10^{-5}	2.13×10^{-3}	2.13×10^{-3}
	3×10^4	2.78×10^{-5}	2.12×10^{-3}	
	4×10^4	2.08×10^{-5}	2.13×10^{-3}	
	5×10^4	1.66×10^{-5}	2.13×10^{-3}	
200	2×10^4	4.11×10^{-5}	2.15×10^{-3}	2.14×10^{-3}
	3×10^4	2.80×10^{-5}	2.11×10^{-3}	
	4×10^4	2.07×10^{-5}	2.14×10^{-3}	
	5×10^4	1.65×10^{-5}	2.14×10^{-3}	
190	2×10^4	4.18×10^{-5}	2.12×10^{-3}	2.12×10^{-3}
	3×10^4	2.76×10^{-5}	2.14×10^{-3}	
	4×10^4	2.10×10^{-5}	2.11×10^{-3}	
	5×10^4	1.67×10^{-5}	2.12×10^{-3}	
180	2×10^4	4.13×10^{-5}	2.14×10^{-3}	2.14×10^{-3}
	3×10^4	2.77×10^{-5}	2.13×10^{-3}	
	4×10^4	2.06×10^{-5}	2.14×10^{-3}	
	5×10^4	1.65×10^{-5}	2.15×10^{-3}	
170	2×10^4	4.17×10^{-5}	2.14×10^{-3}	2.15×10^{-3}
	3×10^4	2.74×10^{-5}	2.16×10^{-3}	
	4×10^4	2.05×10^{-5}	2.15×10^{-3}	
	5×10^4	1.60×10^{-5}	2.12×10^{-3}	
160	2×10^4	4.17×10^{-5}	2.12×10^{-3}	2.14×10^{-3}
	3×10^4	2.75×10^{-5}	2.14×10^{-3}	
	4×10^4	2.06×10^{-5}	2.14×10^{-3}	

	5×10^4	1.65×10^{-5}	2.14×10^{-3}	
150	2×10^4	4.31×10^{-5}	2.06×10^{-3}	2.06×10^{-3}
	3×10^4	2.89×10^{-5}	2.04×10^{-3}	
	4×10^4	2.14×10^{-5}	2.07×10^{-3}	
	5×10^4	1.70×10^{-5}	2.09×10^{-3}	
140	2×10^4	4.32×10^{-5}	2.05×10^{-3}	2.07×10^{-3}
	3×10^4	2.84×10^{-5}	2.08×10^{-3}	
	4×10^4	2.13×10^{-5}	2.08×10^{-3}	
	5×10^4	1.73×10^{-5}	2.05×10^{-3}	
130	2×10^4	4.36×10^{-5}	2.03×10^{-3}	1.99×10^{-3}
	3×10^4	2.96×10^{-5}	1.99×10^{-3}	
	4×10^4	2.22×10^{-5}	2.00×10^{-3}	
	5×10^4	1.78×10^{-5}	1.99×10^{-3}	
120	2×10^4	4.62×10^{-5}	1.92×10^{-3}	1.93×10^{-3}
	3×10^4	3.02×10^{-5}	1.95×10^{-3}	
	4×10^4	2.32×10^{-5}	1.91×10^{-3}	
	5×10^4	1.84×10^{-5}	1.93×10^{-3}	
110	3×10^4	2.00×10^{-5}	2.95×10^{-3}	2.96×10^{-3}
	4×10^4	1.48×10^{-5}	2.98×10^{-3}	
	5×10^4	1.20×10^{-5}	2.95×10^{-3}	
100	3×10^4	2.00×10^{-5}	2.95×10^{-3}	2.95×10^{-5}
	4×10^4	1.50×10^{-5}	2.95×10^{-3}	
	5×10^4	1.20×10^{-5}	2.95×10^{-3}	
90	4×10^4	1.51×10^{-5}	2.93×10^{-3}	2.94×10^{-3}
	5×10^4	1.20×10^{-5}	2.96×10^{-3}	
80	3×10^4	2.03×10^{-5}	2.90×10^{-3}	2.91×10^{-3}
	4×10^4	1.52×10^{-5}	2.91×10^{-3}	

Table S7. TOF photoconductivity (hole) of **DTPTB12** recorded on heating (cell thickness 17.7 μm).

T (°C)	***E*** (V cm^{-1})	τ_{hole} (s)	μ_{hole} (cm^2 V^{-1} s^{-1})	μaverage hole (cm^2 V^{-1} s^{-1})
110	4×10^4	1.51×10^{-5}	2.93×10^{-3}	2.93×10^{-3}
	5×10^4	1.21×10^{-5}	2.93×10^{-3}	
120	4×10^4	1.52×10^{-5}	2.91×10^{-3}	2.93×10^{-3}
	5×10^4	1.20×10^{-5}	2.95×10^{-3}	
130	3×10^4	2.00×10^{-5}	2.95×10^{-3}	2.94×10^{-3}
	4×10^4	1.51×10^{-5}	2.93×10^{-3}	
	5×10^4	1.20×10^{-5}	2.94×10^{-3}	
140	2×10^4	3.14×10^{-5}	2.59×10^{-3}	2.62×10^{-3}
	3×10^4	2.25×10^{-5}	2.62×10^{-3}	
	4×10^4	1.69×10^{-5}	2.62×10^{-3}	
	5×10^4	1.34×10^{-5}	2.64×10^{-3}	
150	2×10^4	3.77×10^{-5}	2.35×10^{-3}	2.35×10^{-3}

	3×10^4	2.50×10^{-5}	2.36×10^{-3}	
	4×10^4	1.88×10^{-5}	2.35×10^{-3}	
	5×10^4	1.50×10^{-5}	2.36×10^{-3}	
160	2×10^4	3.92×10^{-5}	2.26×10^{-3}	2.27×10^{-3}
	3×10^4	2.61×10^{-5}	2.26×10^{-3}	
	4×10^4	1.93×10^{-5}	2.29×10^{-3}	
	5×10^4	1.56×10^{-5}	2.27×10^{-3}	
170	2×10^4	3.96×10^{-5}	2.24×10^{-3}	2.23×10^{-3}
	3×10^4	2.65×10^{-5}	2.22×10^{-3}	
	4×10^4	1.98×10^{-5}	2.23×10^{-3}	
	5×10^4	1.60×10^{-5}	2.22×10^{-3}	
180	2×10^4	4.00×10^{-5}	2.21×10^{-3}	2.21×10^{-3}
	3×10^4	2.68×10^{-5}	2.20×10^{-3}	
	4×10^4	1.99×10^{-5}	2.23×10^{-3}	
	5×10^4	1.60×10^{-5}	2.21×10^{-3}	
190	2×10^4	4.08×10^{-5}	2.17×10^{-3}	2.18×10^{-3}
	3×10^4	2.68×10^{-5}	2.20×10^{-3}	
	4×10^4	2.04×10^{-5}	2.17×10^{-3}	
200	3×10^4	3.07×10^{-5}	2.13×10^{-3}	2.12×10^{-3}
	4×10^4	2.16×10^{-5}	2.14×10^{-3}	
	5×10^4	1.61×10^{-5}	2.11×10^{-3}	
210	2×10^4	4.12×10^{-5}	2.15×10^{-3}	2.13×10^{-3}
	3×10^4	2.84×10^{-5}	2.08×10^{-3}	
	4×10^4	2.08×10^{-5}	2.13×10^{-3}	
	5×10^4	1.64×10^{-5}	2.16×10^{-3}	
220	2×10^4	4.06×10^{-5}	2.18×10^{-3}	2.18×10^{-3}
	3×10^4	2.70×10^{-5}	2.19×10^{-3}	
	4×10^4	2.04×10^{-5}	2.17×10^{-3}	
	5×10^4	1.62×10^{-5}	2.19×10^{-3}	

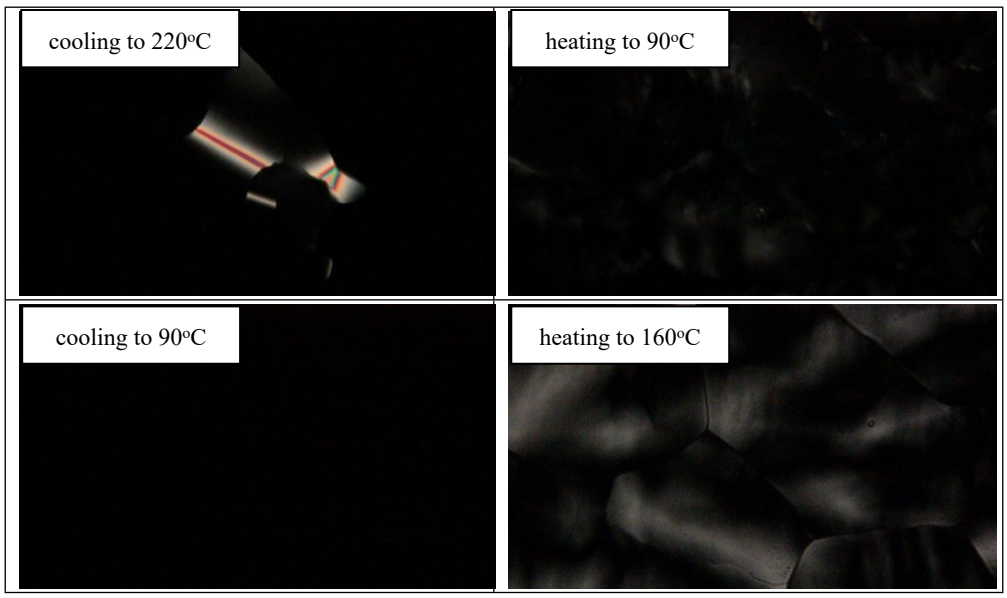

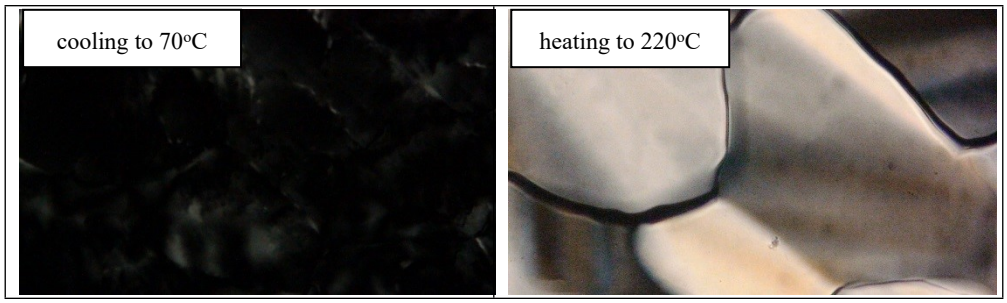

Figure S6. POM images of sample **DTPTB12** in ITO LC cell taken both on heating and cooling run during the TOF measurement.

Table S8. TOF photoconductivity (hole) of **DTPTA12** recorded on cooling (cell thickness 19.7 μm).

T (°C)	***E*** (V cm^{-1})	τ_{hole} (s)	μ_{hole} (cm^2 V^{-1} s^{-1})	μaverage hole (cm^2 V^{-1} s^{-1})
160	3×10^4	1.09×10^{-4}	6.02×10^{-4}	6.36×10^{-4}
	4×10^4	7.72×10^{-5}	6.38×10^{-4}	
	5×10^4	5.90×10^{-5}	6.68×10^{-4}	
150	3×10^4	1.08×10^{-4}	6.08×10^{-4}	6.36×10^{-4}
	4×10^4	7.74×10^{-5}	6.36×10^{-4}	
	5×10^4	5.98×10^{-5}	6.59×10^{-4}	
140	3×10^4	1.11×10^{-4}	5.90×10^{-4}	5.96×10^{-4}
	4×10^4	8.48×10^{-5}	5.81×10^{-4}	
	5×10^4	6.39×10^{-5}	6.16×10^{-4}	
130	3×10^4	1.22×10^{-4}	5.39×10^{-4}	5.75×10^{-4}
	4×10^4	8.39×10^{-5}	5.87×10^{-4}	
	5×10^4	6.56×10^{-5}	6.00×10^{-4}	
120	3×10^4	1.28×10^{-4}	5.14×10^{-4}	5.33×10^{-4}
	4×10^4	9.50×10^{-5}	5.18×10^{-4}	
	5×10^4	6.94×10^{-5}	5.68×10^{-4}	
110	3×10^4	7.89×10^{-5}	5.00×10^{-4}	4.71×10^{-4}
	4×10^4	1.06×10^{-4}	4.67×10^{-4}	
	5×10^4	1.47×10^{-4}	4.47×10^{-4}	
100	3×10^4	1.69×10^{-4}	3.89×10^{-4}	4.06×10^{-4}
	4×10^4	1.21×10^{-4}	4.07×10^{-4}	
	5×10^4	9.37×10^{-5}	4.21×10^{-4}	
90	3×10^4	1.94×10^{-4}	3.39×10^{-4}	3.54×10^{-4}
	4×10^4	1.38×10^{-4}	3.56×10^{-4}	
	5×10^4	1.07×10^{-4}	3.68×10^{-4}	
80	3×10^4	2.28×10^{-4}	2.88×10^{-4}	2.98×10^{-4}
	4×10^4	1.64×10^{-4}	3.00×10^{-4}	
	5×10^4	1.29×10^{-4}	3.07×10^{-4}	
70	3×10^4	2.62×10^{-4}	2.50×10^{-4}	2.66×10^{-4}
	4×10^4	2.05×10^{-4}	2.40×10^{-4}	
	5×10^4	1.48×10^{-4}	2.67×10^{-4}	

Table S9. TOF photoconductivity (hole) of **DTPTA12** recorded on heating (cell thickness 19.7 μm).

T (°C)	*E* (V cm^{-1})	τ_{hole} (s)	μ_{hole} (cm^2 V^{-1} s^{-1})	μaverage hole (cm^2 V^{-1} s^{-1})
70	3×10^4	2.62×10^{-3}	2.50×10^{-5}	2.81×10^{-5}
	4×10^4	1.68×10^{-3}	2.93×10^{-5}	
	5×10^4	1.31×10^{-3}	3.00×10^{-5}	
80	3×10^4	7.02×10^{-4}	9.35×10^{-5}	9.92×10^{-5}
	4×10^4	4.67×10^{-4}	1.05×10^{-4}	
	5×10^4	3.98×10^{-4}	9.90×10^{-5}	
90	3×10^4	1.98×10^{-4}	3.32×10^{-4}	3.35×10^{-4}
	4×10^4	1.45×10^{-4}	3.40×10^{-4}	
	5×10^4	1.19×10^{-4}	3.32×10^{-4}	
100	3×10^4	1.79×10^{-4}	3.63×10^{-4}	3.66×10^{-4}
	4×10^4	1.39×10^{-4}	3.53×10^{-4}	
	5×10^4	1.04×10^{-4}	3.77×10^{-4}	
110	3×10^4	1.51×10^{-4}	4.35×10^{-4}	4.12×10^{-4}
	4×10^4	1.12×10^{-4}	4.05×10^{-4}	
	5×10^4	9.94×10^{-5}	3.96×10^{-4}	
120	3×10^4	1.54×10^{-4}	4.28×10^{-4}	4.40×10^{-4}
	4×10^4	1.07×10^{-4}	4.60×10^{-4}	
	5×10^4	9.11×10^{-5}	4.32×10^{-4}	
130	3×10^4	7.56×10^{-5}	5.21×10^{-4}	5.34×10^{-4}
	4×10^4	9.12×10^{-5}	5.40×10^{-4}	
	5×10^4	1.21×10^{-4}	5.41×10^{-4}	
140	3×10^4	1.33×10^{-4}	4.95×10^{-4}	5.05×10^{-4}
	4×10^4	9.86×10^{-5}	5.00×10^{-4}	
	5×10^4	7.58×10^{-5}	5.20×10^{-4}	
150	3×10^4	6.62×10^{-5}	5.95×10^{-4}	5.95×10^{-4}
	4×10^4	8.14×10^{-5}	6.05×10^{-4}	
	5×10^4	1.14×10^{-4}	5.85×10^{-4}	
160	3×10^4	1.15×10^{-4}	5.71×10^{-4}	5.97×10^{-4}
	4×10^4	8.45×10^{-5}	5.83×10^{-4}	
	5×10^4	6.20×10^{-5}	6.36×10^{-4}	

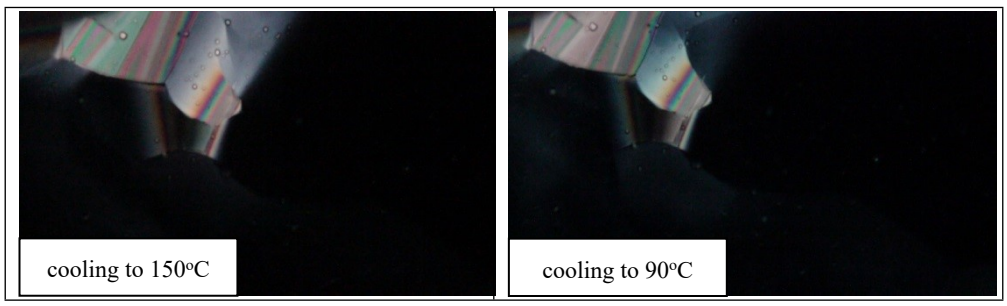

Figure S7. POM images of sample **DTPTA12** in ITO LC cell taken on cooling during the TOF measurement.

9. Relationship of TOF charge carrier mobility and Mesophase/Molecular structures

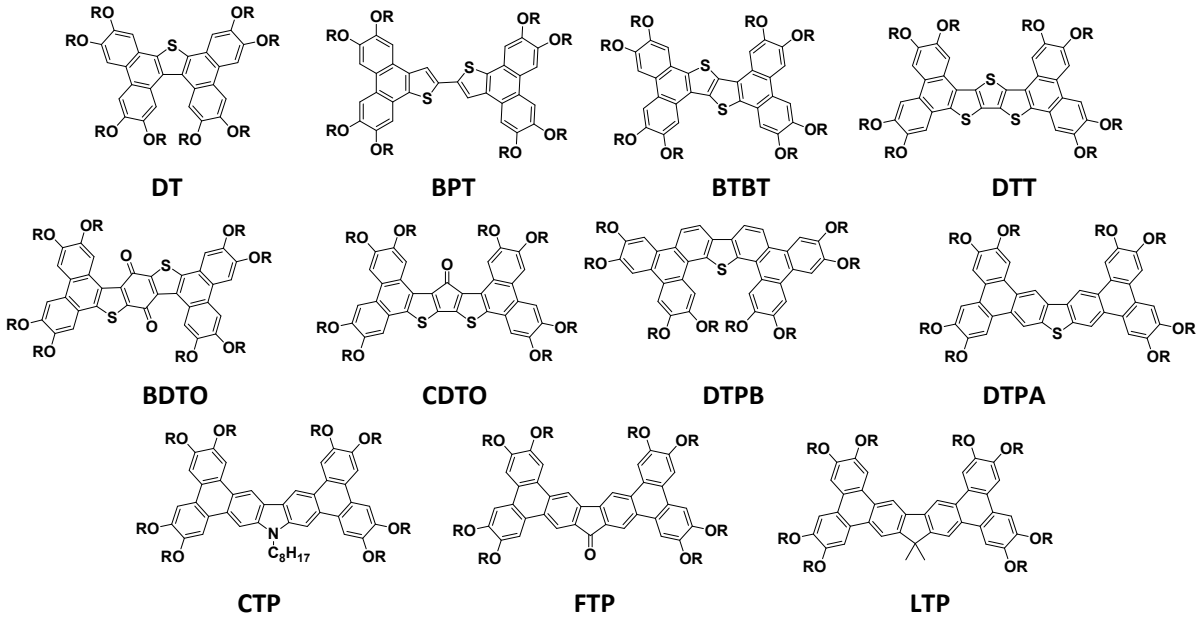

Figure S8. Butterfly-shape columnar mesogens.

Table S10. Charge carrier mobility (μ, TOF) of butterfly-shape molecules

Compound	R	Phase	Temperature (°C)	Mobility x 10^{-3} cm^2/Vs	Ref
DT	OC_5H_{11}	Col_{hex} Cr	120 30	1.15 (μ+) 10 (μ+)	6
BPT	OC_6H_{13}	Col_{rec} Cr	210 170	4.39 (μ+) 30 (μ+)	6
BTBT	$OC_{10}H_{21}$	Col_{hex}	230	1.7 (μ+)/2.0 (μ-)	7
DTT	$OC_{14}H_{29}$	Col_{hex}	220-70	1.5 (μ+)	8
DTT	$OC_{16}H_{33}$	Col_{hex}	200-160 150-80	1.2 (μ+) 0.4 (μ+)	8
BDTO	$OC_{14}H_{29}$	Col_{hex}	180/120	4.5 (μ+)/6.6 (μ-)	9

[6] K. C. Zhao, J. Q. Du, H. F. Wang, K. Q. Zhao, P. Hu, B. Q. Wang, H. Monobe, B. Heinrich and B. Donnio, *Chem. Asian J.*, 2019, **14**, 462-470.
[7] C. X. Liu, H. Wang, J. Q. Du, K. Q. Zhao, P. Hu, B. Q. Wang, H. Monobe, B. Heinrich and B. Donnio, *J. Mater. Chem. C*, 2018, **6**, 4471-4778.
[8] T. Ma, H. F. Wang, K. Q. Zhao, B. Q. Wang, P. Hu, H. Monobe, B. Heinrich and B. Donnio, *ChemPlusChem.*, 2019, **84**, 1439-1488.

CDTO	$OC_{14}H_{29}$	Col_{hex}	80-220	1.5-2.1(μ+)	9
DTPTA	$OC_{12}H_{25}$	Col_{hex}	160	0.6 (μ+)	This work
DTPTB	$OC_{12}H_{25}$	Col_{hex}	100	3.0 (μ+)	This work
CTP	$OC_{12}H_{25}$	Col_{hex}	190	1.3 (μ+)	10
FTP		Col_{hex}	110-220	7.3 (μ+)	10
LTP	$OC_{10}H_{21}$	Col_{hex} Col_{rec}	180 110	5.6 (μ+) 25.7 (μ+)	10
LTP	$OC_{12}H_{25}$	Col_{hex} Col_{rec}	160 90	0.4 (μ+) 8.0 (μ+)	10

10. DFT

Table S11. Molecular structures of compounds **T**, **D**, **DTPTB** and **DTPTA**.

Compd.	molecular structure
T	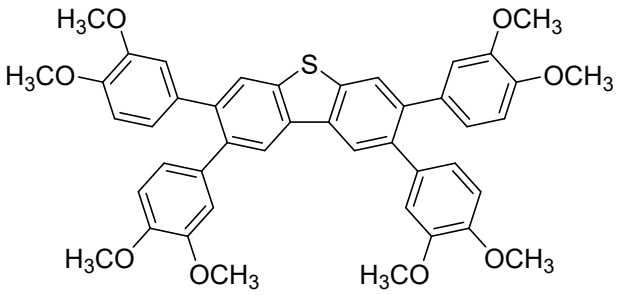
D	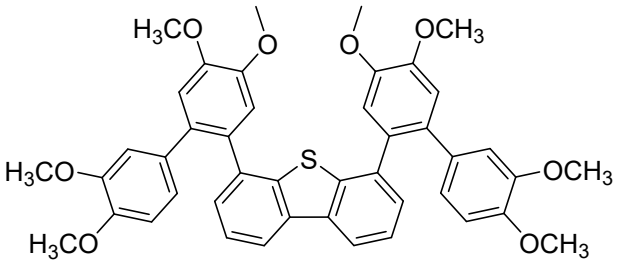
DTPTB	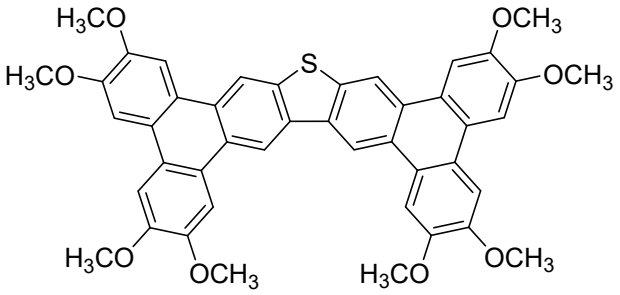

[9] T. Ma, Y. J. Zhong, H. F. Wang, K. Q. Zhao, B. Q. Wang, P. Hu, H. Monobe and B. Donnio, *Chem. Asian. J.*, 2021, **16**, 1106-1117.

[10] J. F. Hang, H. Lin, K. Q. Zhao, P. Hu, B. Q. Wang, H. Monobe, C. H. Zhu and B. Donnio. *Eur. J. Org. Chem.*, 2021, **2021**, 1989-2002.

DTPTA	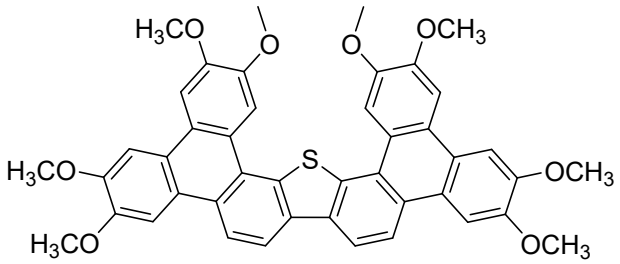

Table S12. List of selected molecular orbital energies for **T**, **D**, **DTPTB**, **DTPTA** and their HOMO-LUMO energy gaps (△E).

	HOMO-2 (eV)	HOMO-1 (eV)	HOMO (eV)	△E (eV)	LUMO (eV)	LUMO+1 (eV)	LUMO+2 (eV)
T	-5.57	-5.23	-5.04	3.99	-1.05	-0.42	-0.30
D	-5.73	-5.42	-5.38	4.41	-0.97	-0.62	-0.52
DTPTB	-5.31	-5.07	-4.95	3.65	-1.30	-0.83	-0.70
DTPTA	-5.43	-5.20	-5.09	3.87	-1.22	-0.81	-0.81

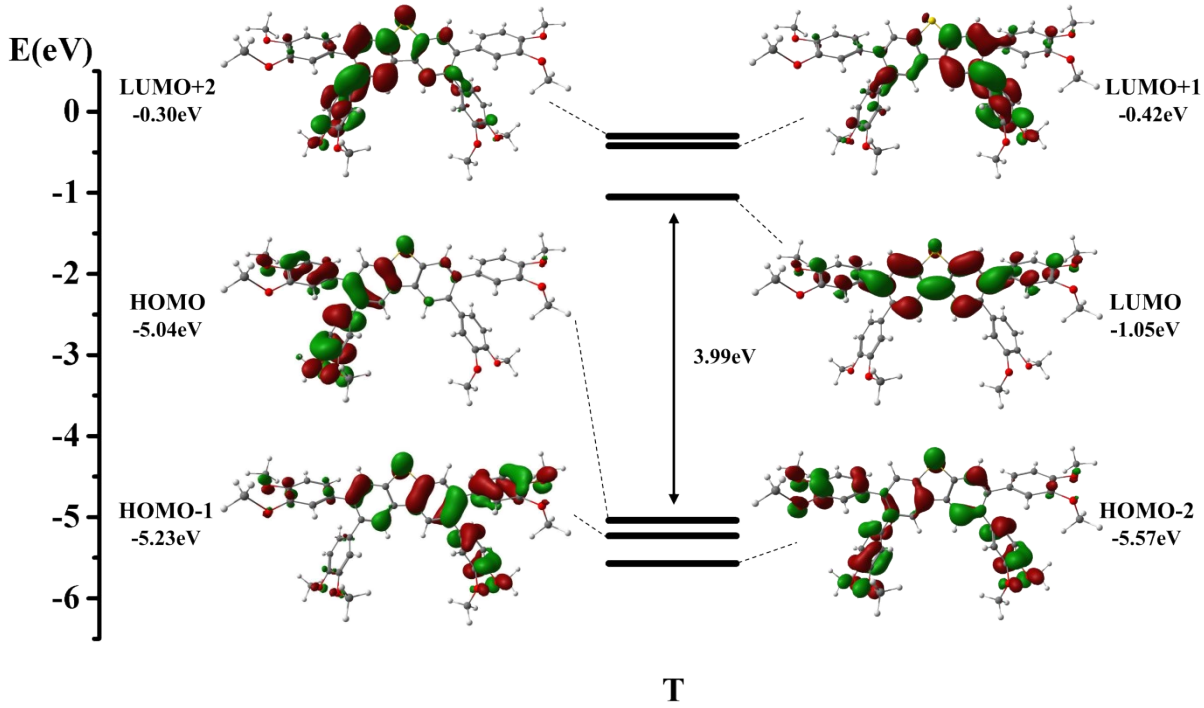

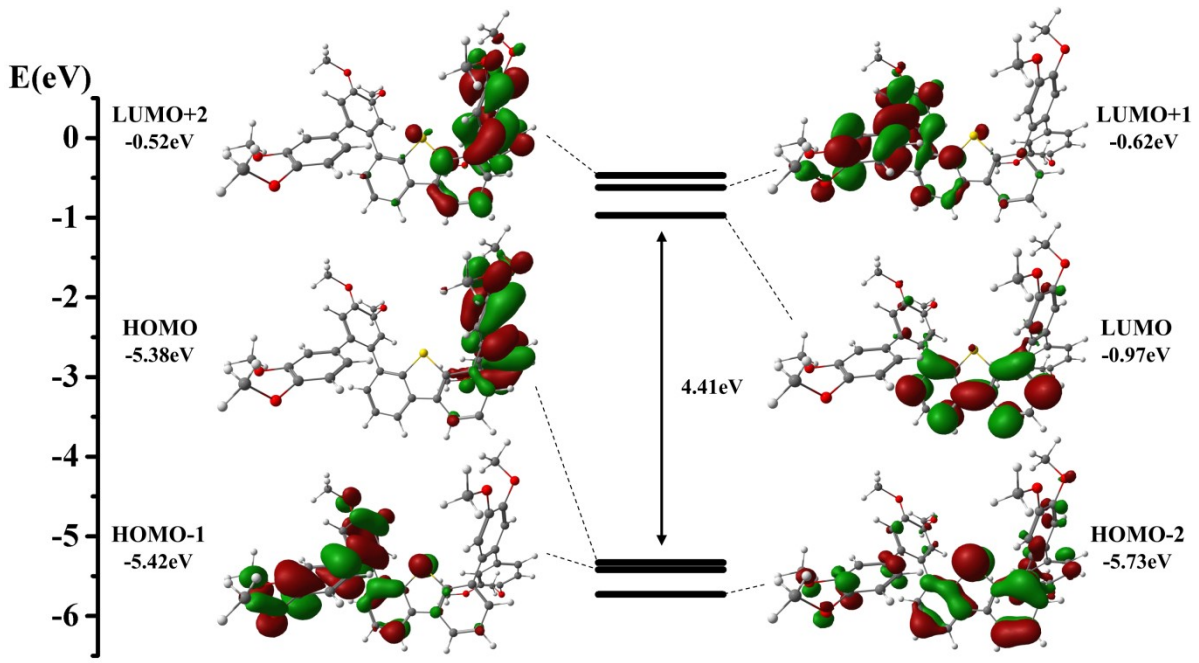
E(eV)
0
-1
-2
-3
-4
-5
-6
LUMO+2
-0.52eV
HOMO
-5.38eV
HOMO-1
-5.42eV
4.41eV
LUMO+1
-0.62eV
LUMO
-0.97eV
HOMO-2
-5.73eV

D

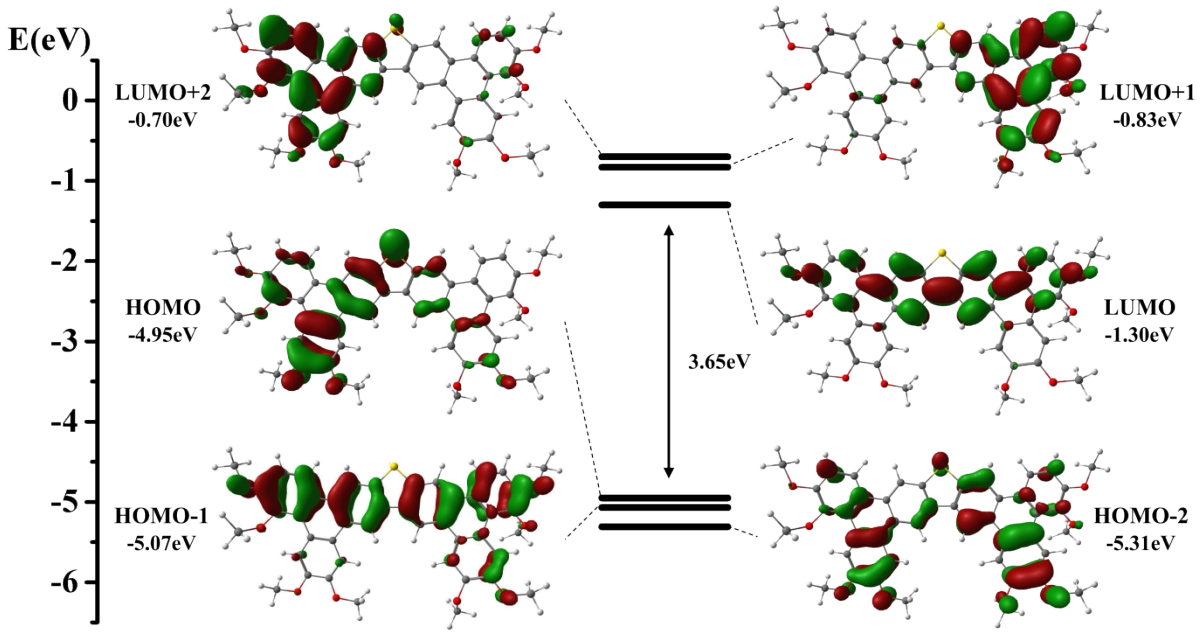
E(eV)
0
-1
-2
-3
-4
-5
-6
LUMO+2
-0.70eV
HOMO
-4.95eV
HOMO-1
-5.07eV
3.65eV
LUMO+1
-0.83eV
LUMO
-1.30eV
HOMO-2
-5.31eV

DTPTB

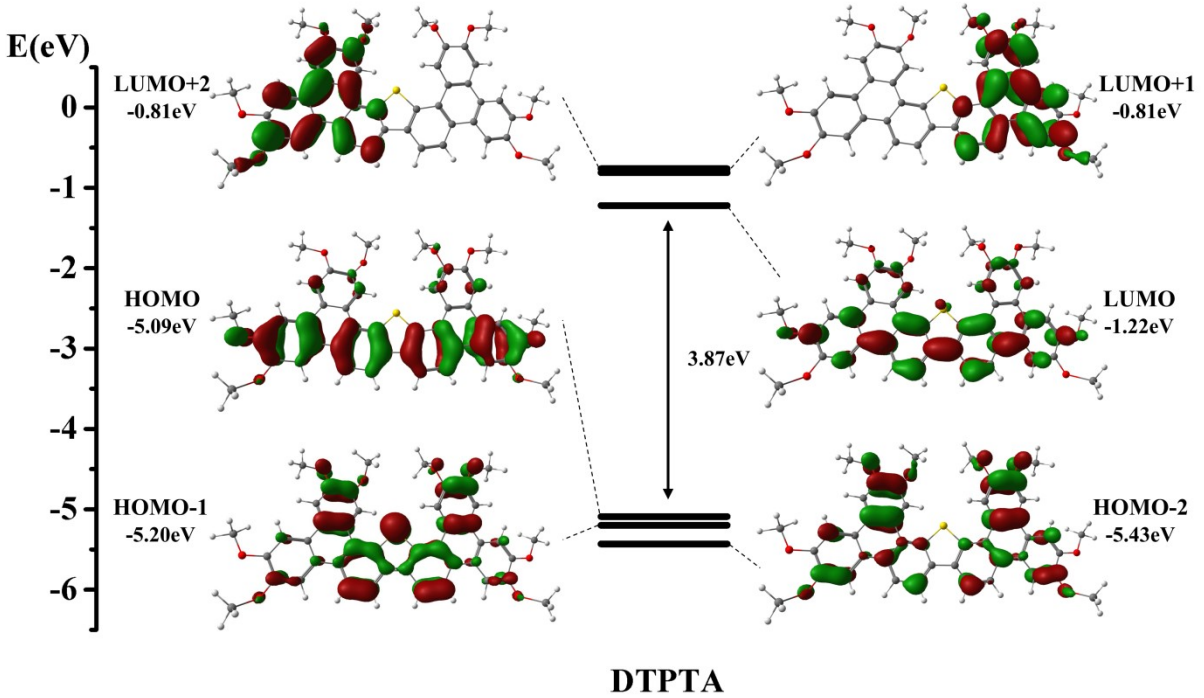

Figure S9. Partial molecular orbital diagrams for **T**, **D**, **DTPTB** and **DTPTA** with some selected isodensity frontier molecular orbital mainly involved in the electronic transitions. All the DFT energy values are given in electronvolts. The arrows are intended to highlight the HOMO-LUMO energy gaps.

Table S13. Selected calculated excitation energies (ΔE), oscillator strengths (f), main orbital components, and assignment for the **T**, **D**, **DTPTB**, **DTPTA** in THF solution.[a]

Compd.	λ_{exc}/nm	ΔE/eV	f	Transitions (Percentage Contribution)
T	353.3	3.51	0.1326	H-1→L+0(+12%), H-0→L+0(+68%)
	334.7	3.70	0.4978	H-1→L+0(+67%), H-2→L+0(+10%)
	310.0	4.00	0.3620	H-2→L+0(+59%), H-3→L+0(+22%), H-1→L+1(+18%)
	301.9	4.11	0.1027	H-3→L+0(+47%), H-0→L+2(+28%), H-4→L+0(+15%)
	295.1	4.20	0.3490	H-0→L+1(+46%), H-3→L+0(+31%), H-1→L+1(+27%)
	292.1	4.24	0.0062	H-0→L+2(+45%), H-0→L+1(+42%), H-2→L+0(+13%)
	287.4	4.31	0.1786	H-4→L+0(+48%), H-1→L+1(+36%)
	283.0	4.38	0.2495	H-1→L+1(+39%), H-0→L+2(+30%), H-1→L+2(+26%)
	277.7	4.46	0.0596	H-1→L+2(+52%), H-4→L+0(+27%), H-0→L+4(+12%)
	271.8	4.56	0.1334	H-0→L+5(+50%), H-5→L+0(+18%)
	270.7	4.58	0.0438	H-1→L+3(+45%), H-0→L+5(+24%), H-7→L+0(+13%)
	268.6	4.62	0.0191	H-5→L+0(+39%), H-1→L+3(+29%), H-0→L+3(+24%)
	266.2	4.66	0.0528	H-0→L+3(+47%), H-0→L+4(+20%), H-0→L+5(+16%)
	264.8	4.68	0.1139	H-6→L+0(+45%), H-2→L+1(+24%), H-0→L+5(+23%)
	263.3	4.71	0.0464	H-6→L+0(+37%), H-0→L+3(+31%), H-2→L+2(+15%)
	261.3	4.75	0.0786	H-3→L+1(+38%), H-2→L+2(+29%), H-2→L+1(+17%)
	259.6	4.78	0.0214	H-0→L+4(+35%), H-2→L+2(+32%), H-3→L+1(+22%)
	258.6	4.79	0.0155	H-7→L+0(+37%), H-0→L+3(+13%), H-2→L+5(+11%)

	257.3	4.82	0.0870	H-3→L+1(+42%), H-9→L+0(+14%), H-6→L+0(+13%)
	255.7	4.85	0.2356	H-1→L+4(+38%), H-2→L+1(+15%), H-2→L+2(+15%)
	253.9	4.88	0.0641	H-1→L+6(+33%), H-3→L+2(+27%), H-2→L+3(+11%)
	252.5	4.91	0.0089	H-8→L+0(+37%), H-7→L+0(+32%), H-1→L+4(+29%)
	252.2	4.92	0.0110	H-8→L+0(+31%), H-4→L+1(+23%), H-7→L+0(+14%)
	250.6	4.95	0.0366	H-0→L+7(+32%), H-1→L+6(+12%), H-1→L+7(+11%)
	249.2	4.97	0.0506	H-3→L+2(+33%), H-1→L+3(+15%), H-1→L+4(+14%)
	248.5	4.99	0.0081	H-4→L+1(+48%), H-3→L+2(+25%), H-9→L+0(+18%)
	247.7	5.01	0.0066	H-1→L+5(+46%), H-7→L+0(+30%), H-1→L+6(+14%)
	246.3	5.03	0.0050	H-0→L+6(+56%), H-2→L+3(+16%), H-1→L+5(+13%)
	245.2	5.06	0.0749	H-2→L+3(+45%), H-3→L+3(+20%), H-1→L+5(+12%)
	243.4	5.09	0.0359	H-9→L+0(+46%), H-2→L+3(+16%), H-1→L+6(+14%)
D	318.6	3.89	0.0441	H-0→L+0(+62%)
	315.9	3.93	0.0280	H-1→L+0(+60%), H-0→L+0(+32%)
	298.9	4.15	0.0364	H-2→L+0(+61%), H-1→L+0(+16%), H-4→L+0(+13%)
	292.5	4.24	0.3647	H-1→L+1(+66%), H-2→L+0(+17%)
	285.5	4.34	0.2912	H-0→L+2(+67%)
	282.0	4.40	0.0247	H-0→L+1(+65%), H-0→L+2(+15%), H-3→L+0(+14%)
	279.7	4.43	0.0110	H-3→L+0(+58%), H-5→L+0(+17%)
	277.5	4.47	0.0151	H-1→L+2(+56%), H-2→L+1(+11%)
	275.9	4.49	0.0757	H-4→L+0(+59%), H-3→L+0(+23%), H-5→L+0(+19%)
	274.1	4.52	0.0712	H-2→L+1(+37%), H-4→L+0(+18%)
	271.4	4.57	0.0582	H-5→L+0(+34%), H-2→L+2(+27%), H-1→L+2(+27%)
	269.8	4.60	0.1265	H-0→L+4(+57%), H-0→L+3(+19%)
	268.1	4.62	0.0787	H-2→L+2(+35%), H-1→L+3(+33%), H-2→L+1(+26%)
	266.0	4.66	0.2270	H-2→L+1(+42%), H-5→L+0(+28%), H-1→L+3(+20%)
	261.6	4.74	0.1503	H-3→L+1(+44%), H-4→L+1(+33%), H-1→L+6(+13%)
	258.7	4.79	0.0283	H-0→L+5(+35%), H-4→L+2(+26%), H-2→L+2(+23%)
	256.9	4.83	0.0035	H-0→L+3(+59%), H-2→L+3(+14%), H-5→L+2(+14%)
	255.8	4.85	0.0381	H-5→L+1(+39%), H-1→L+4(+32%), H-4→L+1(+20%)
	254.5	4.87	0.0092	H-1→L+4(+37%), H-1→L+3(+13%), H-1→L+6(+13%)
	252.9	4.90	0.0796	H-6→L+0(+40%), H-1→L+4(+28%), H-3→L+1(+15%)
	252.3	4.91	0.0801	H-0→L+5(+33%), H-3→L+2(+27%), H-0→L+4(+17%)
	251.4	4.93	0.1089	H-5→L+2(+31%), H-2→L+3(+24%), H-1→L+6(+20%)
	251.0	4.94	0.0808	H-7→L+0(+31%), H-6→L+0(+29%), H-1→L+6(+27%)
	249.7	4.97	0.0008	H-4→L+1(+42%), H-2→L+3(+14%)
	249.0	4.98	0.0032	H-7→L+0(+49%), H-5→L+2(+26%), H-2→L+3(+20%)
	246.9	5.02	0.0132	H-2→L+4(+37%), H-2→L+3(+28%), H-0→L+8(+18%)
	245.5	5.05	0.0226	H-1→L+5(+41%), H-1→L+7(+33%), H-2→L+4(+20%)
	243.9	5.08	0.0894	H-2→L+3(+40%), H-8→L+0(+16%), H-5→L+1(+14%)
	243.7	5.09	0.0313	H-3→L+2(+49%), H-4→L+2(+43%)
	241.7	5.13	0.0525	H-8→L+0(+42%), H-5→L+3(+26%), H-2→L+4(+19%)
DTPTB	353.3	3.51	0.1326	H-1→L+0(+12%), H-0→L+0(+68%)

	334.7	3.70	0.4978	H-1→L+0(+67%), H-2→L+0(+10%)
	310.0	4.00	0.3620	H-2→L+0(+59%), H-3→L+0(+22%), H-1→L+1(+18%)
	301.9	4.11	0.1027	H-3→L+0(+47%), H-0→L+2(+28%), H-4→L+0(+15%)
	295.1	4.20	0.3490	H-0→L+1(+46%), H-3→L+0(+31%), H-1→L+1(+27%)
	292.1	4.24	0.0062	H-0→L+2(+45%), H-0→L+1(+42%), H-2→L+0(+13%)
	287.4	4.31	0.1786	H-4→L+0(+48%), H-1→L+1(+36%)
	283.0	4.38	0.2495	H-1→L+1(+39%), H-0→L+2(+30%), H-1→L+2(+26%)
	277.7	4.46	0.0596	H-1→L+2(+52%), H-4→L+0(+27%), H-0→L+4(+12%)
	271.8	4.56	0.1334	H-0→L+5(+50%), H-5→L+0(+18%)
	270.7	4.58	0.0438	H-1→L+3(+45%), H-0→L+5(+24%), H-7→L+0(+13%)
	268.6	4.62	0.0191	H-5→L+0(+39%), H-1→L+3(+29%), H-0→L+3(+24%)
	266.2	4.66	0.0528	H-0→L+3(+47%), H-0→L+4(+20%), H-0→L+5(+16%)
	264.8	4.68	0.1139	H-6→L+0(+45%), H-2→L+1(+24%), H-0→L+5(+23%)
	263.3	4.71	0.0464	H-6→L+0(+37%), H-0→L+3(+31%), H-2→L+2(+15%)
	261.3	4.75	0.0786	H-3→L+1(+38%), H-2→L+2(+29%), H-2→L+1(+17%)
	259.6	4.78	0.0214	H-0→L+4(+35%), H-2→L+2(+32%), H-3→L+1(+22%)
	258.6	4.79	0.0155	H-7→L+0(+37%), H-0→L+3(+13%), H-2→L+5(+11%)
	257.3	4.82	0.0870	H-3→L+1(+42%), H-9→L+0(+14%), H-6→L+0(+13%)
	255.7	4.85	0.2356	H-1→L+4(+38%), H-2→L+1(+15%), H-2→L+2(+15%)
	253.9	4.88	0.0641	H-1→L+6(+33%), H-3→L+2(+27%), H-2→L+3(+11%)
	252.5	4.91	0.0089	H-8→L+0(+37%), H-7→L+0(+32%), H-1→L+4(+29%)
	252.2	4.92	0.0110	H-8→L+0(+31%), H-4→L+1(+23%), H-7→L+0(+14%)
	250.6	4.95	0.0366	H-0→L+7(+32%), H-1→L+6(+12%), H-1→L+7(+11%)
	249.2	4.97	0.0506	H-3→L+2(+33%), H-1→L+3(+15%), H-1→L+4(+14%)
	248.5	4.99	0.0081	H-4→L+1(+48%), H-3→L+2(+25%), H-9→L+0(+18%)
	247.7	5.01	0.0066	H-1→L+5(+46%), H-7→L+0(+30%), H-1→L+6(+14%)
	246.3	5.03	0.0050	H-0→L+6(+56%), H-2→L+3(+16%), H-1→L+5(+13%)
	245.2	5.06	0.0749	H-2→L+3(+45%), H-3→L+3(+20%), H-1→L+5(+12%)
	243.4	5.09	0.0359	H-9→L+0(+46%), H-2→L+3(+16%), H-1→L+6(+14%)
DTPTA	364.3	3.40	0.0259	H-1→L+0(+61%)
	361.1	3.43	0.6278	H-0→L+0(+66%), H-1→L+1(+12%)
	345.5	3.59	0.0164	H-2→L+0(+49%), H-0→L+2(+33%), H-0→L+0(+12%)
	323.9	3.83	0.0008	H-3→L+0(+44%), H-1→L+1(+30%), H-2→L+1(+14%)
	317.2	3.91	0.1086	H-0→L+3(+37%), H-0→L+1(+36%), H-0→L+2(+29%)
	315.3	3.93	0.5043	H-1→L+1(+46%), H-1→L+2(+36%), H-2→L+0(+24%)
	312.0	3.97	0.5640	H-2→L+0(+39%), H-1→L+3(+27%), H-0→L+1(+24%)
	310.6	4.00	0.0780	H-0→L+3(+37%), H-3→L+0(+36%), H-1→L+2(+14%)
	304.7	4.07	0.0368	H-1→L+2(+31%), H-3→L+0(+26%), H-2→L+1(+20%)
	304.5	4.07	0.0040	H-1→L+3(+54%), H-0→L+4(+22%), H-0→L+2(+21%)
	301.4	4.11	0.0289	H-0→L+4(+59%), H-5→L+0(+25%)
	296.1	4.19	0.0285	H-1→L+4(+35%), H-3→L+2(+21%), H-0→L+3(+15%)
	292.1	4.24	0.0532	H-4→L+0(+45%), H-1→L+4(+36%)
	292.0	4.25	0.5454	H-2→L+2(+52%), H-1→L+3(+11%), H-3→L+3(+10%)

	290.0	4.28	0.0022	H-0→L+5(+41%), H-3→L+0(+25%), H-2→L+3(+22%)
	283.0	4.38	0.0264	H-3→L+1(+38%), H-3→L+2(+30%), H-1→L+5(+28%)
	281.6	4.40	0.0093	H-1→L+4(+38%), H-2→L+3(+30%), H-3→L+1(+20%)
	280.4	4.42	0.0068	H-1→L+5(+42%), H-2→L+4(+35%), H-5→L+0(+33%)
	279.4	4.44	0.0970	H-5→L+0(+41%), H-3→L+1(+21%), H-3→L+2(+16%)
	273.9	4.53	0.2988	H-2→L+3(+36%), H-3→L+2(+33%), H-1→L+4(+15%)
	270.2	4.59	0.0515	H-3→L+3(+56%), H-1→L+5(+21%), H-4→L+1(+18%)
	268.1	4.62	0.0978	H-0→L+5(+42%), H-2→L+1(+20%), H-6→L+0(+17%)
	267.4	4.64	0.0812	H-1→L+5(+40%)
	263.5	4.70	0.0478	H-3→L+4(+57%), H-6→L+0(+32%)
	262.4	4.72	0.0138	H-4→L+1(+41%), H-4→L+2(+31%), H-2→L+4(+21%)
	261.9	4.73	0.1681	H-2→L+5(+43%), H-4→L+2(+31%), H-6→L+0(+29%)
	257.5	4.82	0.0081	H-2→L+5(+44%), H-4→L+1(+26%), H-3→L+4(+14%)
	255.8	4.85	0.0131	H-6→L+0(+48%), H-4→L+1(+12%)
	255.2	4.86	0.0168	H-4→L+3(+44%), H-5→L+1(+23%), H-3→L+5(+19%)
	252.8	4.90	0.3876	H-5→L+1(+47%), H-5→L+2(+34%), H-2→L+3(+18%)
[a]H = HOMO, L = LUMO, H-n = HOMO-n and L+n = LUMO+n.				

11. NMR

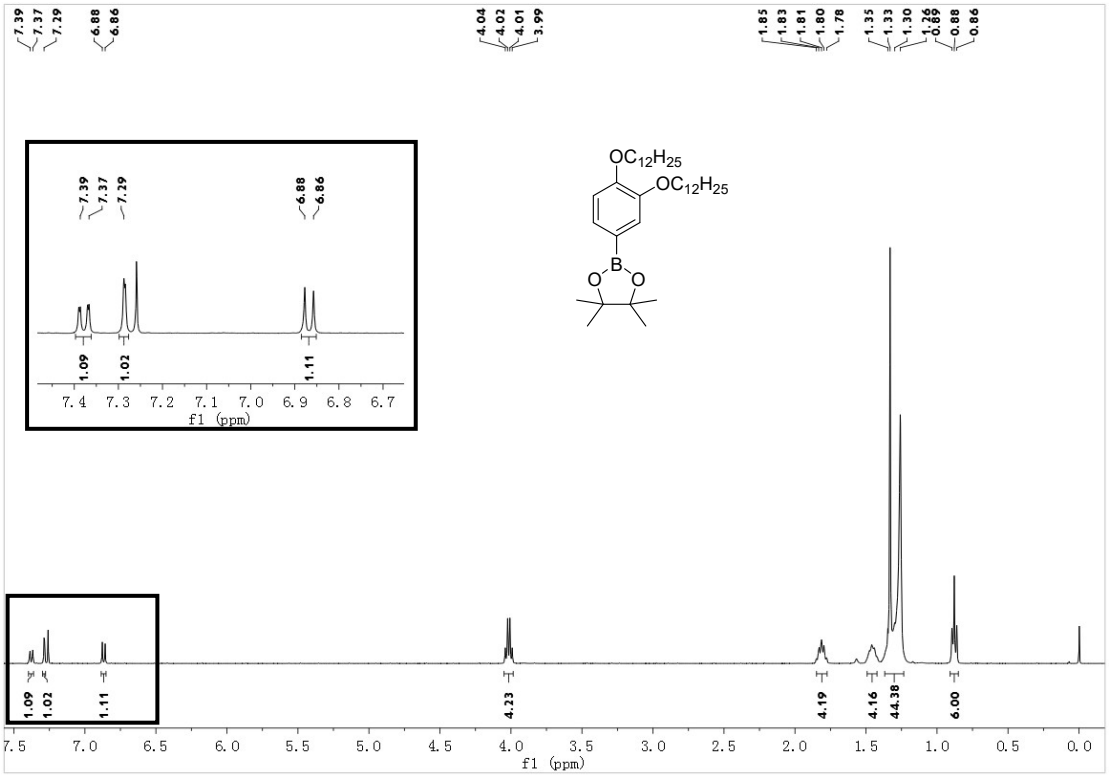

^{1}H NMR ($CDCl_3$, 400 MHz) spectrum of **3a**

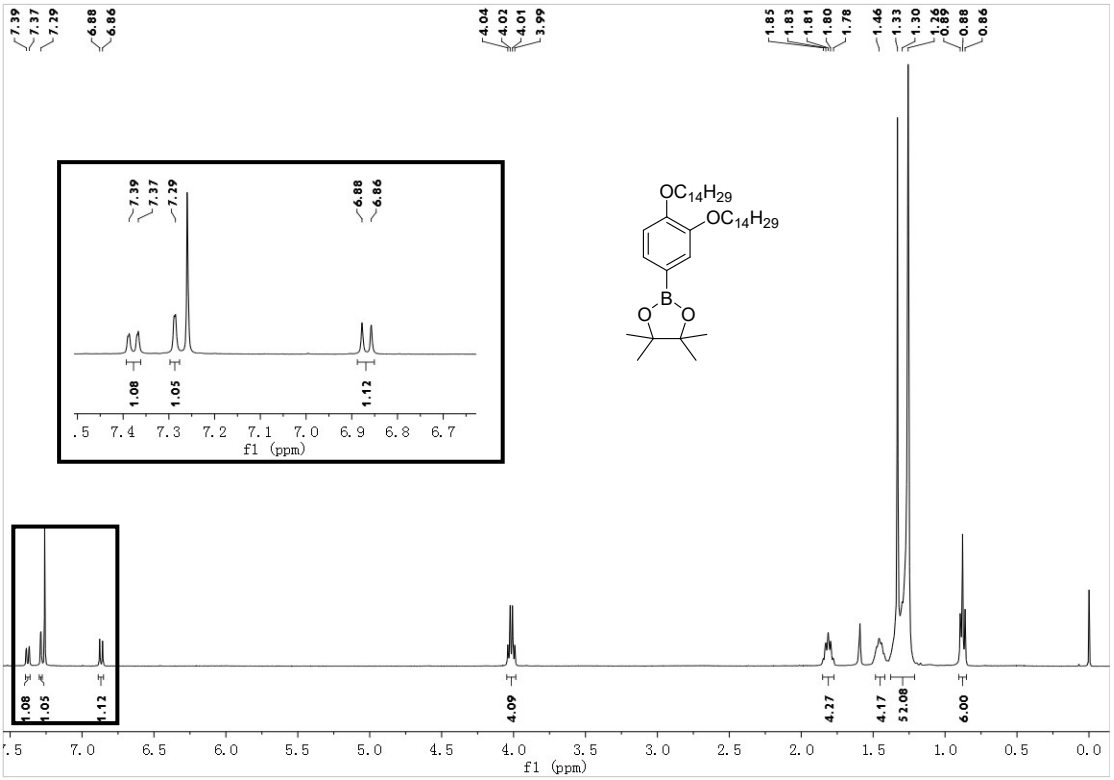

^{1}H NMR ($CDCl_3$, 400 MHz) spectrum of **3b**

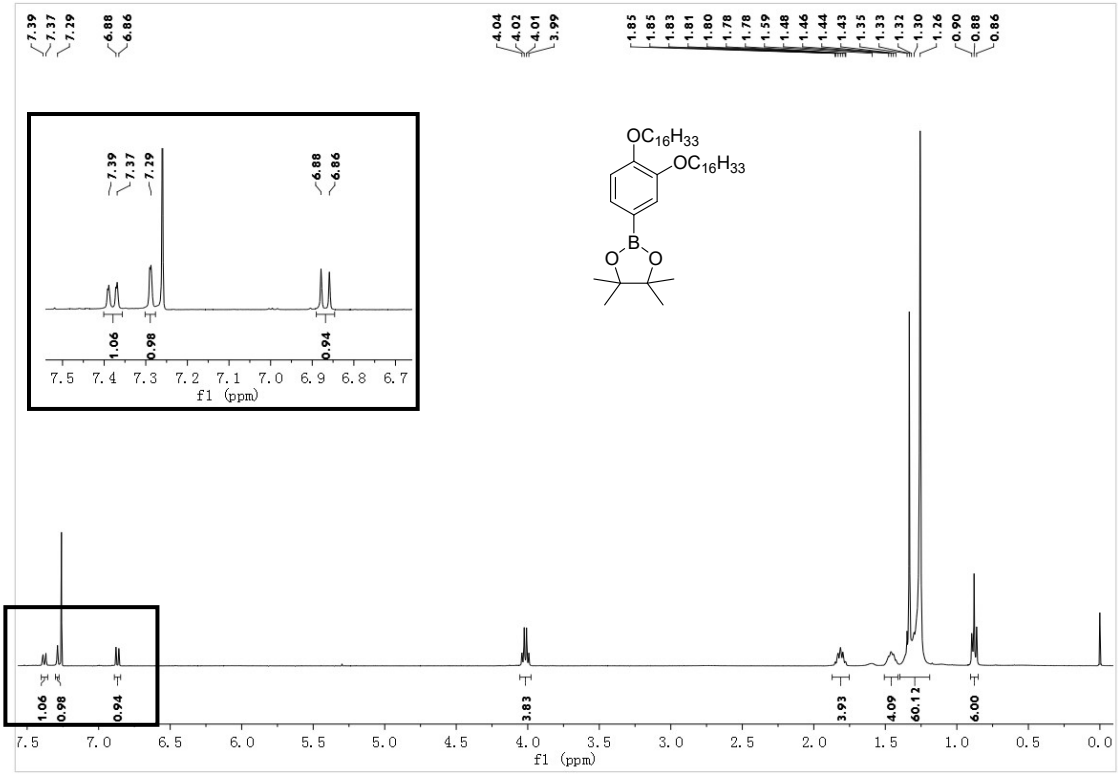

^{1}H NMR ($CDCl_3$, 400 MHz) spectrum of **3c**

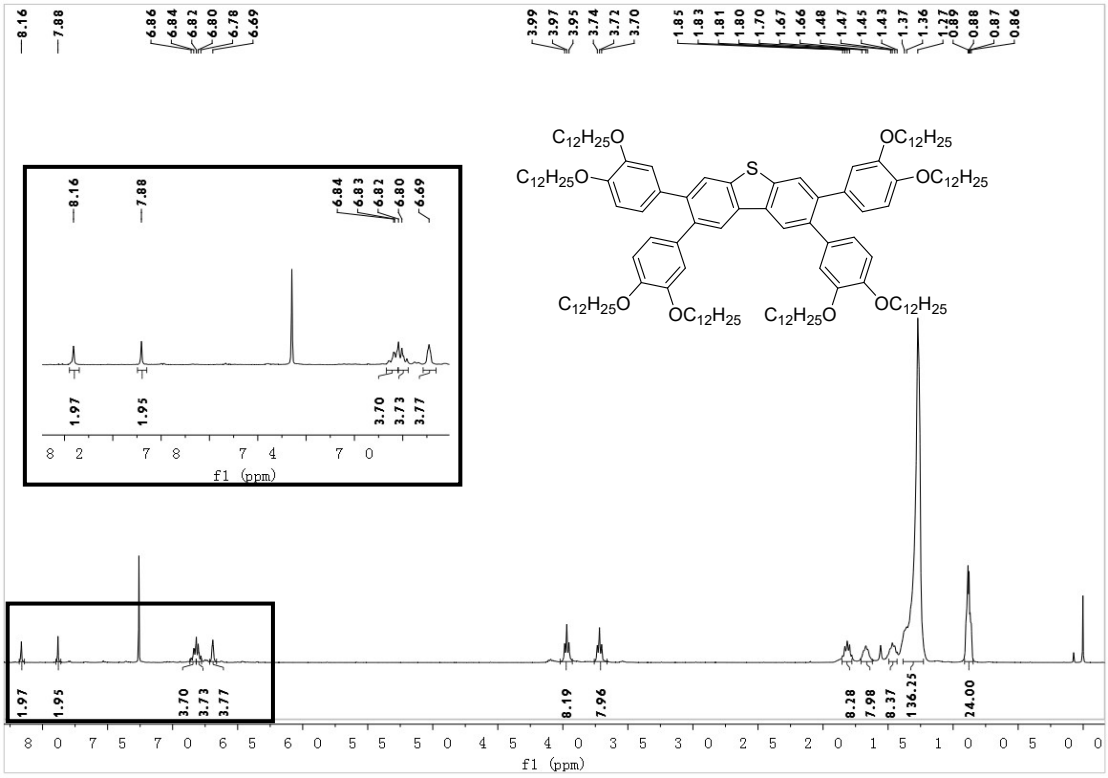

^{1}H NMR ($CDCl_3$, 400 MHz) spectrum of **T12**

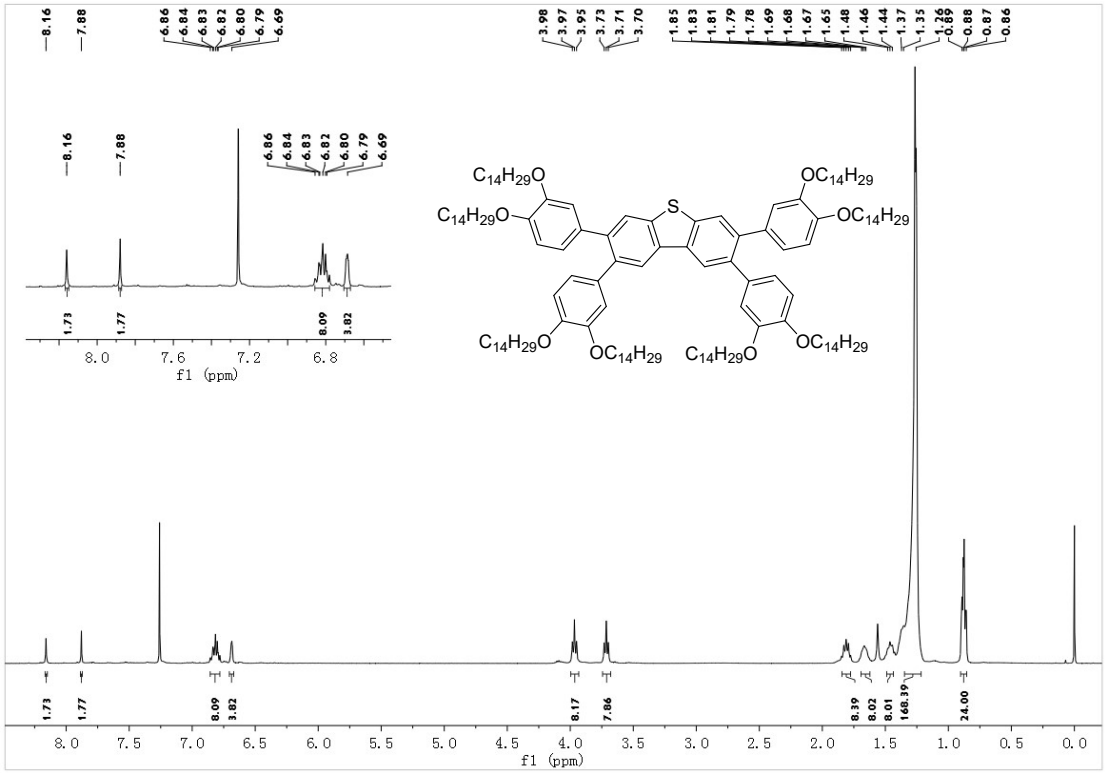

^{1}H NMR ($CDCl_3$, 400 MHz) spectrum of **T14**

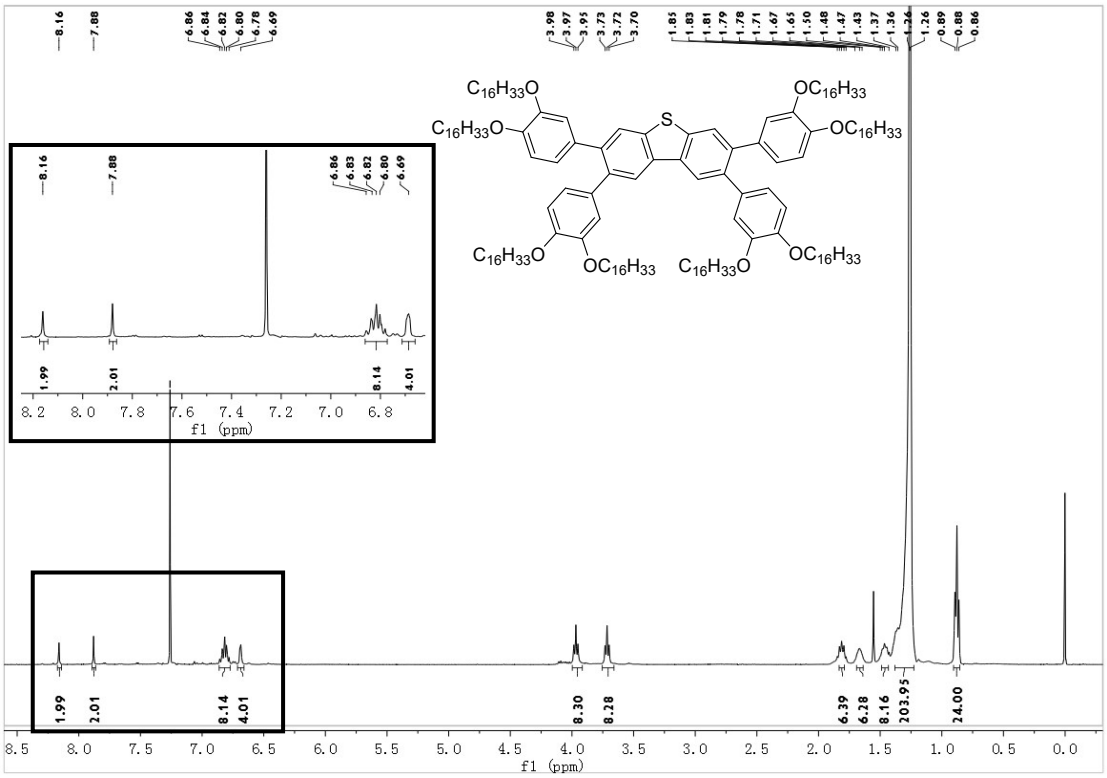

^{1}H NMR ($CDCl_3$, 400 MHz) spectrum of **T16**

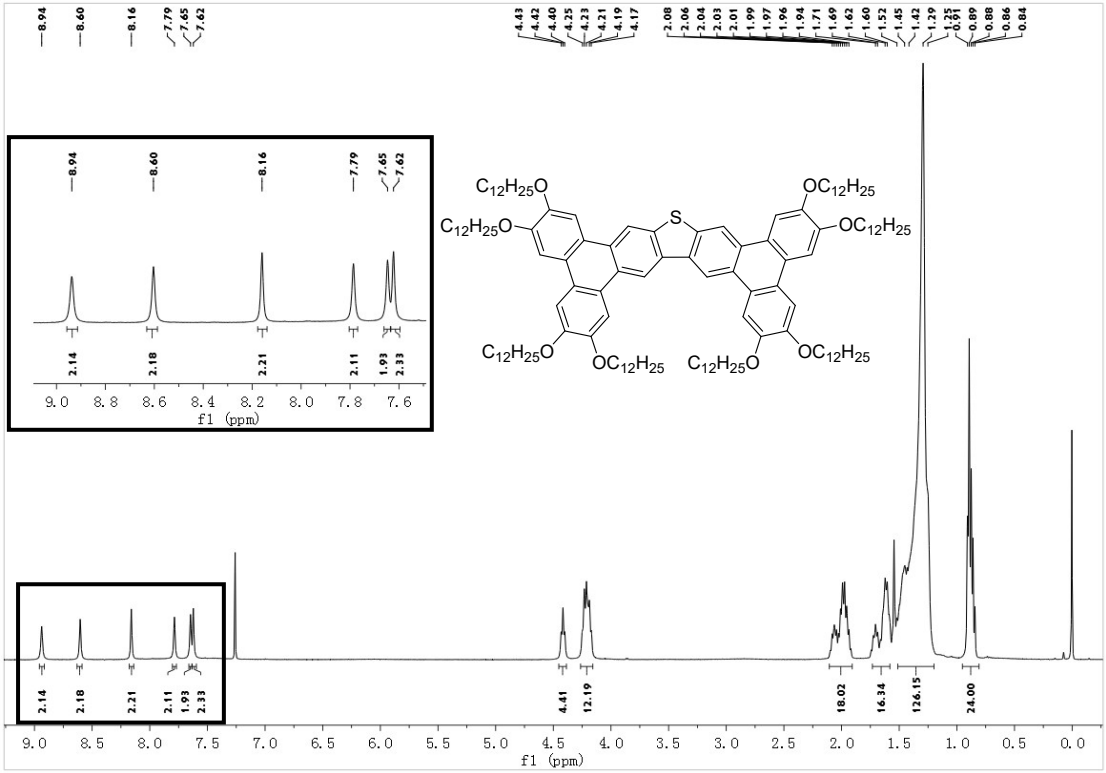

^{1}H NMR ($CDCl_3$, 400 MHz) spectrum of **DTPTB12**

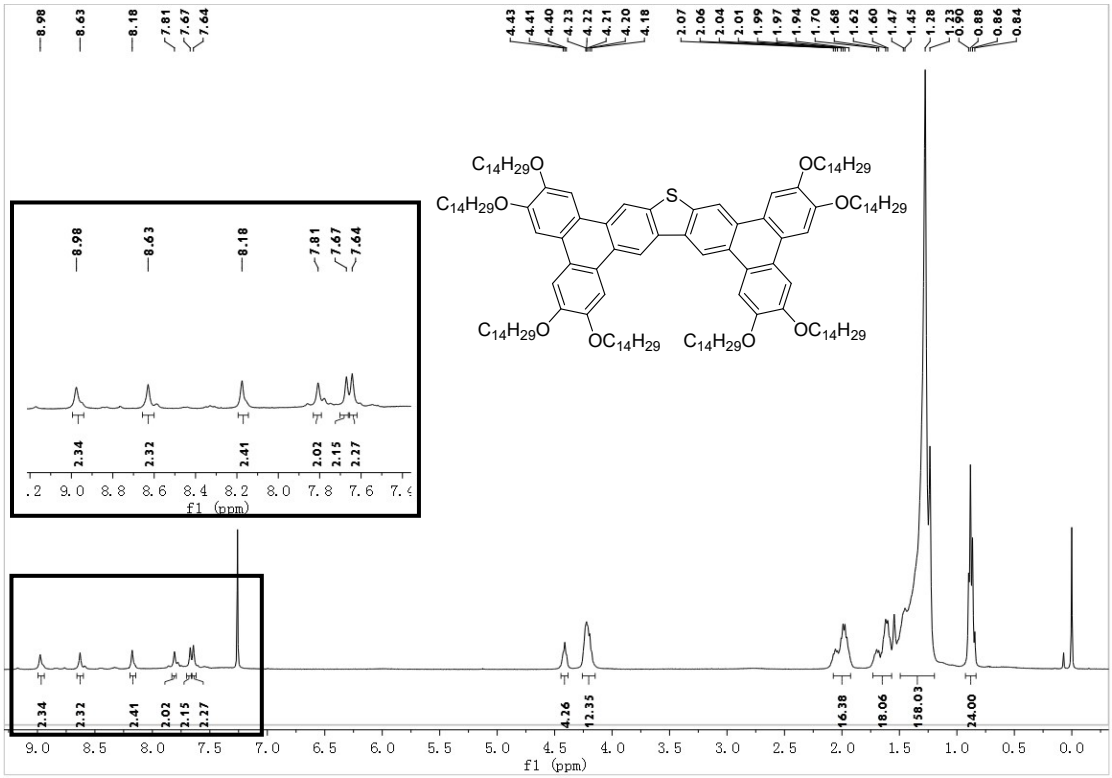

^{1}H NMR ($CDCl_3$, 400 MHz) spectrum of **DTPTB14**

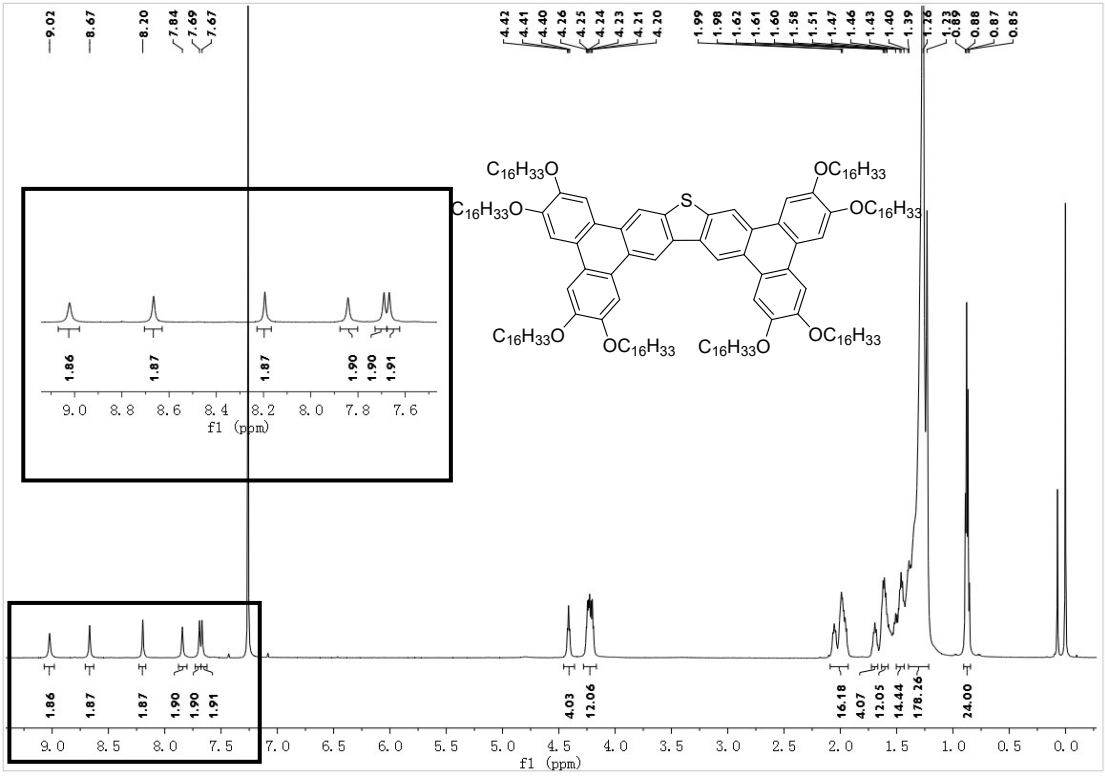

^{1}H NMR ($CDCl_3$, 600 MHz) spectrum of **DTPTB16**

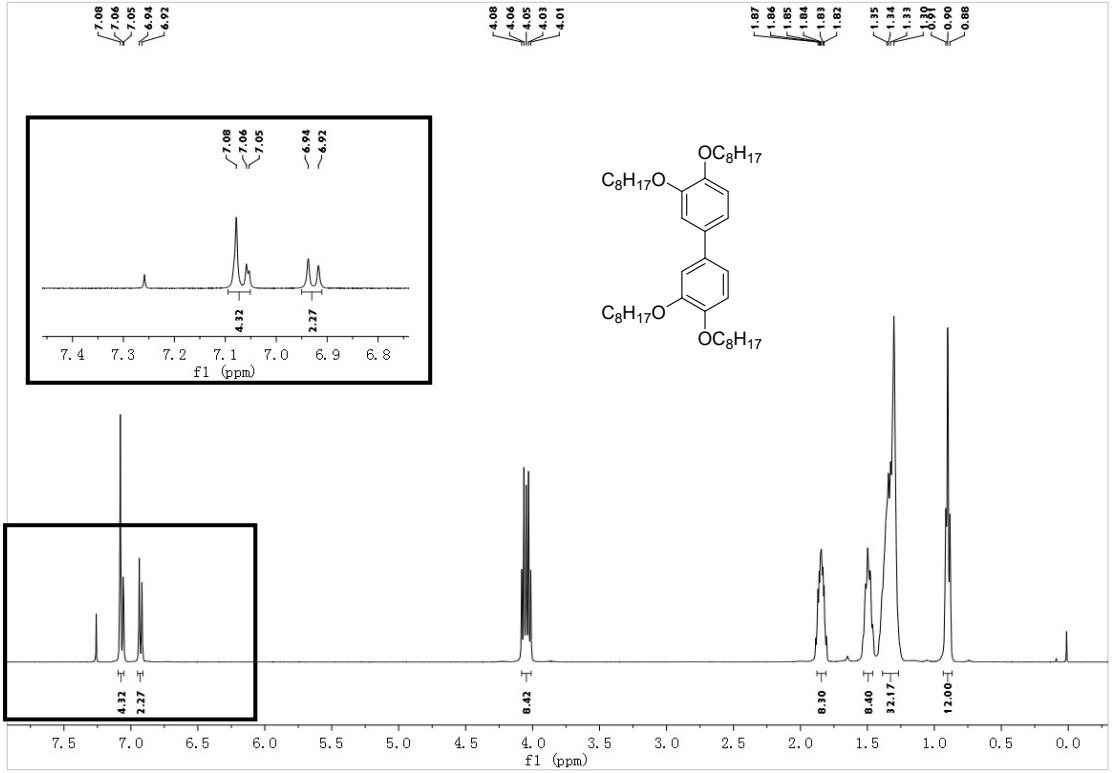

^{1}H NMR ($CDCl_3$, 400 MHz) spectrum of **5a**

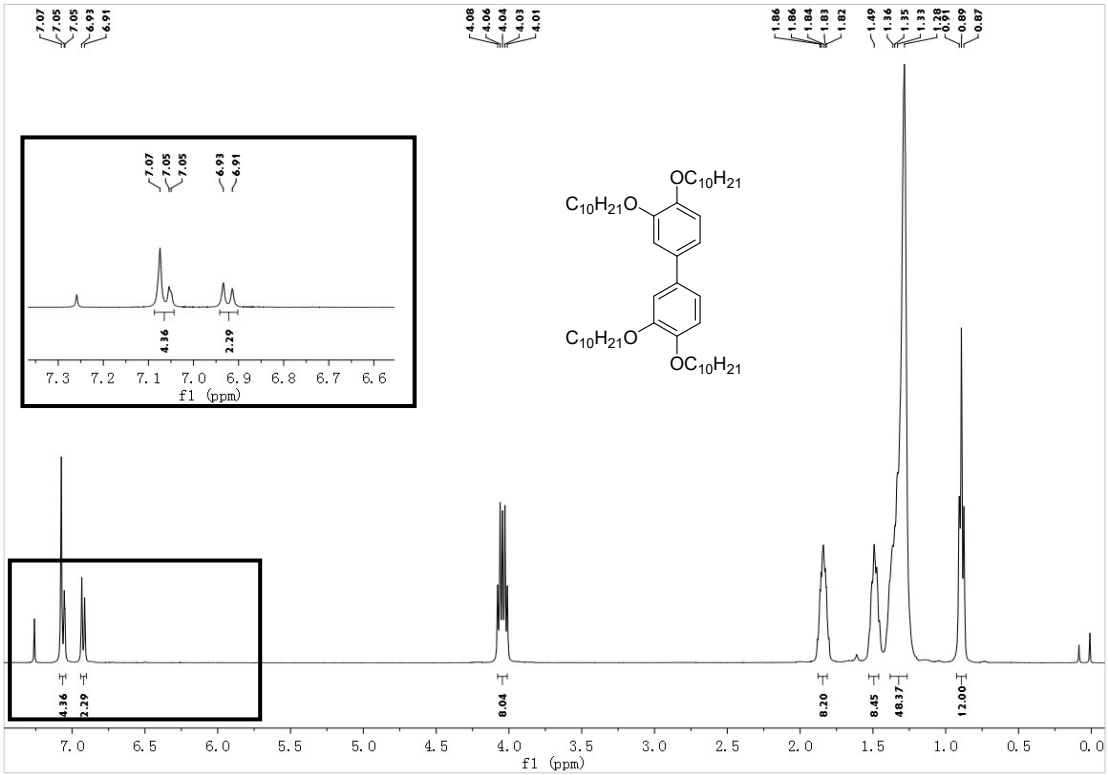

^{1}H NMR ($CDCl_3$, 400 MHz) spectrum of **5b**

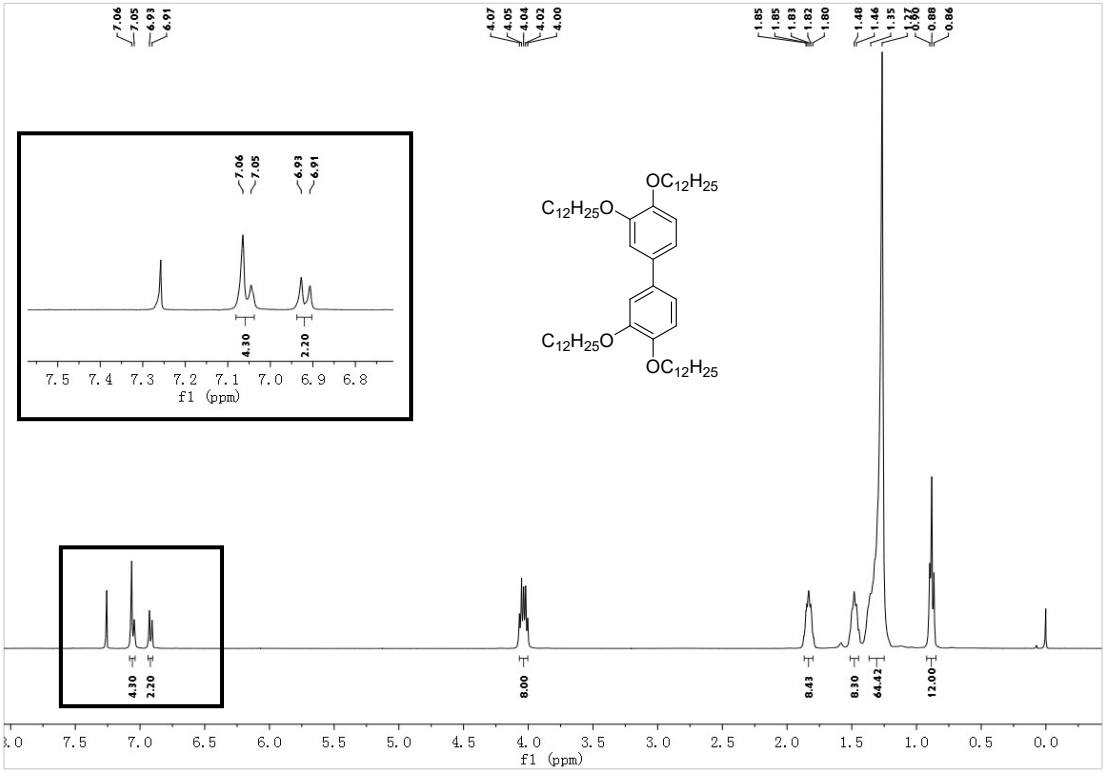

^{1}H NMR ($CDCl_3$, 400 MHz) spectrum of **5c**

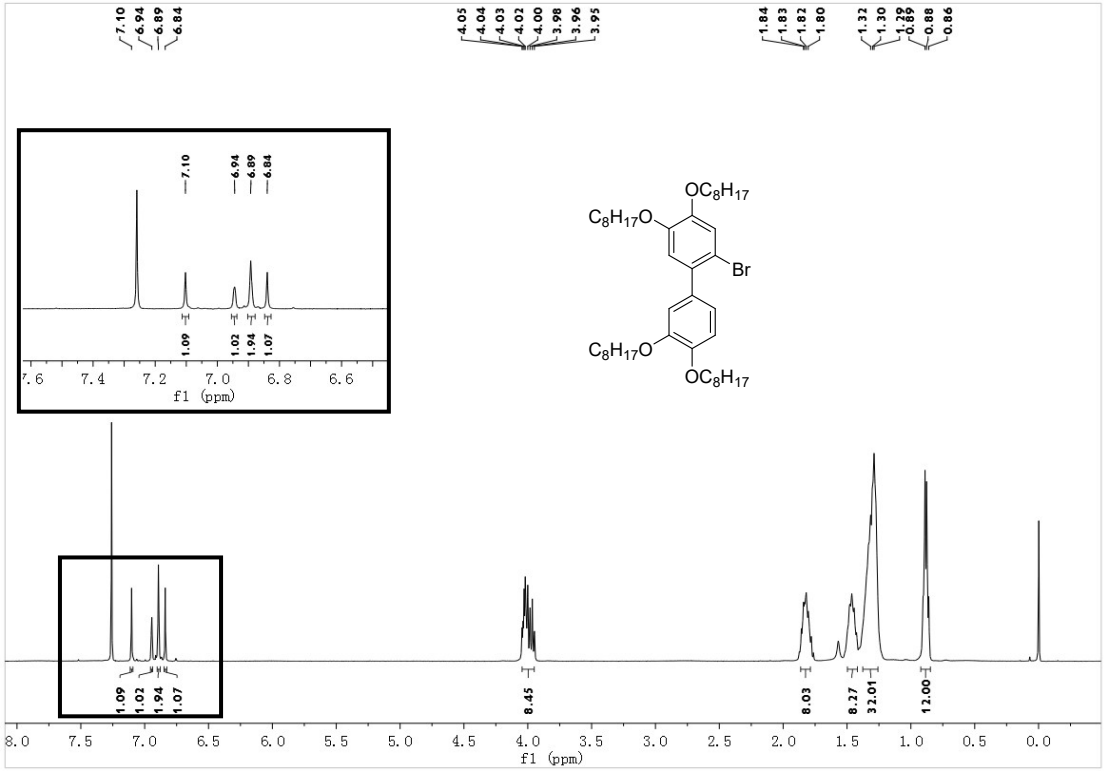

^{1}H NMR ($CDCl_3$, 400 MHz) spectrum of **6a**

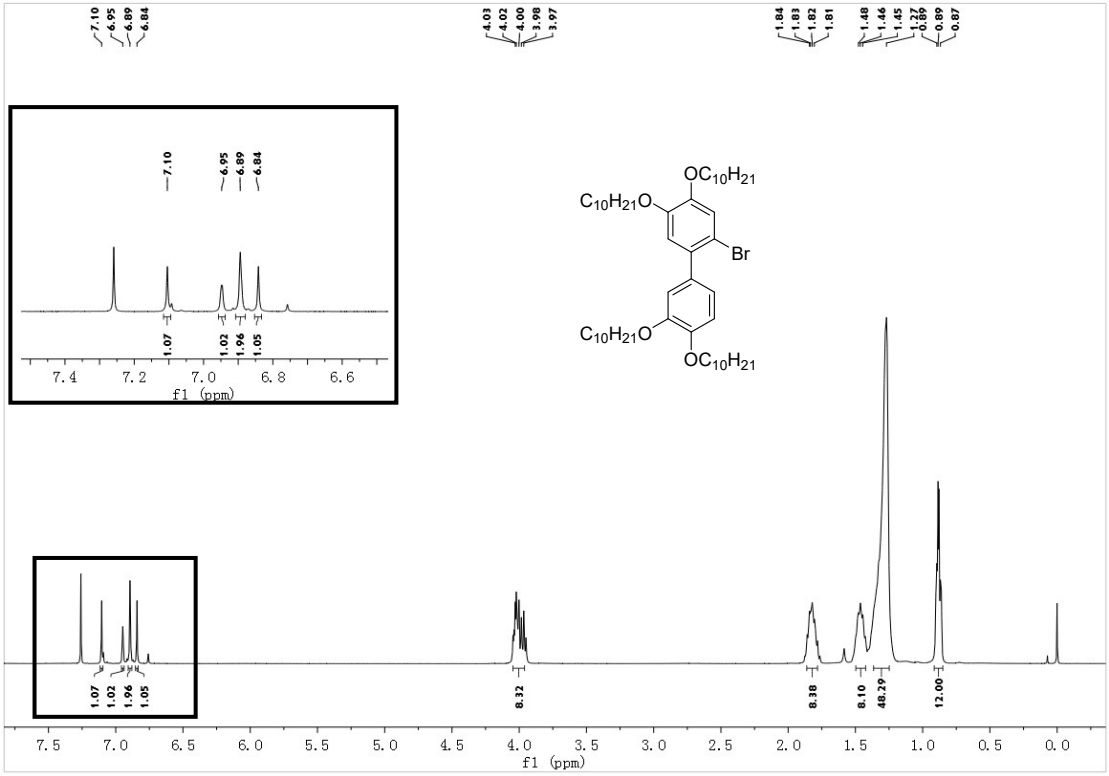

^{1}H NMR ($CDCl_3$, 400 MHz) spectrum of **6b**

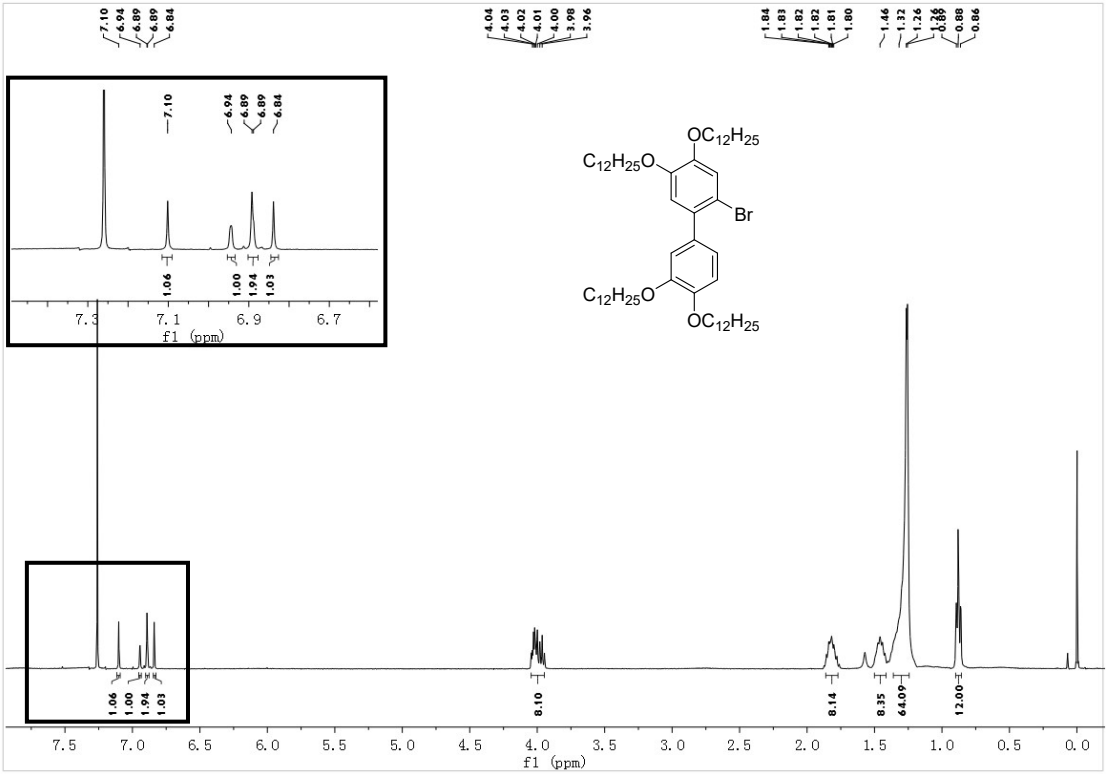

^{1}H NMR ($CDCl_3$, 400 MHz) spectrum of **6c**

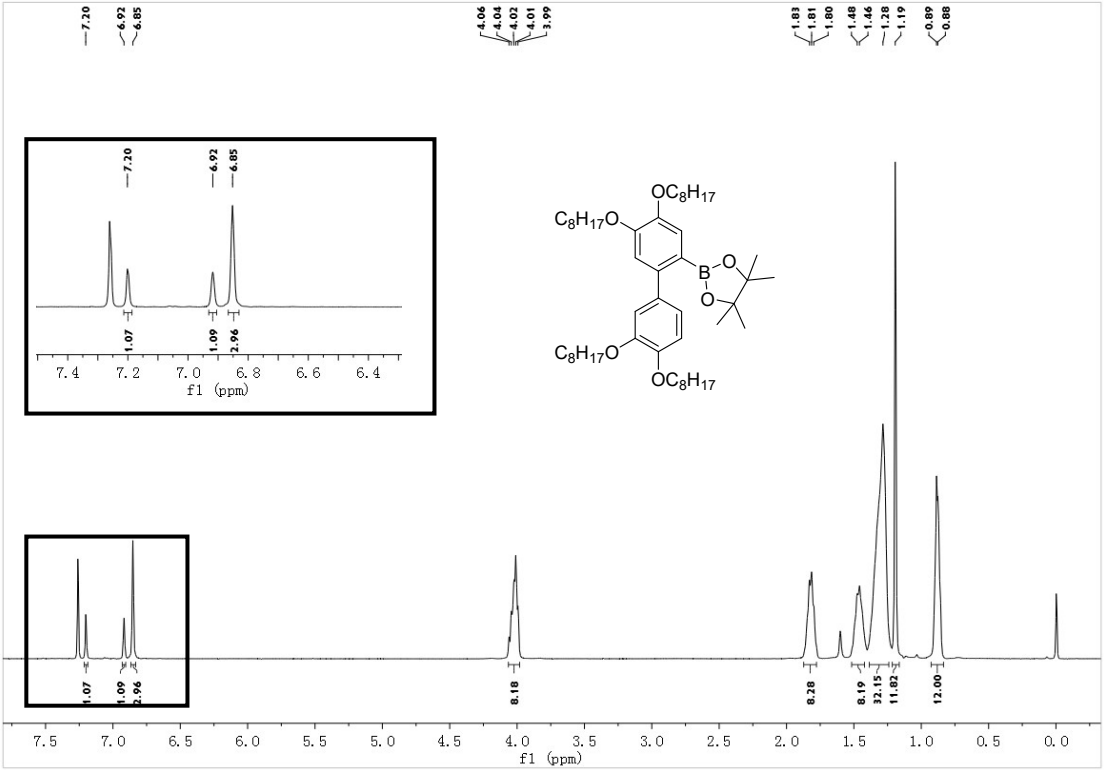

^{1}H NMR ($CDCl_3$, 400 MHz) spectrum of **7a**

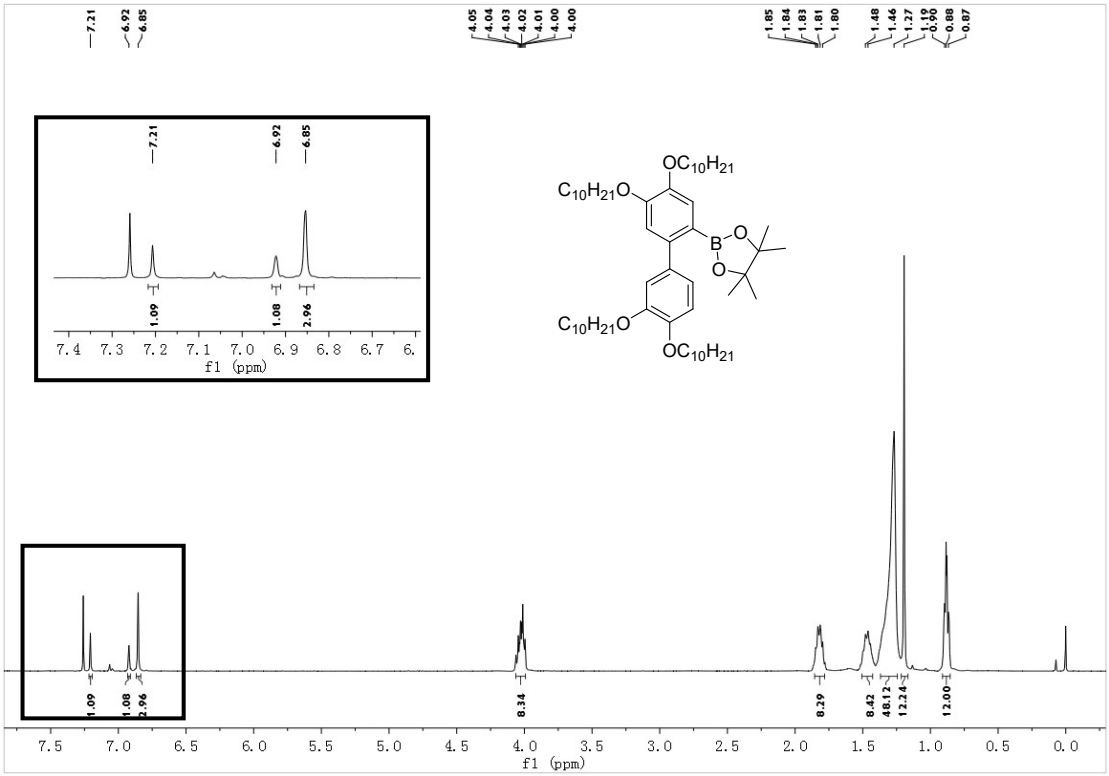

^{1}H NMR ($CDCl_3$, 400 MHz) spectrum of **7b**

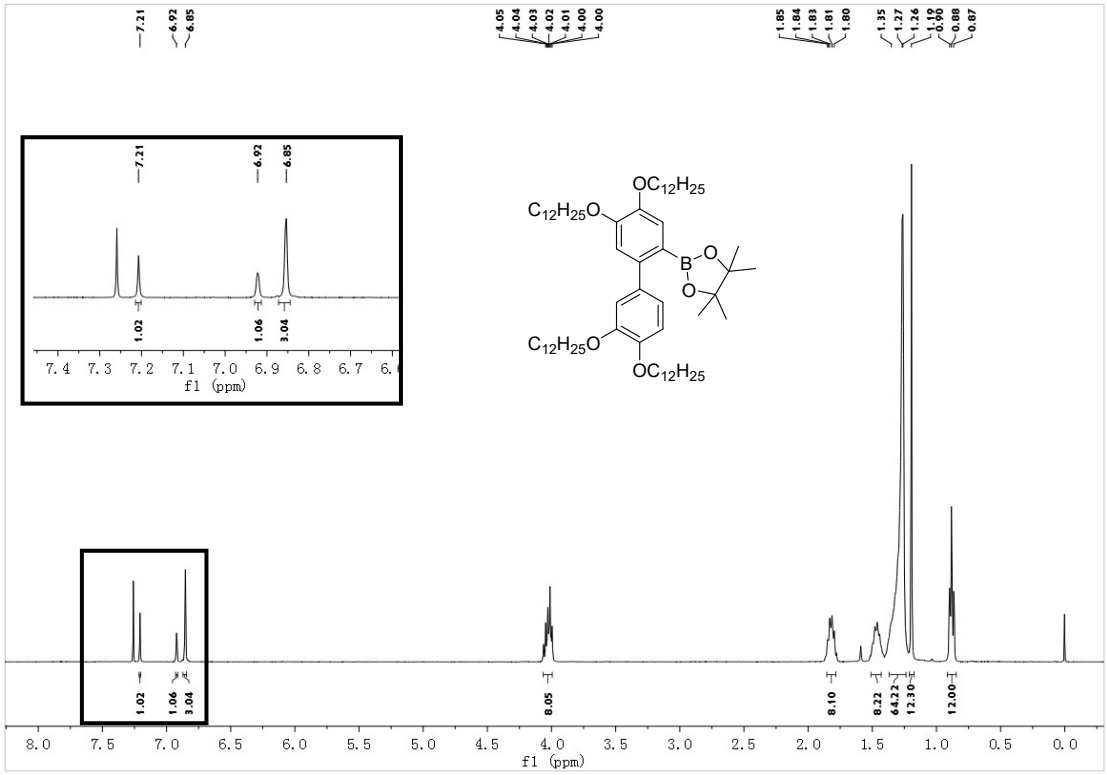

^{1}H NMR ($CDCl_3$, 400 MHz) spectrum of **7c**

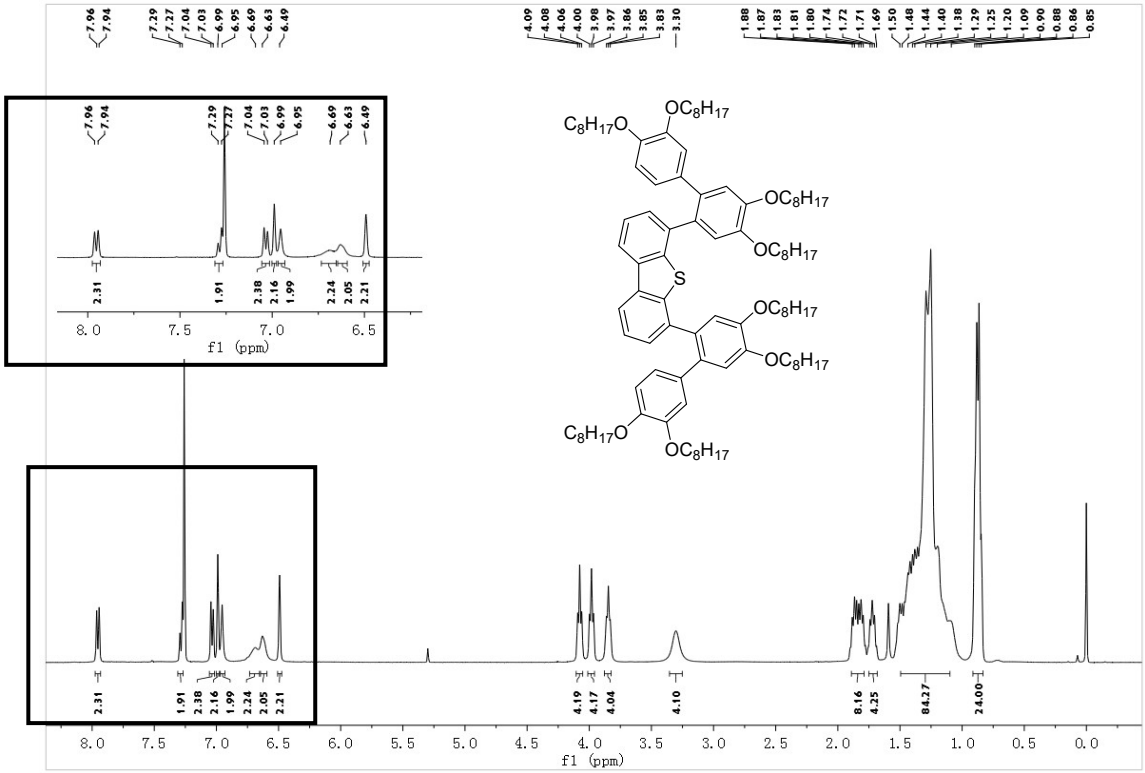

^{1}H NMR ($CDCl_3$, 400 MHz) spectrum of **D8**

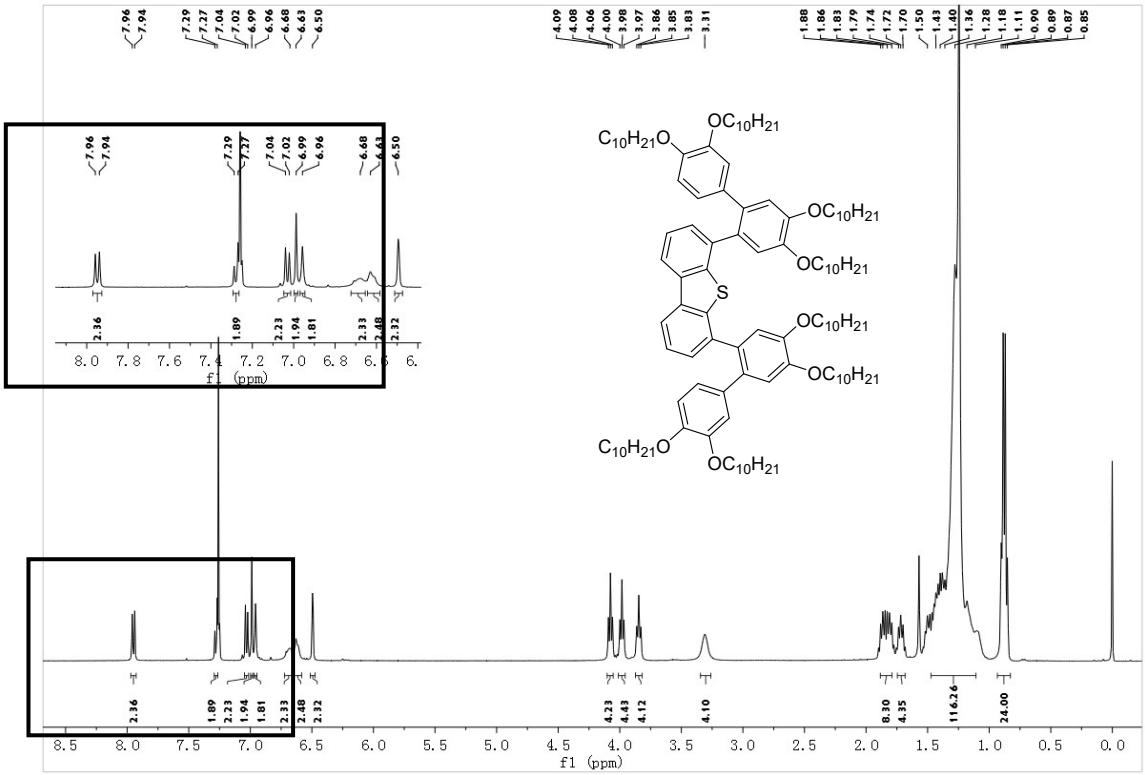

^{1}H NMR ($CDCl_3$, 400 MHz) spectrum of **D10**

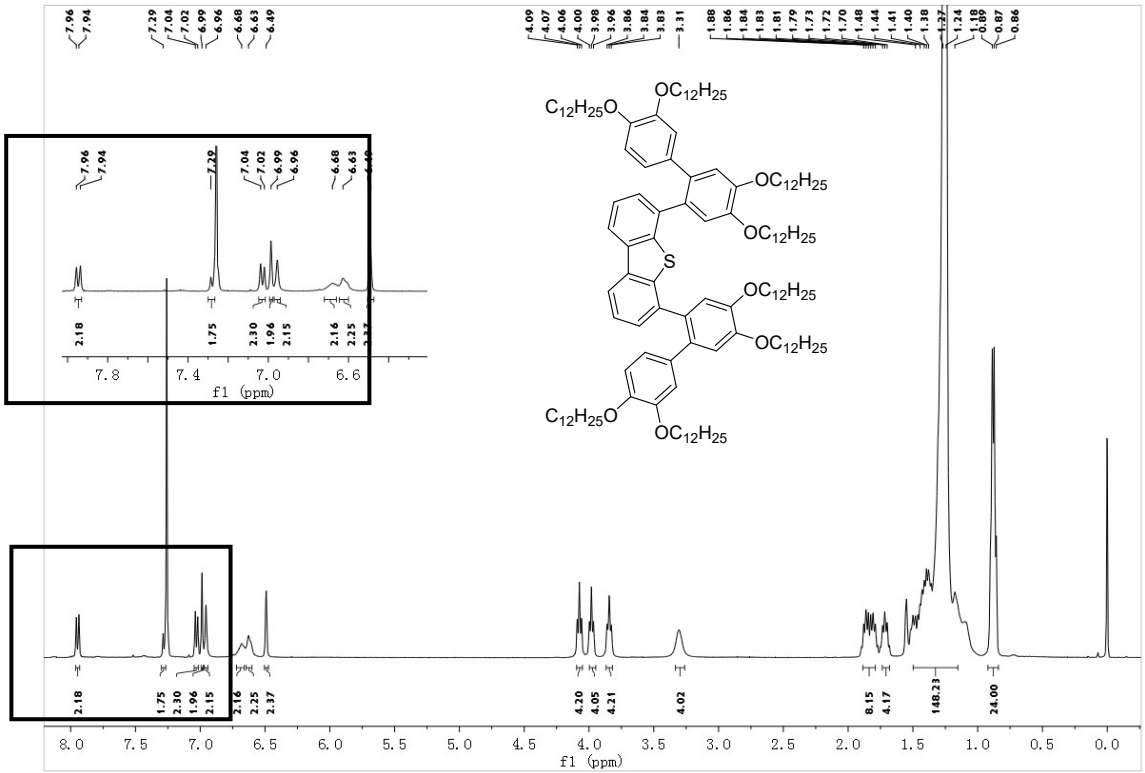

^{1}H NMR ($CDCl_3$, 400 MHz) spectrum of **D12**

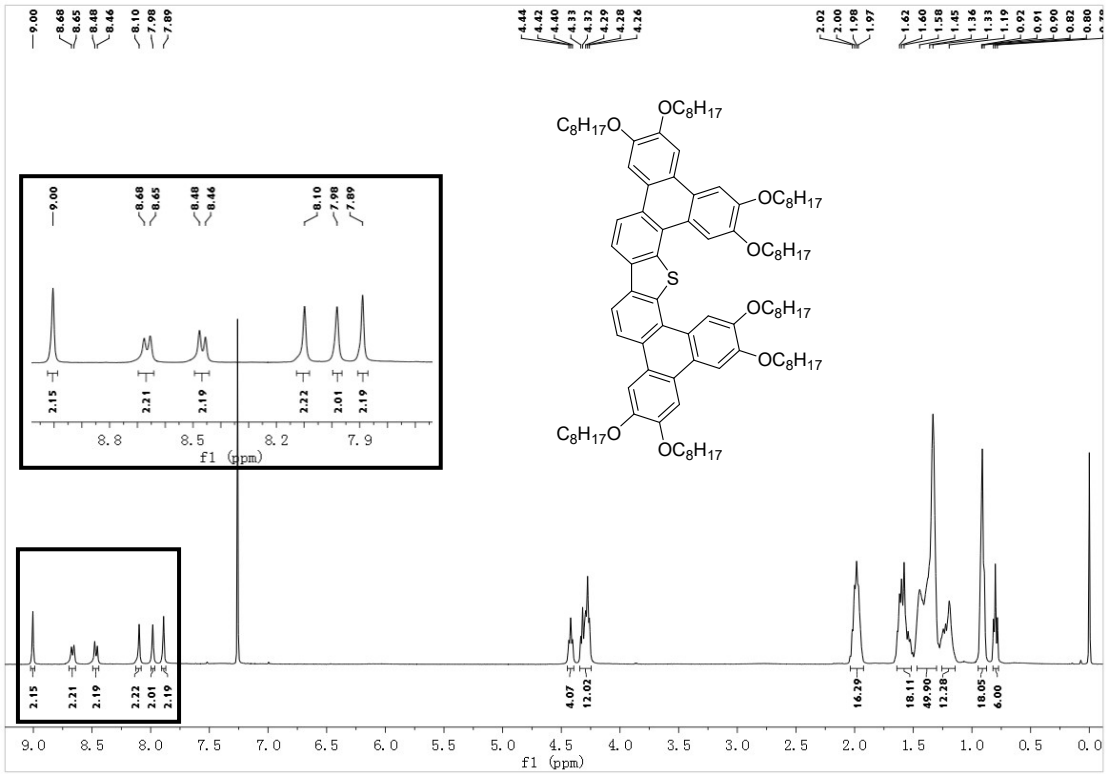

^{1}H NMR ($CDCl_3$, 400 MHz) spectrum of **DTPTA8**

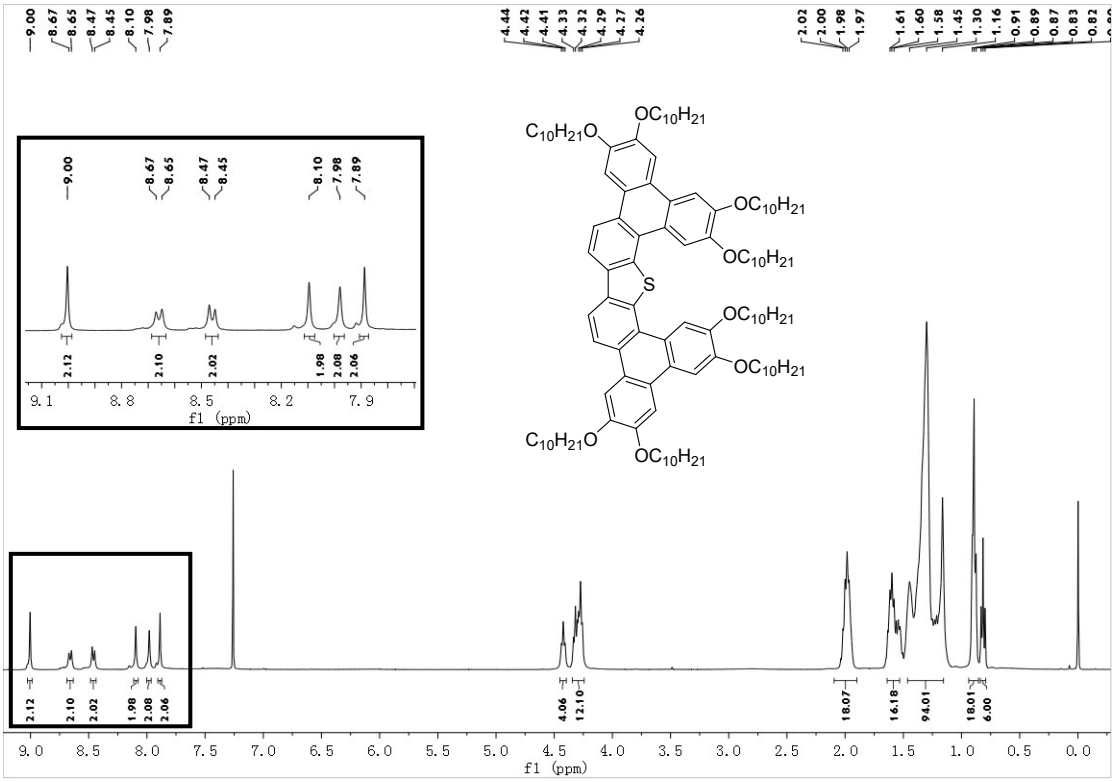

^{1}H NMR ($CDCl_3$, 400 MHz) spectrum of **DTPTA10**

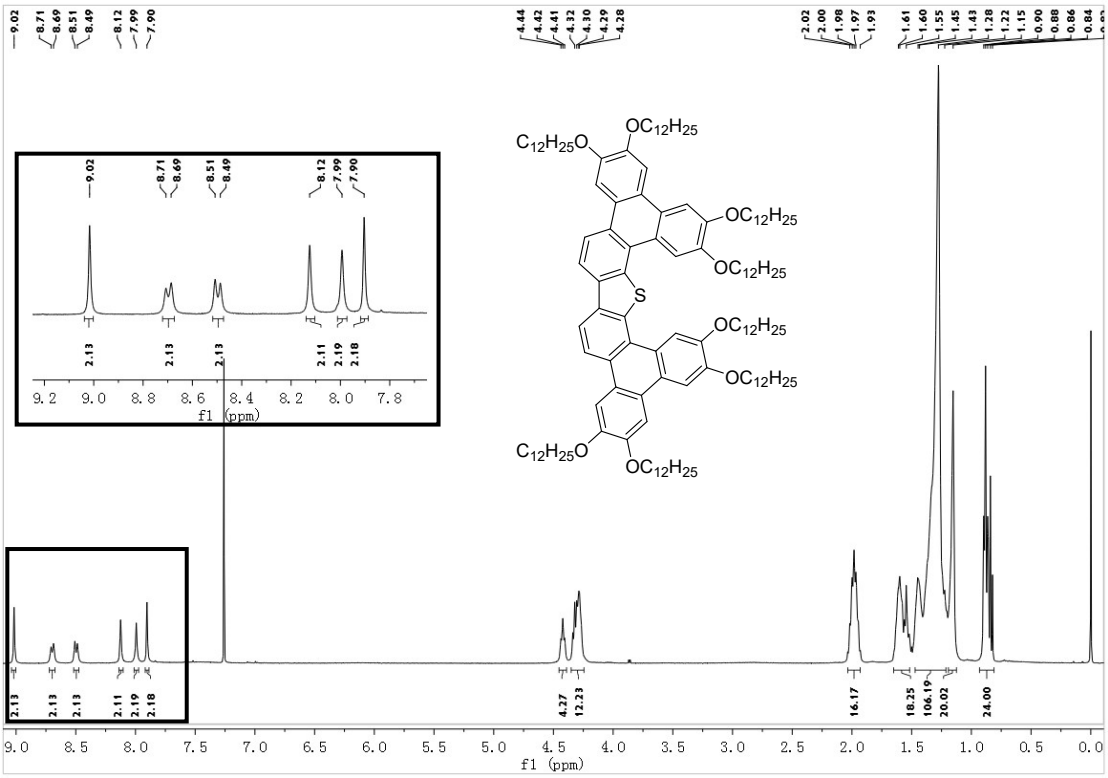

^{1}H NMR ($CDCl_3$, 400 MHz) spectrum of **DTPTA12**

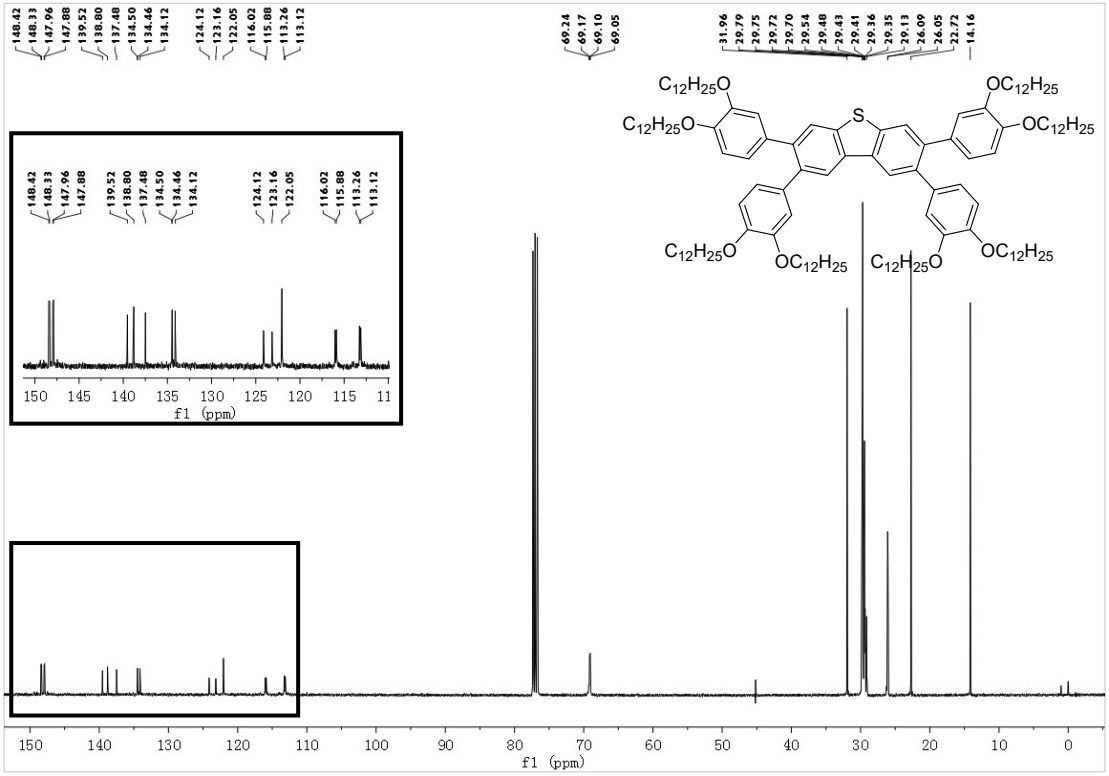

^{13}C NMR ($CDCl_3$, 101 MHz) spectrum of **T12**

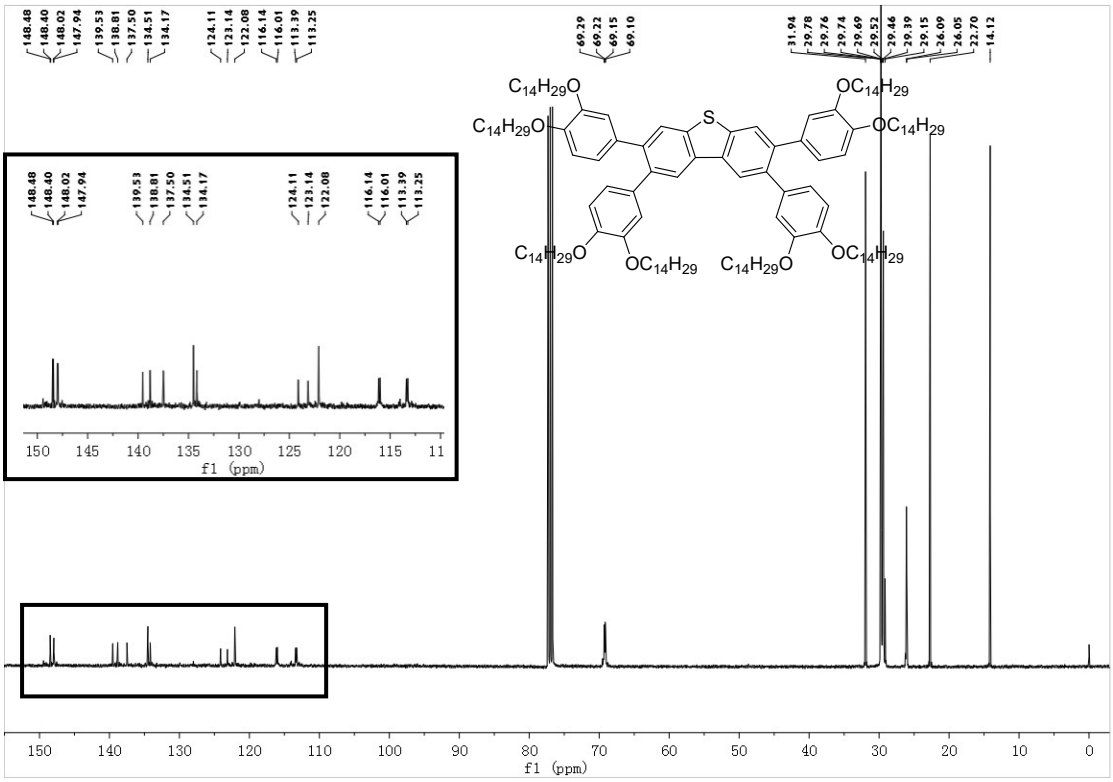

^{13}C NMR ($CDCl_3$, 101 MHz) spectrum of **T14**

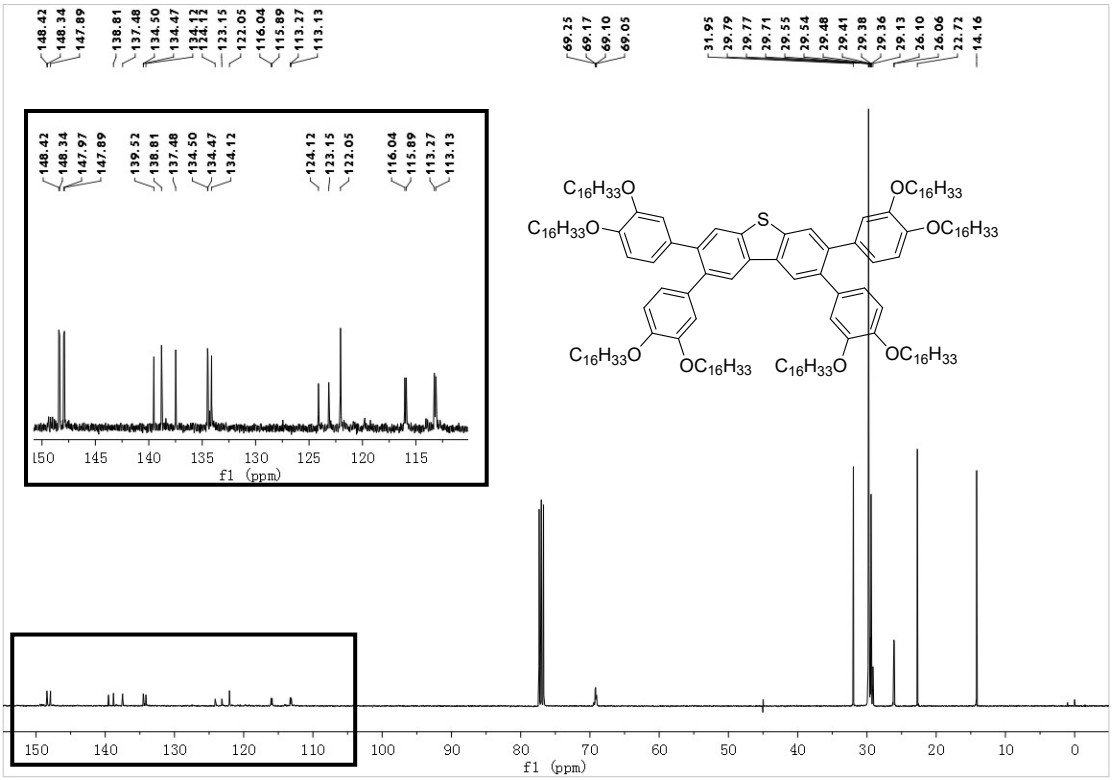

^{13}C NMR ($CDCl_3$, 101 MHz) spectrum of **T16**

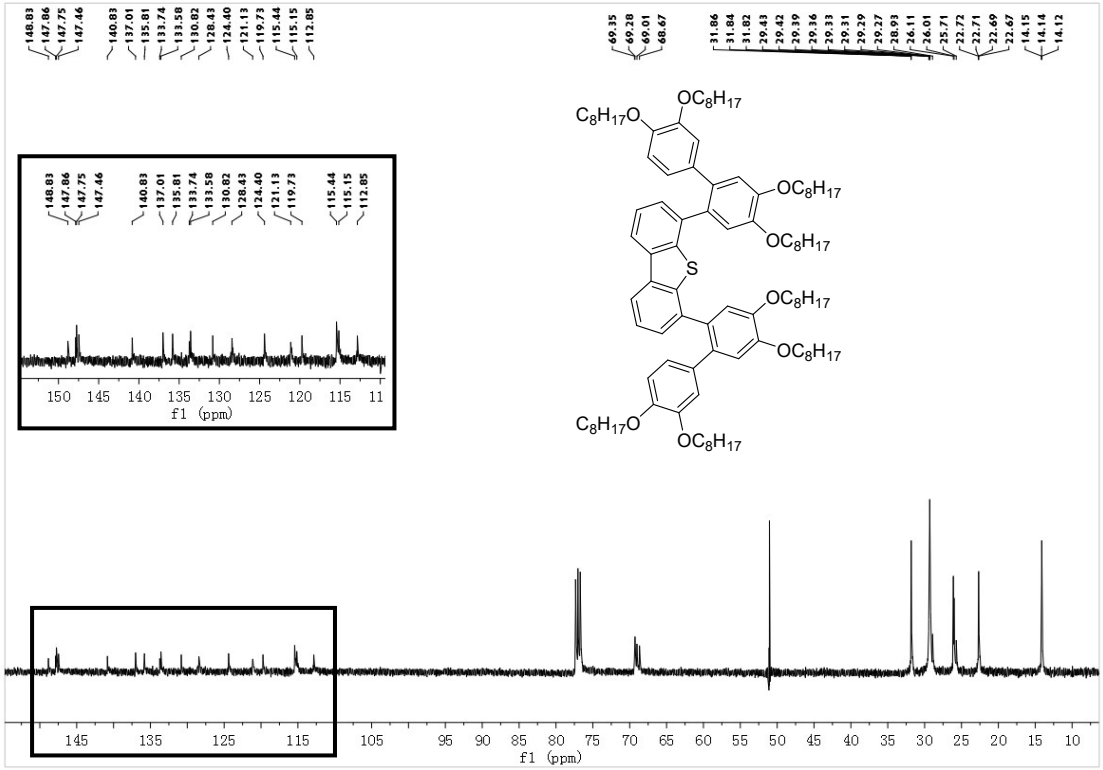

^{13}C NMR ($CDCl_3$, 101 MHz) spectrum of **D8**

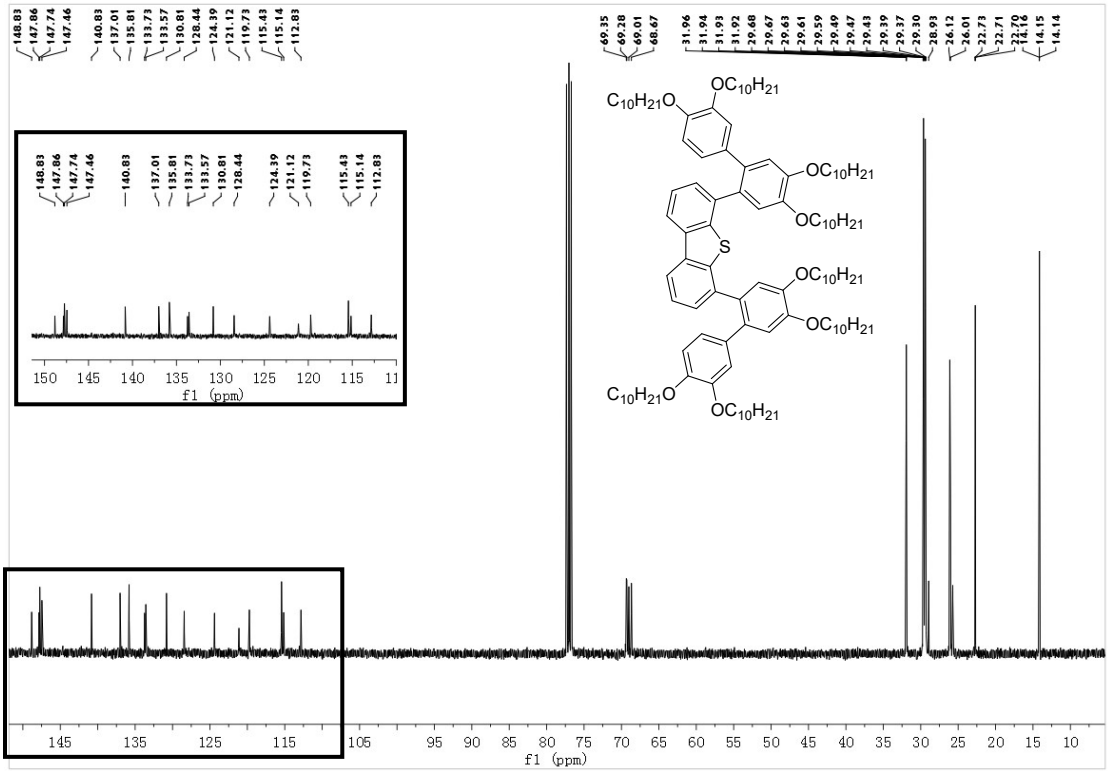

^{13}C NMR ($CDCl_3$, 101 MHz) spectrum of **D10**

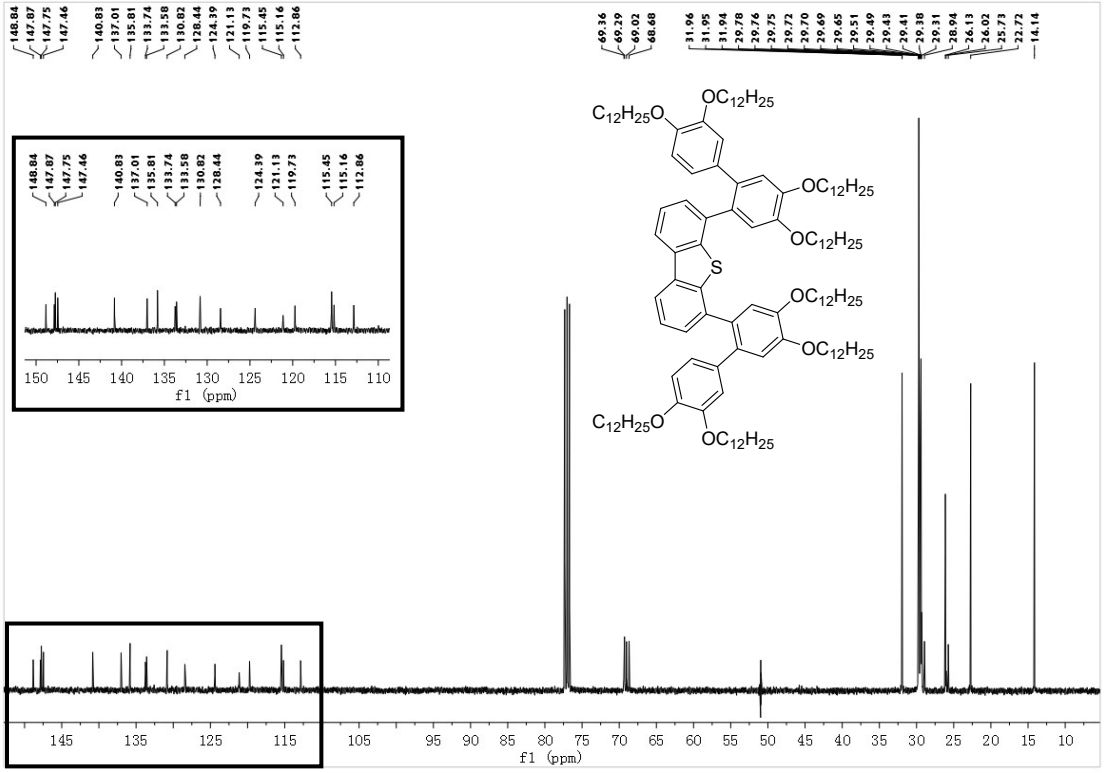

^{13}C NMR ($CDCl_3$, 101 MHz) spectrum of **D12**

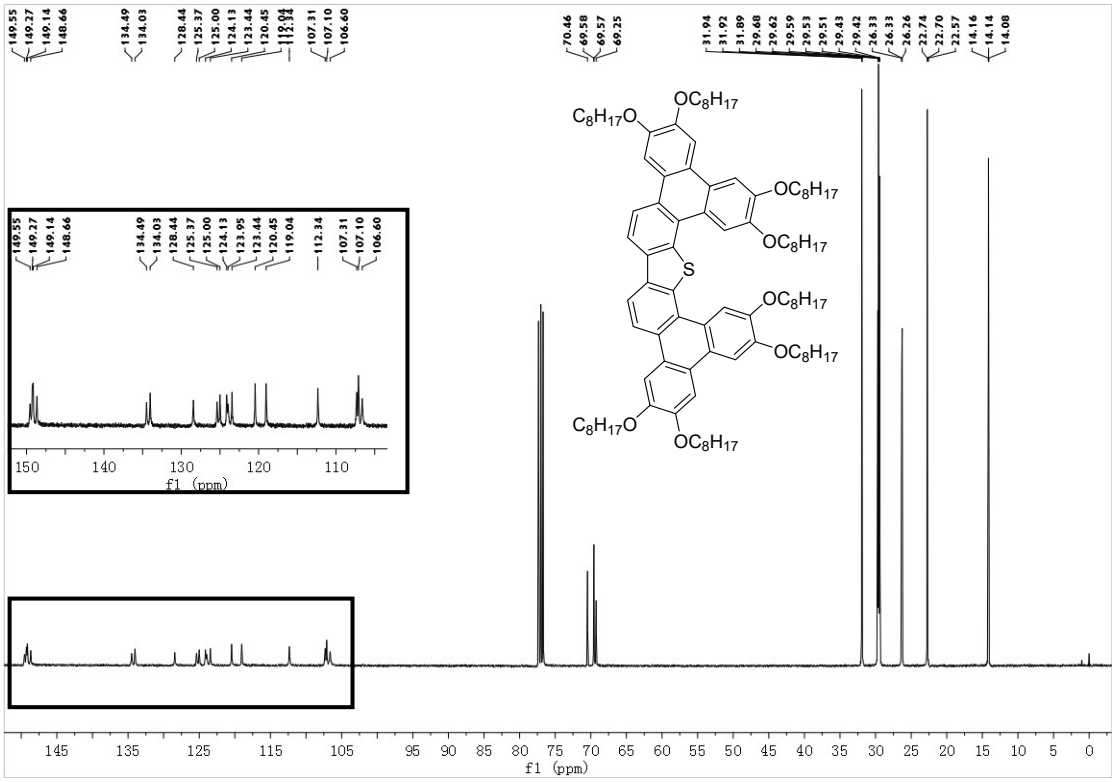

^{13}C NMR ($CDCl_3$, 101 MHz) spectrum of **DTPTA8**

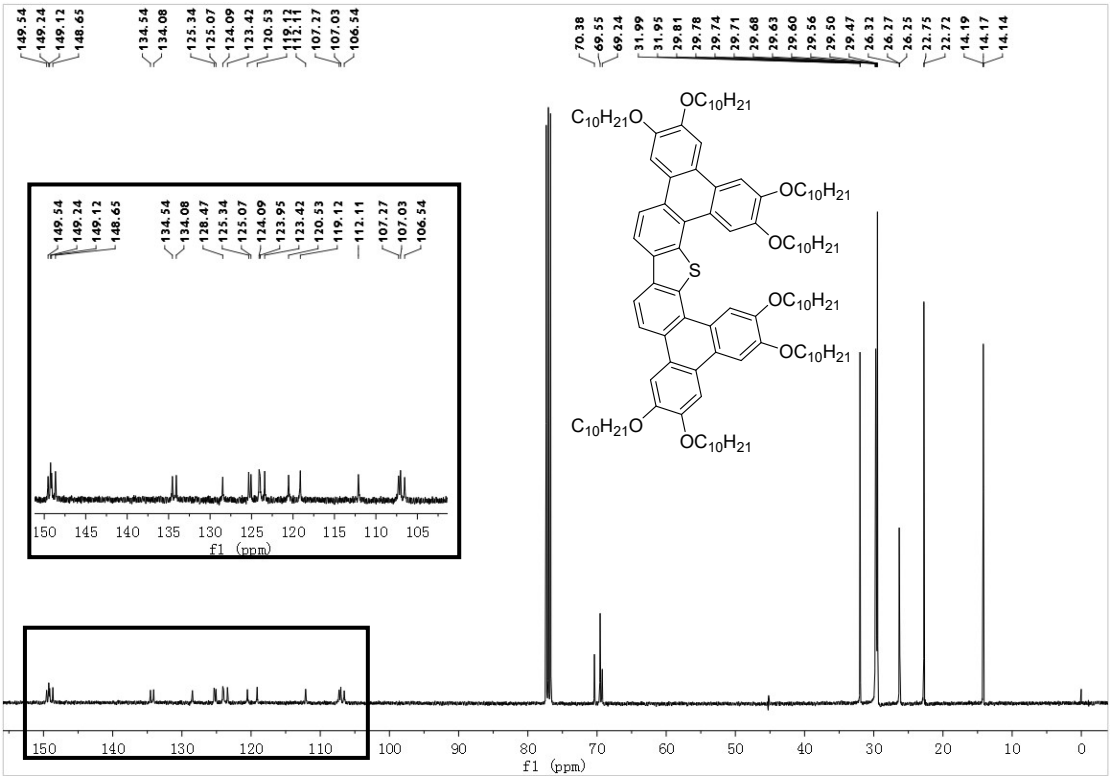

^{13}C NMR ($CDCl_3$, 101 MHz) spectrum of **DTPTA10**

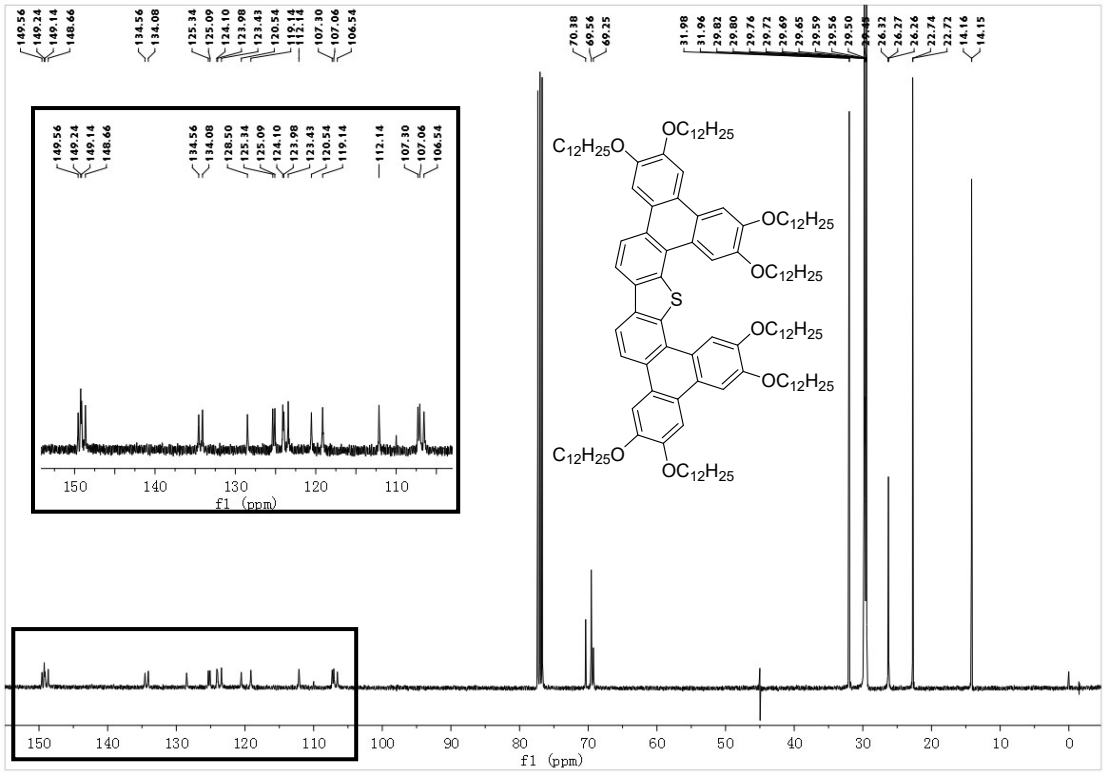

^{13}C NMR ($CDCl_3$, 101 MHz) spectrum of **DTPTA12**

Figure S10. NMR spectra.

12. HRMS

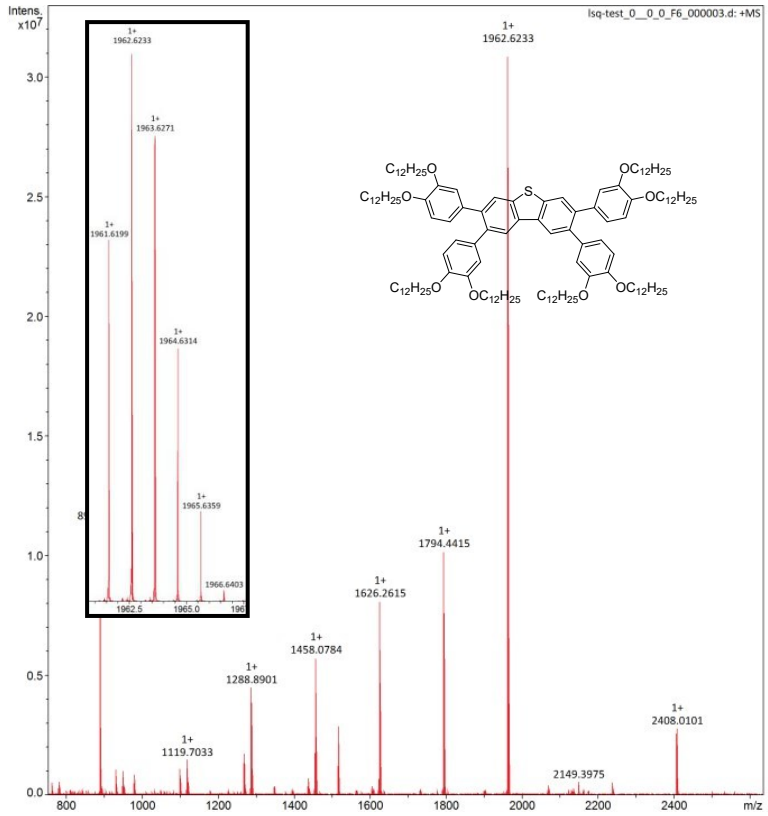

HRMS of **T12**

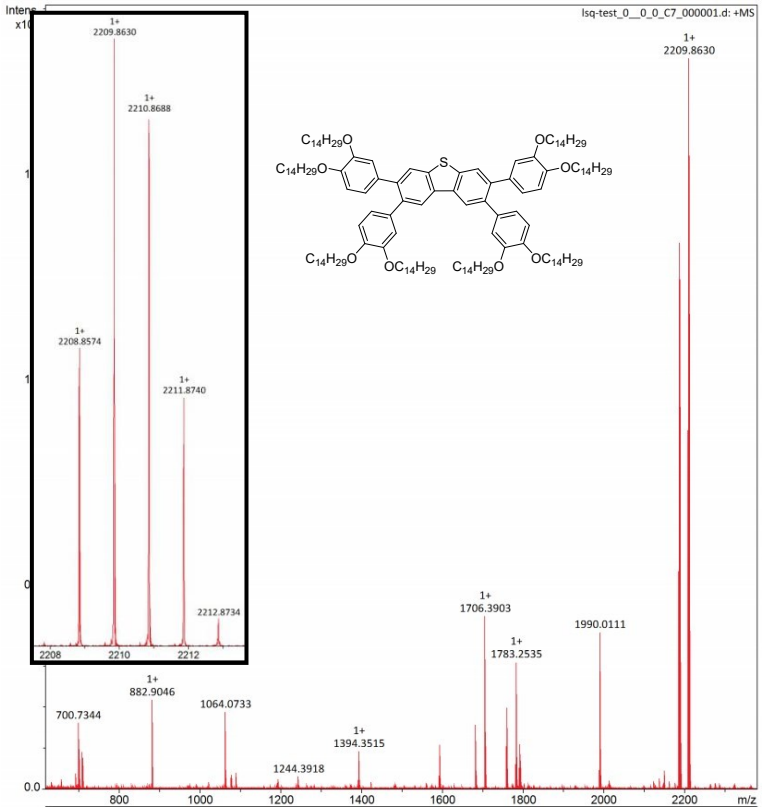

HRMS of **T14**

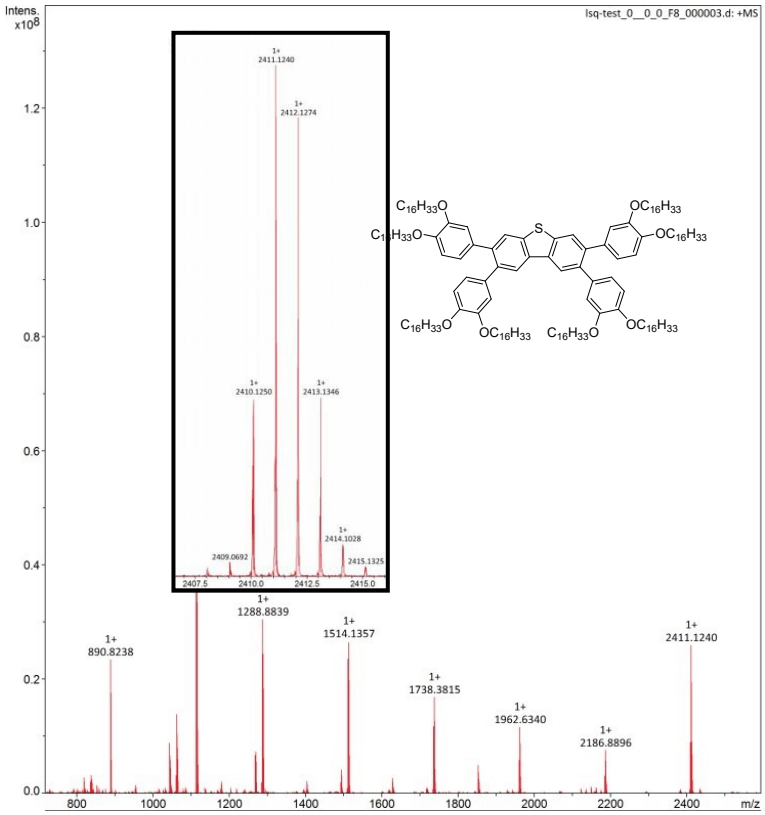

HRMS of **T16**

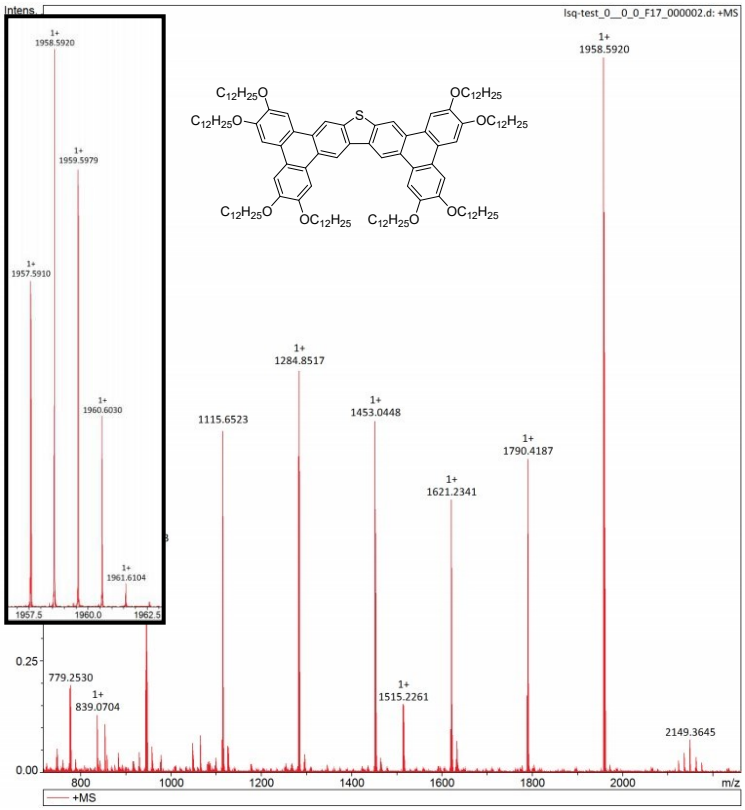

HRMS of **DTPTB12**

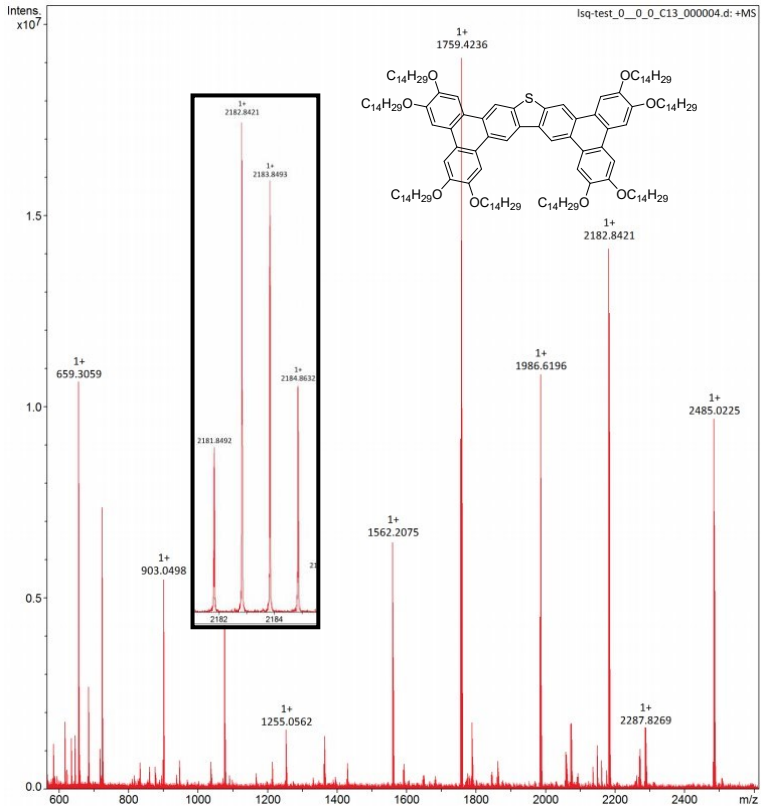

HRMS of **DTPTB14**

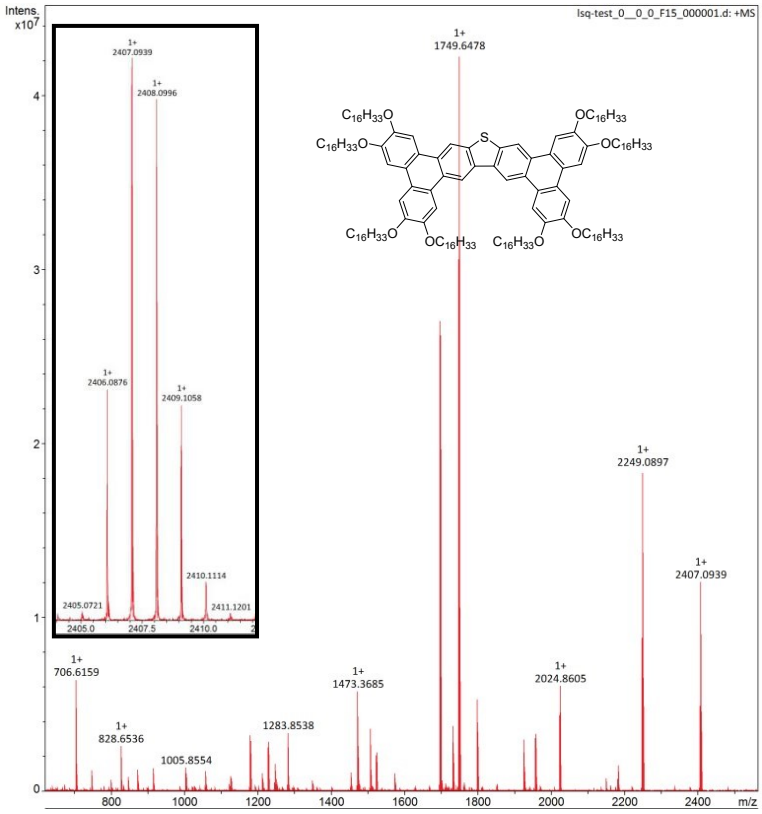

HRMS of **DTPTB16**

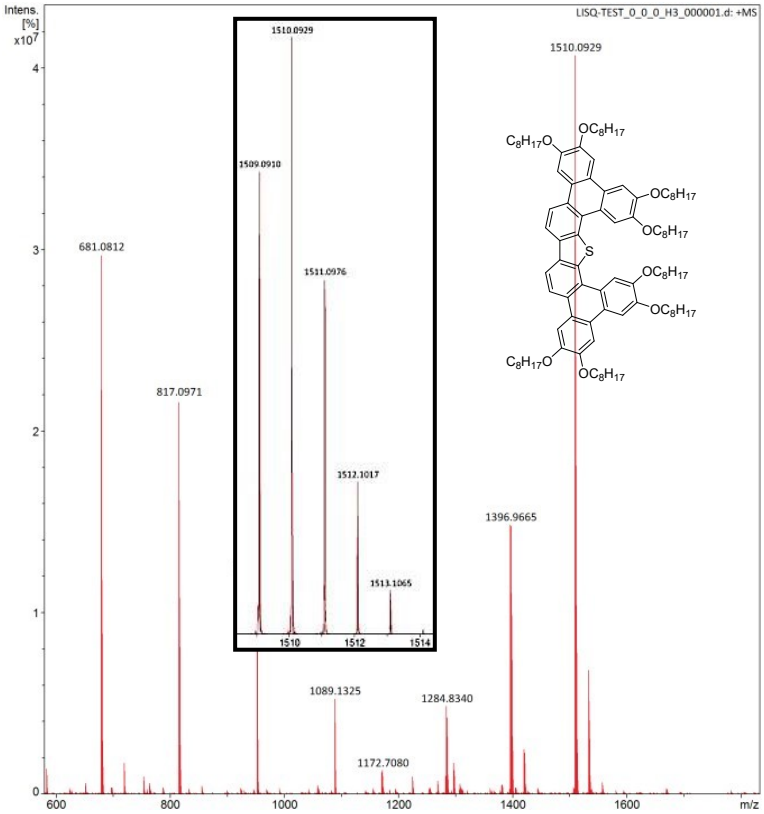

HRMS of **DTPTA8**

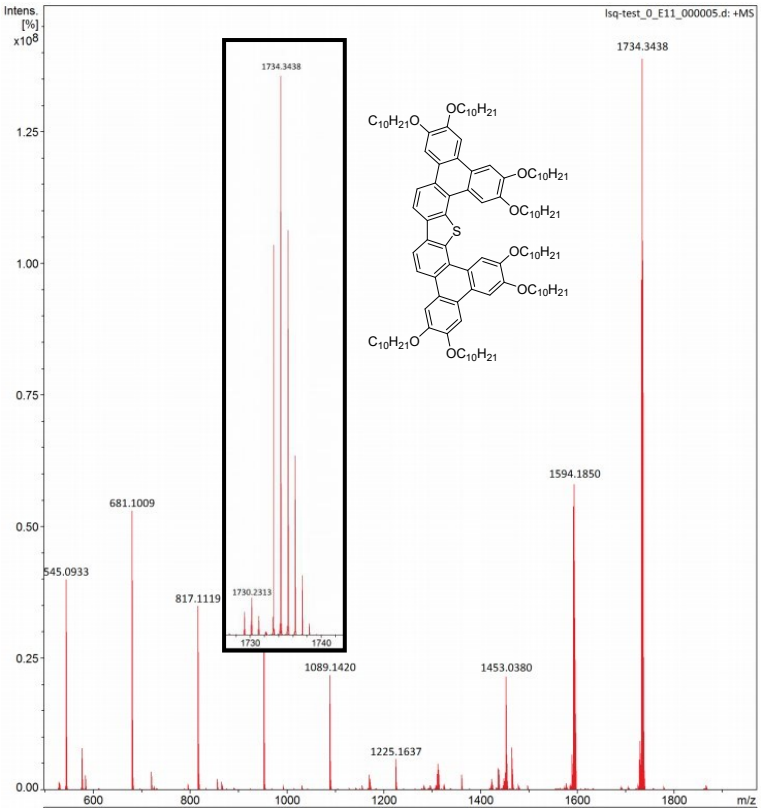

HRMS of **DTPTA10**

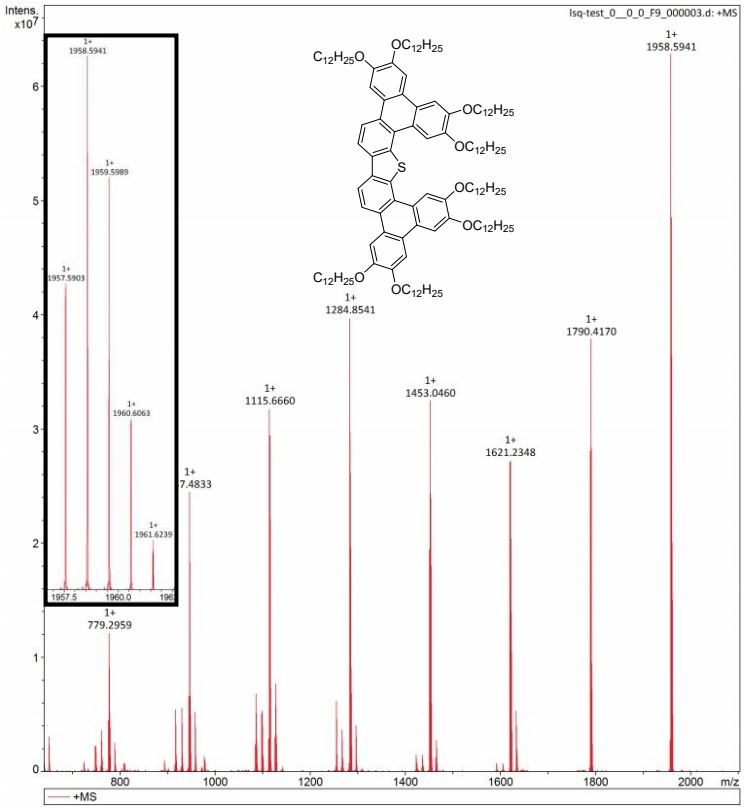

HRMS of **DTPTA12**

Figure S11. HMRS spectra.